

INFORMATION TO USERS

This manuscript has been reproduced from the microfilm master. UMI films the text directly from the original or copy submitted. Thus, some thesis and dissertation copies are in typewriter face, while others may be from any type of computer printer.

The quality of this reproduction is dependent upon the quality of the copy submitted. Broken or indistinct print, colored or poor quality illustrations and photographs, print bleedthrough, substandard margins, and improper alignment can adversely affect reproduction.

In the unlikely event that the author did not send UMI a complete manuscript and there are missing pages, these will be noted. Also, if unauthorized copyright material had to be removed, a note will indicate the deletion.

Oversize materials (e.g., maps, drawings, charts) are reproduced by sectioning the original, beginning at the upper left-hand corner and continuing from left to right in equal sections with small overlaps.

ProQuest Information and Learning
300 North Zeeb Road, Ann Arbor, MI 48106-1346 USA
800-521-0600

UMI[®]



52

VAPOR-LIQUID EQUILIBRIUM

PART I: Vapor-liquid Equilibrium at Atmospheric
Pressure and at 55°C for Binary and Ternary Systems
Containing n-Hexane, Ethyl Alcohol and Benzene.

PART II: Prediction of Binary Vapor-Liquid Equilibrium
Data

by

James C. K. Ho



A Thesis submitted to the Department of Chemical Engineering
of the University of Ottawa in partial fulfillment of the
requirements for the degree of M.Sc.



Author

Director

1962

UMI Number: EC52252

INFORMATION TO USERS

The quality of this reproduction is dependent upon the quality of the copy submitted. Broken or indistinct print, colored or poor quality illustrations and photographs, print bleed-through, substandard margins, and improper alignment can adversely affect reproduction.

In the unlikely event that the author did not send a complete manuscript and there are missing pages, these will be noted. Also, if unauthorized copyright material had to be removed, a note will indicate the deletion.

UMI[®]

UMI Microform EC52252
Copyright 2007 by ProQuest LLC
All rights reserved. This microform edition is protected against
unauthorized copying under Title 17, United States Code.

ProQuest LLC
789 East Eisenhower Parkway
P.O. Box 1346
Ann Arbor, MI 48106-1346

TABLE OF CONTENTS

	<u>PAGE</u>
TABLE OF CONTENTS	i
INDEX OF TABLES, FIGURES AND REPRINT	iv
ABSTRACT	ix
PART I	1
INTRODUCTION	2
HISTORICAL DISCUSSION	3
THEORETICAL PRINCIPLES	4
(A) VAPOR-LIQUID EQUILIBRIUM	4
(B) CORRELATION OF DATA	6
(1) Margules Equations	6
(2) van Laar Equations	6
(3) Redlich-Kister Equations	6
(C) TEST OF THERMODYNAMIC CONSISTENCY	10
(1) Consistency of the binary system	10
(2) Consistency of the ternary system	11
EXPERIMENTAL DETAILS	13
(A) MATERIAL AND PROPERTIES	13
(1) n-Hexane	13
(2) Ethyl Alcohol	13
(3) Benzene	13
(B) DESCRIPTION OF EQUIPMENT	13
(1) Equilibrium Still	13

	<u>PAGE</u>
(2) Accessory Equipment with Still	15
(3) Equipment for Quantitative Analysis of Sample	15
(a) Chromatograph	15
(b) Refractometer	16
(C) EXPERIMENTAL PROCEDURES	17
(1) Binary systems of n-hexane-benzene and ethyl alcohol-benzene	17
(a) Planning of experiment	17
(b) Determination of vapor-liquid equilibrium data	17
(c) Analytical method	19
(2) Ternary system and binary system of n-hexane-ethyl alcohol	20
(a) Planning of experiment	20
(b) Determination of vapor-liquid equilibrium data	20
(c) Analytical method	21
RESULTS	23
CORRELATION OF RESULTS	63
SAMPLE CALCULATIONS	65
DISCUSSION	72
CONCLUSION	75
APPENDIX I	77
PART II	100
INTRODUCTION	108

	111
	<u>PAGE</u>
PROPOSED METHOD	102
TESTING THE PROPOSED METHOD	106
SAMPLE CALCULATIONS	108
CONCLUSION	110
APPENDIX II	111
ACKNOWLEDGEMENT	118
NOMENCLATURE	119
REFERENCES	121

INDEX OF TABLES AND FIGURES

	<u>PAGE</u>
(a) TABLES	
1. Vapor-liquid equilibrium data for n-hexane(1)-ethyl alcohol(2) system at 760 mm. Hg.	24
2. Vapor-liquid equilibrium data for n-hexane(1)-ethyl alcohol(2) system at 55°C.	25
3. Vapor-liquid equilibrium data for n-hexane(1)-benzene(3) system at 760 mm.Hg.	26
4. Vapor-liquid equilibrium data for n-hexane(1)-benzene(3) system at 55°C.	27
5. Vapor-liquid equilibrium data for ethyl alcohol(2)-benzene(3) system at 760 mm.Hg.	28
6. Vapor-liquid equilibrium data for ethyl alcohol(2)-benzene(3) system at 55°C.	29
7. Vapor-liquid equilibrium data for n-hexane(1)-ethyl alcohol(2)-benzene(3) system at 760 mm. Hg.	30
8. Vapor-liquid equilibrium data for n-hexane(1)-ethyl alcohol(2)-benzene(3) system at 55°C.	33
9. Operating conditions for gas chromatographic analysis	79
10. Calibration of temperature - absolute millivolts for the copper constantan thermocouple	80
11. Calibration of composition-refractive index for the system n-hexane-benzene	82
12. Calibration of composition-refractive index for the system ethyl alcohol-benzene	84
13. Calibration of mole fraction ratio vs. area ratio for the system of n-hexane-ethyl alcohol	86
14. Calibration of mole fraction ratio vs. area ratio for the system of n-hexane-ethyl alcohol-benzene	88

	<u>PAGE</u>
15. Redlich-Kister constants for the binary systems of n-hexane-ethanol, n-hexane-benzene and ethanol-benzene at 55°C.	92
16. Equations for solving the ternary constants in the Redlich-Kister equation	93
17. Comparison of experimental and calculated values of Q_{123}	94
18. Comparison of experimental and calculated values from the proposed prediction	112
19. Pseudo mole fraction values calculated for system heptane-ethylbenzene from the experimental equilibrium data at 760 mm.Hg.	114

(b) FIGURES

1. Temperature vs. composition diagram for n-hexane(1)-ethyl alcohol(2) system at 760 mm. Hg.	37
2. Logarithmic activity coefficients vs. composition for n-hexane(1)-ethyl alcohol(2) system at 760 mm. Hg.	38
3. Logarithm of ratios of γ_1/γ_2 vs. x_1 for n-hexane(1)-ethyl alcohol(2) system at 760 mm.Hg.	39
4. Total pressure vs. composition diagram for n-hexane(1)-ethyl alcohol(2) system at 55°C.	40
5. Logarithmic activity coefficients vs. composition for n-hexane(1)-ethyl alcohol(2) system at 55°C.	41
6. Logarithm of ratios of γ_1/γ_2 vs. x_1 for n-hexane(1)-ethyl alcohol(2) system at 55°C.	42
7. Temperature vs. composition diagram for n-hexane(1)-benzene(3) system at 760 mm. Hg.	43
8. Logarithmic activity coefficients vs. composition for n-hexane(1)-benzene(3) system at 760 mm. Hg.	44
9. Logarithm of ratios of γ_3/γ_1 vs. x_3 for n-hexane(1)-benzene(3) system at 760 mm.Hg.	45

	<u>PAGE</u>
10. Total pressure vs. composition diagram for n-hexane(1)-benzene(3) system at 55°C.	46
11. Logarithmic activity coefficients vs. composition for n-hexane(1)-benzene(3) system at 55°C.	47
12. Logarithm of ratios of γ_3/γ_1 vs. x_3 for n-hexane(1)-benzene(3) system at 55°C.	48
13. Temperature vs. composition diagram for ethyl alcohol(2)-benzene(3) system at 760 mm. Hg.	49
14. Logarithmic activity coefficients vs. composition for ethyl alcohol(2)-benzene(3) system at 760 mm. Hg.	50
15. Logarithm of ratios of γ_2/γ_3 vs. x_2 for ethyl alcohol(2)-benzene(3) system at 760 mm. Hg.	51
16. Total pressure vs. composition diagram for ethyl alcohol(2)-benzene(3) system at 55°C.	52
17. Logarithmic activity coefficients vs. composition for ethyl alcohol(2)-benzene(3) system at 55°C.	53
18. Logarithm of ratios of γ_2/γ_3 vs. x_2 for ethyl alcohol(2)-benzene(3) system at 55°C.	54
19. Bubble point (°C)-liquid phase composition diagram for the ternary system of n-hexane(1)-ethyl alcohol(2)-benzene(3) at 760 mm. Hg.	55
20. n-Hexane activity coefficients vs. liquid phase composition in the ternary system at 760 mm. Hg.	56
21. Ethyl alcohol activity coefficients vs. liquid phase composition in the ternary system at 760 mm. Hg.	57
22. Benzene activity coefficients vs. liquid phase composition in the ternary system at 760 mm. Hg.	58
23. Total pressure (mm. Hg.)-liquid phase composition diagram for the ternary system of n-hexane(1)-ethyl alcohol(2)-benzene(3) at 55°C.	59

	<u>PAGE</u>
24. n-Hexane activity coefficients vs. liquid phase composition in the ternary system at 55°C.	60
25. Ethyl alcohol activity coefficients vs. liquid phase composition in the ternary system at 55°C.	61
26. Benzene activity coefficients vs. liquid phase composition in the ternary system at 55°C.	62
27. Modified Oillepie Equilibrium Still	78
28. Calibration curve of copper constantan thermocouple	81
29. Calibration curve of composition-refractive index for the system n-hexane-benzene	83
30. Calibration curve of composition-refractive index for the system ethyl alcohol-benzene	85
31. Calibration curve of (Ethanol/n-Hexane) mole fraction vs. (Ethanol/n-Hexane) area for the binary system of n-hexane-ethanol	87
32. Calibration curve of (Ethanol/Benzene) mole fraction vs. (Ethanol/Benzene) area for the ternary system	89
33. Calibration curve of (Benzene/n-Hexane) mole fraction vs. (Benzene/n-Hexane) area for the ternary system	90
34. Calibration curve of (Ethanol/n-Hexane) mole fraction vs. (Ethanol/n-Hexane) area for the ternary system	91
35. Thermodynamic consistency of vapor-liquid equilibrium data for the ternary system at 760 mm. Hg. (Percentages indicated are overall deviations)	96
36. Vapor-liquid equilibrium diagram for the ternary system at 760 mm. Hg.	97
37. Thermodynamic consistency of vapor-liquid equilibrium data for the ternary system at 55°C. (Percentages indicated are overall deviations)	98
38. Vapor-liquid equilibrium diagram for the ternary system at 55°C.	99

	<u>PAGE</u>
39. Calculated $t-x^l-y^l$ values for the system heptane-ethylbenzene at 100 mm. Hg.	115
40. Predicted vapor-liquid equilibrium curve and data (2) for the system heptane-ethylbenzene	116
(e) Reprint of Part. II Thesis from Ind. Eng. Chem., <u>53</u> , 384-386 (1961)	117

ABSTRACT

This thesis comprises of two parts.

The first part is the determination of vapor-liquid equilibrium data at atmospheric pressure and 55°C for the ternary system n-hexane-ethyl alcohol-benzene and for the three possible binary systems n-hexane-ethyl alcohol, n-hexane-benzene and ethyl alcohol-benzene which constituted the ternary system.

A modified Gillespie equilibrium still is employed to conduct the investigation. The equilibrium data for the three binary systems and the ternary system appear to be consistent as shown from the thermodynamic consistency tests.

The experimental results indicate that two binary systems, namely, n-hexane-ethyl alcohol and ethyl alcohol-benzene form azeotrope at 760 mm. Hg. and 55°C. The ternary system deviates considerably from ideal liquid phase behavior. However, no ternary azeotrope is found from the experiment.

The second part presents a method for predicting binary vapor-liquid equilibrium data at various conditions if the equilibrium data for the system concerned are available over the complete concentration range at any one isothermal or isobaric condition. The proposed method is limited to nonazeotropic solutions.

PART I

Vapor-Liquid Equilibrium at Atmospheric
Pressure and at 55°C for Binary and Ternary
Systems Containing n-Hexane, Ethyl Alcohol
and Benzene

INTRODUCTION

Vapor-liquid equilibrium data at atmospheric pressure and 55°C were determined by means of a modified Gillespie still for the ternary system n-hexane-ethyl alcohol-benzene and for the possible three binaries which constituted the ternary system.

This particular ternary system was investigated because of the different types of hydrocarbon compounds involved, n-hexane being a straight-chain saturated paraffin and benzene being an aromatic, and ethyl alcohol being a polar compound of straight-chain saturated alcohol. Furthermore, this ternary system was chosen because it could be expected to show large deviations from ideal liquid phase behavior. The data reported in this investigation and those reported from other workers (1, 2, 3, 4, 5) should be useful in seeking some means of predicting multicomponent equilibrium data from binary equilibrium data and extending the equilibrium data of the multicomponent systems from one basic condition to various desired conditions. It is also intended to correlate the data by the Redlich-Kister equations (6).

HISTORICAL DISCUSSION

Due to the limitation of the reliable vapor-liquid equilibrium data for multicomponent systems in the past, many investigators and research workers in the recent years concentrated their effort in seeking more data for industrial applications and better understanding of the physico-chemical relationship for theoretical development and correlation of ternary systems.

In the design of azeotropic and extractive distillation equipment, reliable multicomponent vapor-liquid equilibria are necessary for the estimation of heat requirements, column capacities and separation efficiencies. It would be most helpful to be able to predict equilibrium relationship from properties of the pure components or, failing this, from a minimum of experimental data. Such information would be useful for the selection of a suitable third component to facilitate the ease of separation of two close-boiling or azeotropic liquids by distillation. The combination of the knowledge obtained from the experiments and the use of empirical and semi-empirical equations for prediction or extension of ternary vapor-liquid equilibrium data to multi-component systems is desirable.

THEORETICAL PRINCIPLES

Vapor-Liquid Equilibrium

The evaluation of the liquid phase activity coefficient, allowing for non-ideal solutions of the vapor and liquid phase, some investigators (7) proposed the following equation.

For simplicity, binary system is considered.

$$v_1 = \frac{y_1 P}{x_1 p_1} \exp. \left[\frac{(p_1 - P)(v_1^* - B_{11})}{RT} \right] \exp. \left(\frac{y_2^2 S P}{RT} \right) \quad (1)$$

where y = mole fraction of component in the vapor phase

x = mole fraction of component in the liquid phase

P = total pressure

p = vapor pressure of component

v_1^* = molal volume of the liquid in the vapor state

B_{11} = second coefficient in the virial equation of state

R = gas law constant

T = temperature of the system

S = interaction parameter

$$= 2 B_{12} - B_{11} - B_{22}$$

or

$$v_1 = \frac{y_1 P}{x_1 p_1} z_1 z_2 \quad (2)$$

where

$$z_1 = \exp. \left[\frac{(p_1 - P)(v_1^* - B_{11})}{RT} \right]$$

and is a correction for deviation of the pure vapor from the perfect gas law and $Z_2 = \exp. (y_2^2 \frac{P}{RT})$ which corrects for deviation from the laws of ideal solution.

The two exponential terms can be evaluated if the virial coefficients for the two components are known. Scheibel (8) has prepared a nomograph for the estimation of Z_1 from the knowledge of reduced temperature (T_r), critical pressure (P_c) and the difference between vapor pressure of pure component and total pressure ($p - P$) on the system. In most cases, the value of Z is ranging from 0.85 to 1.70. Z_2 is ignored in most literature but will have a value greater than unity if there is a positive deviation from Raoult's law in the liquid phase. Thus the product of Z_1 and Z_2 may be greater or less than unity, depending on the magnitude of each. As Z_2 could not be calculated conveniently, this author therefore decided also to neglect Z_1 . If Z_1 correction is applied alone, additional error might be introduced. Thus a simplified form of Equation 1 for liquid phase activity coefficient is employed as shown in the following equation.

$$\gamma_1 = \frac{y_1 P}{x_1 P_1} \quad (3)$$

For multicomponent system, the following equation is used to evaluate liquid phase activity coefficient of component i.

$$\gamma_i = \frac{y_i P}{x_i P_i} \quad (4)$$

Correlation of Data

The activity coefficients in binary solutions may be represented by the following common equations.

(1) Margules Equation. The following equations are proposed by Margules (9) and modified by Carlson and Colburn (10).

$$\begin{aligned}\log \gamma_1 &= x_2^2 \left[A + 2 (B-A) x_1 \right] \\ &= (2 B-A) x_2^2 + 2(A-B) x_2^3\end{aligned}\quad (5)$$

$$\begin{aligned}\log \gamma_2 &= x_1^2 \left[B + 2 (A-B) x_2 \right] \\ &= (2 A-B) x_1^2 + 2 (B-A) x_1^3\end{aligned}\quad (6)$$

where A, B = constants of Margules equation.

(2) van Laar Equations. The following equations are developed by van Laar (11, 12) and rearranged by Carlson and Colburn (10).

$$\log \gamma_1 = \frac{A}{\left(1 + \frac{A}{B} \frac{x_1}{x_2}\right)^2}\quad (7)$$

$$\log \gamma_2 = \frac{B}{\left(1 + \frac{B}{A} \frac{x_2}{x_1}\right)^2}\quad (8)$$

where A, B = constants of van Laar equation.

(3) Redlich-Kister Equations. The Redlich-Kister equation (6) is the most commonly used equation for relating activity coefficients. The

authors expanded Scatchard excess free energy and divided by 2.303 RT to obtain the excess free energy function Q.

For liquid phase,

$$Q = \frac{Q^E}{2.303 RT} = x_1 \log \gamma_1 + x_2 \log \gamma_2 \quad (9)$$

or in the form of

$$\frac{dQ}{dx_1} = \log (\gamma_1/\gamma_2) \quad (10)$$

The degree of this function is one unit lower than Q as well as the functions.

The following two equations may also be obtained conveniently.

$$\log \gamma_1 = Q + x_2 \frac{dQ}{dx_1} \quad (11)$$

$$\log \gamma_2 = Q - x_1 \frac{dQ}{dx_1} \quad (12)$$

Assuming the usual convention that $\gamma_1 = 1$ at $x_1 = 1$, Q may be represented by an appropriate power series which satisfies the theoretical limits that $Q = 0$ at $x_1 = 1$ and $x_2 = 1$. Redlich and Kister (6) have related the excess free energy of constant temperature and pressure to liquid composition by a series function shown below.

$$Q = x_1 x_2 \left[B_{12} + C_{12} (x_1 - x_2) + D_{12} (x_1 - x_2)^2 + \dots \right] \quad (\text{at } P, T) \quad (13)$$

where B_{12} , C_{12} , D_{12} = constants of Redlich-Kister equation.

Formulation of individual activity coefficients is obtained by differentiation of Equation 13.

$$\log \gamma_1 = x_2^2 \left[B_{12} + C_{12} (3x_1 - x_2) + D_{12} (x_1 - x_2) (5x_1 - x_2) + \dots \right] \quad (14)$$

$$\log \gamma_2 = x_1^2 \left[B_{12} + C_{12} (x_1 - 3x_2) + D_{12} (x_1 - x_2) (x_1 - 5x_2) + \dots \right] \quad (15)$$

Subtracting Equation 15 from Equation 14, one obtains

$$\begin{aligned} \log (\gamma_1/\gamma_2) = dQ/dx_1 = & B_{12} (x_2 - x_1) \\ & + C_{12} (6x_1 x_2 - 1) + D_{12} (x_2 - x_1)(1 - 6x_1 x_2) \\ & + \dots \end{aligned} \quad (16)$$

The selection of the proper suffix equation depends on the molecular complexity of the system and the precision of the experimental data. Where an equation is chosen that fits the experimental data, the constants will be different for conditions of constant temperature or constant pressure. It should also be mentioned that the Margules equations (Equations 5 and 6) are one of the typical forms of the Redlich-Kister equations. Furthermore, the Redlich-Kister equations do not have to be limited to three constants as shown in Equations 14 and 15. Redlich, Kister and Turnquist (13) illustrated the flexibility

of Equation 13 and stated that van Laar equations are much more cumbersome for solutions which can be represented by Equation 13, with one or two terms and are always entirely insufficient for solutions which require three or four terms in Equation 13. It may be stated in general that Equations 14 and 15 are adequate for representing activity coefficient curves. The only question remains is that how many terms should be employed. According to Redlich, Kister and Turnquist (13), only very accurate measurements for an extremely imperfect solution requires four terms. The investigation by Ho, Bostko and Lu (14) further supports the suggestion (13) that three-constant Redlich-Kister equation is adequate for representing liquid activity coefficients for most systems.

The activity coefficient for multicomponent systems may be expressed by the expansion of Redlich-Kister power series (6) without difficulty. The series for a ternary system is then conveniently represented by

$$G_{123} = G_{12} + G_{23} + G_{31} + x_1 x_2 x_3 \left[G_{123} + D_1 (x_2 - x_3) + D_2 (x_3 - x_1) + D_3 (x_1 - x_2) + \dots \right] \quad (17)$$

where the first three terms on the right-hand side of Equation 17 represent contributions by the separate binaries and the last term represents ternary effects,

$$\text{and,} \quad G_{123} = x_1 \log \gamma_1 + x_2 \log \gamma_2 + x_3 \log \gamma_3 \quad (18)$$

Test of Thermodynamic Consistency

(1) Consistency of the binary system. The thermodynamic consistency of the binary systems may be tested by the methods recommended by Lu, Spinner and Ho (15), Redlich and Kister (6) and Thijssen (16). In et al (15) proposed that consistency of data can be tested by visual methods by using the Gibbs-Duhem equation on a $\log \gamma$ vs. x plot at strategic liquid compositions of 0.00, 0.25, 0.50, 0.75 and 1.00 mole fractions provided that the boiling intervals are small, and by direct tests of P-T-composition data.

Redlich and Kister (6) derived the relation shown below.

$$\int_{x_2=0}^{x_2=1} \log (\gamma_1/\gamma_2) dx_1 = 0 \quad (19)$$

By plotting experimental data of $\log (\gamma_1/\gamma_2)$ against x_1 from 0.0 to 1.0, the net area of the curve is equal to zero. Or, the area above the abscissa axis is equal to the area below that axis. However, Herington (17) has shown that a small correction should be made to Equation 19 for the heat of mixing effect.

As the heat of mixing data are not available for the systems investigated, it could not be applied for test of consistency. However, the correction is small for azeotropic systems.

The concept of heat of mixing led to various new proposals for data consistency test. Thijssen (16) has shown that for consistent

data the following relations must be held,

$$\int_{x_1=0}^{x_1=1} \log \frac{\gamma_1}{\gamma_2} dx_1 = \frac{1}{2.303} \int_{x_1=0}^{x_1=1} \frac{\Delta H^M}{RT^2} \frac{dT}{dx_1} dx_1 \quad (20)$$

where ΔH^M = isobaric and isothermal heat of mixing.

(2) Consistency of the ternary system. Checking the consistency of binary equilibrium data is a well developed process, but there is no wholly satisfactory method for testing the thermodynamic consistency of ternary vapor-liquid data. Several methods (18, 19, 20, 21, 22) based on the definition of excess free energy have been proposed for testing of data consistency.

Recently, Li and Lu (23) have proposed graphical and numerical integration methods for testing the thermodynamic consistency of ternary vapor-liquid equilibrium data, in which the integration of the Gibbs-Duhem equation can be performed under isothermal and isobaric conditions. No data-fitting procedure is involved in the proposed method, therefore, the uncertainty as to whether deviations are due to experimental errors or to the inadequacy of the employed equation can be avoided. The authors have suggested the following equation for integration.

$$Q_b - Q_a = \int_a^b \log \gamma_1 dx_1 + \int_a^b \log \gamma_2 dx_2 + \int_a^b \log \gamma_3 dx_3 \quad (\text{at } T, P) \quad (21)$$

where a and b are any two points on the same curve. A direct method would be integrating each of the integrals graphically. In performing the integration, plots of $\log \gamma_1$ against x_1 , $\log \gamma_2$ against x_2 and $\log \gamma_3$ against x_3 are required. The points have to be in the sequence from point a to point b. The evaluation of the integrals of Equation 21 may also be carried out by means of a numerical integration. This method has the advantage that it can be applied to almost any set of data without using any graphical procedure, provided that the experimental points are reasonably spaced. Experimental data over the entire concentration range may be conveniently divided into several small sets and the thermodynamic consistency can be tested on each of them. In doing so, the less reliable region may be easily spotted. If one of the experimental points is much in error in a set of data, it may be singled out by successively including points, one by one, in a set.

EXPERIMENTAL DETAILS

Materials and Properties

The chemicals used in this investigation were n-hexane, ethyl alcohol and benzene. They were not purified further. When these compounds were run separately through the Vapor-Fractionator, no small peaks appeared. This indicated the purity of the chemicals. The purity of the chemicals is listed below.

(1) n-Hexane. n-Hexane (Matheson, Coleman and Bell) had a boiling point range of 68° to 69°C and was spectro quality solvent grade. The refractive index at 25°C was 1.3722 compared with a literature value (24) of 1.37226. The normal boiling point was 68.61°C compared with a literature value (24) of 68.74°C.

(2) Ethyl Alcohol. Ethyl alcohol (Canadian Industrial Alcohols and Chemicals Ltd.) was absolute grade. The refractive index at 25°C was 1.3591 compared with a literature value (25) of 1.35914. The normal boiling was 78.24°C compared with a literature value (25) of 78.33°C.

(3) Benzene. Benzene (Matheson, Coleman and Bell) was spectro quality reagent. The refractive index at 25°C was 1.4977 compared with a literature value (25) of 1.49790. The normal boiling point was 79.95°C compared with a literature value (25) of 80.103.

Description of Equipment

(1) Equilibrium Still. There are six main methods for determination of vapor-liquid equilibria: recirculation, static, dynamic flow, dew

and bubble point, differential distillation and continuous distillation methods.

Details of these methods and the advantages and disadvantages of each are discussed by Robinson and Gilliland (26). After a careful study of the performance of each type, a Fowler-Norris still of Gillespie type (27) was chosen. However, further modifications were necessary to improve the operation of the still. Figure 27 shows the equilibrium still used for this study. For the sake of clarity, the insulation, electrical windings, and supports were omitted from Figure 27. The capacity of charge of the still was about 170 mls. The modifications had the following features:

(a) In order to obtain better measurement of equilibrium temperature, a vacuum-sealed, double-jacketed glass thermowell was used as the hot junction of the thermocouple.

(b) Teflon plug-valves were used instead of glass stopcocks for permitting the elimination of all stopcock grease and any possible contamination.

(c) To ensure mixing of liquid and vapor condensate in the receiver, a double-jacketed tube was used instead of simple tubing.

(d) The interval heater is placed at the bottom of the boiler instead of at the top, as in the original design. This would eliminate any possible leakage of liquid or forming of air bubbles around the opening.

(2) Accessory Equipment with Still. The accessories were classified into two main parts, namely, temperature and pressure measurements.

Temperatures were measured by copper-constantan thermocouple inserted into the thermowell of the equilibrium chamber of the still and were believed to be accurate within $\pm 0.05^{\circ}\text{C}$. A micro-step potentiometer of type 442h8 manufactured by Cambridge Instrument Co. Ltd., England, in conjunction with the accessories mentioned below, was used to measure the thermocouple e.m.f. The accessories were: (a) A 2-volt battery and a 4-volt battery (lead acid type); (b) A galvanometer, type 4500/5R4 (Tinsley Instrument), and (c) Type 4305 saturated standard cell (Tinsley Instrument).

For isobaric operations, pressure in the still was measured by means of a barometer at atmospheric pressure and corrected to 760 mm. Hg. For isothermal operations, the desired temperature of 55°C was obtained and regulated by a Cartesian manostat of Type 7A (28) incorporated with a vacuum pump and surge reservoir. The pressure was read from a glass manometer.

(3) Equipment for Quantitative Analysis of Sample. Two main apparatus were employed for sample analysis. They were vapor-fractometer and refractometer.

(a) Chromatograph: A Perkin-Elmer Vapor Fractometer was employed to analyze samples. Two 2-meter, 1/4 inch columns packed with Perkin-Elmer's Type R packing material were used to affect the separation of the components. The separating agent or fixed phase in Column R

was polypropylene glycol which was mixed with a new form of diatomaceous earth that had been powdered into fine granules. Micro-Dipper sample introduction system was used for injection of samples. A L and H, 0-10 mv., Type G Speedomax recorder was used incorporated with the Vapor Fractometer.

(b) Refractometer: The refractometer used in this work was the Abbe refractometer (Bausch and Lomb Optical Co.).

Experimental Procedure

(1) Binary systems of n-hexane-benzene and ethyl alcohol-benzene.

(a) Planning of experiment:

In order to obtain reasonable composition range of vapor-liquid equilibrium data with reduced experiment for a system, predetermined compositions were desired before starting each run. The procedure was carried out by adding a known amount of one component to another.

(b) Determination of vapor-liquid equilibrium data:

(i) Charging the assembly:

Before starting the experiment, the charging of the still was necessary. The reboiler, liquid sample chamber and vapor condensate chamber were charged with solution to the appropriate level. The heater in the reboiler should always be fully immersed in liquid before starting of heating. Electrical tape was wound evenly outside the reboiler. The heat input to the heater and electrical tape was controlled separately by powerstat.

(ii) Arrangement of apparatus:

For atmospheric operation, a drying tube filled with silica gel was placed on the top of the vapor condenser line to prevent moisture from getting into the system. For isothermal operation, a vacuum system was connected to the vapor condenser line. When vacuum was in operation, the apparatus was arranged in the following manner: vacuum pump connected to a surge tank, from the surge tank to

the upper arm of the Cartesian manostat, the lower arm of the manostat connected to another surge tank to ensure cabling effect, from it to a 3-way joint, one way of the joint connected to the still, the other way directed to another 3-way joint from which one way connected to the manometer and the other way to the vent. The vent line was closed when vacuum was in operation.

(iii) Temperature measurement:

Temperature was measured by means of a micro-step potentiometer of Cambridge Instrument Co. Ltd. in conjunction with copper constantan thermocouples. The thermocouples were calibrated in a stirred bath by comparison with a standard resistance thermometer. The reference junctions were held at 0°C. The uncertainty of calibration was 0.02°C. The calibration curve is shown in Figure 26 and listed in Table 10. The thermocouples were placed in the thermowell in which some silicone oil 704 of Dow Corning Silicone Ltd. was provided to ensure fast response of the thermocouples to temperature. Before taking any reading, the potentiometer was standardized with standard cell.

(iv) Duration of run:

The still was allowed to operate for approximately 3 hours before samples were drawn. Constant still temperature was also a criterion for equilibrium state. Prior to sampling, preliminary samples were taken to flush the lines. Sample receivers were placed in ice bath to minimise evaporation losses during sampling.

Same solution was used for the determination of vapor-liquid equilibrium data at isobaric and isothermal conditions. New desired solution was then prepared accordingly.

(c) Analytical method:

In a case where a sufficient difference in the refractive index of the two components existed, analysis of the mixtures was made with an Abbe refractometer. Since the refractive index difference between pure n-hexane and pure benzene is 0.1256 and between pure ethanol and pure benzene is 0.1389, the compositions can be measured to better than ± 0.1 of 1 mole %. However, the refractive index difference between pure n-hexane and pure ethanol is 0.0132, the sensitivity of determining the composition of that system is much reduced. It was therefore concluded that refractive index method was employed to analyze the systems of n-hexane-benzene and ethyl alcohol-benzene. Gas chromatograph method was employed to analyze the binary system of n-hexane-ethanol.

Prior to the determination of the composition of the mixture by means of the Abbe refractometer, a calibration for the refractive index-composition of the system under studied was carried out by observation of the refractive indices of known composition of mixture. The known composition of the mixture was determined analytically by weighing samples individually with an analytical balance. The refractive indices were observed at 25°C. Table 11 shows the composition-refractive indices of the calibration and Figure 29 is the calibration plot for the

system n-hexane-benzene. Table 12 shows the composition-refractive indices of the calibration and Figure 30 is the calibration plot for the system ethyl alcohol-benzene.

The unknown samples were analyzed in the same manner by means of the refractive index method. The refractometer was kept at 25°C by running through water which was regulated by constant temperature device. Prior to any determination, the refractometer should be standardized by a test piece with contact liquid 1-bromonaphthalene provided with the instrument.

(2) Ternary system and the binary system of n-hexane-ethyl alcohol.

(a) Planning of experiments:

The planning of experiment for binary system of n-hexane-ethanol was exactly the same as that described previously for the other two binaries. For the ternary system, a procedure similar to that of Severns et al (29) was followed for taking ternary vapor-liquid equilibrium data which would reduce appreciably the number of experiments required to investigate a system adequately. Severns et al (29) proposed thirteen strategic compositions to be investigated. The author extended the original 13 compositions to 43 compositions to cover a much complete concentration of the ternary system. In order to obtain the planned concentration as close as possible, a method to prepare the desired concentration was necessary. It was carried out by adding a known amount of one component to the mixture.

(b) Determination of vapor-liquid equilibrium data.

The vapor-liquid equilibrium data were obtained

using the same apparatus and experimental techniques as for the binaries described previously.

(c) Analytical method:

The ternary system and the binary system of n-hexane-ethyl alcohol were analyzed by means of gas chromatograph.

The instrument used for the technique of gas chromatograph was a Perkin-Elmer Vapor-Fractometer, Model 154-C. Before a complete analysis of a sample could be carried out satisfactorily, instrument conditions must be determined which would allow complete separation of all components, with a maximum accuracy and speed of measurement. Therefore, various operating conditions were employed by injecting the samples. Finally, the operating variables were chosen as follows. Two 2-meter x 1/4 inch Perkin-Elmer B-type column filled with polypropylene glycol packing was used to separate the three components. The fractometer was operated at 100°C, 25 psig column pressure and a bridge voltage of 8 volts. Under these conditions and a helium flow rate of 152 c.c. per minute, one complete analysis of a sample of the ternary system was about 15 minutes. The peaks were well spaced and completely separated. Operating conditions for gas chromatographic analysis are listed in Table 9. The retention time for the three components in the column was in the following order, starting from shortest: n-hexane, ethanol and benzene. The peak area of each component was recorded in a recorder and was measured with a planimeter.

Calibration of the fractometer was found to be necessary to convert peak area fractions to mole fractions because the peak areas and mole fractions of the components are not directly proportional. Numerous known samples of binary system of n-hexane-ethanol and ternary system were separated for calibration purpose. The calibration method was similar to that of Wagner and Weber (30). Table 13 and Figure 31 show the calibration of the binary system of n-hexane-ethanol. From Figure 31, the following relation is obtained:

$$\frac{\left(\frac{\text{Ethanol}}{\text{n-Hexane}}\right) \text{ mole fraction}}{\left(\frac{\text{Ethanol}}{\text{n-Hexane}}\right) \text{ area}} = 1.5625$$

Table 14 and Figures 32, 33 and 34 show the calibration of the ternary system. From Figure 32, the following relation is obtained:

$$\frac{\left(\frac{\text{Ethanol}}{\text{Benzene}}\right) \text{ mole fraction}}{\left(\frac{\text{Ethanol}}{\text{Benzene}}\right) \text{ area}} = 1.4667$$

From Figure 33, the following relation is obtained:

$$\frac{\left(\frac{\text{Benzene}}{\text{n-Hexane}}\right) \text{ mole fraction}}{\left(\frac{\text{Benzene}}{\text{n-Hexane}}\right) \text{ area}} = 1.2085$$

From Figure 34, the following relation is obtained:

$$\frac{\left(\frac{\text{Ethanol}}{\text{n-Hexane}}\right) \text{ mole fraction}}{\left(\frac{\text{Ethanol}}{\text{n-Hexane}}\right) \text{ area}} = 1.8000$$

These constants and the fact that the sum of the mole fractions of any sample must be one were used to calculate the compositions.

RESULTS

The experimental vapor-liquid equilibria data for the binary systems are presented from Table 1 to Table 6, and from Figure 1 to Figure 18. The data of the ternary systems are presented in Table 7 and Table 8, and from Figure 19 to Figure 26.

TABLE I

Vapor-Liquid Equilibrium Data for n-Heptane(1)-Ethyl Alcohol(2) system at 760 mm. Hg.

Temp., °C.	Liquid Mole Fraction X ₁	Vapor mole Fraction Y ₁	Activity Coefficient				Log Y	Log $\frac{Y_1}{X_1}$
			γ ₁	γ ₂	log γ ₁	log γ ₂		
63.00	0.9850	0.8350	1.019	20.821	0.0080	1.3185	-1.3105	
58.99	0.8750	0.6940	1.076	6.020	0.0319	0.7796	-0.7477	
58.25	0.7080	0.6100	1.332	2.644	0.1245	0.4223	-0.2978	
58.24	0.5920	0.6460	1.568	1.991	0.1953	0.2991	-0.1038	
58.24	0.5050	0.6100	1.784	1.702	0.2514	0.2309	+0.0205	
58.53	0.4400	0.6280	1.990	1.534	0.2989	0.1858	0.1131	
58.94	0.3070	0.6150	2.755	1.260	0.4401	0.1004	0.3394	
59.97	0.2190	0.5850	3.546	1.151	0.5500	0.0611	0.4889	
62.90	0.1455	0.5250	4.496	1.105	0.6528	0.0433	0.6095	
66.07	0.0831	0.4110	5.369	1.066	0.7299	0.0278	0.7021	
73.23	0.0277	0.1750	8.605	1.031	0.9348	0.0132	0.9216	

TABLE 2

Vapor-Liquid Equilibrium Data for n-hexane (1)-ethyl Alcohol(2) System at 55°C.

Temp., °C	Total Pressure mm. Hg.	Liquid Mole Fraction x_1	Vapor Mole Fraction y_1	Activity Coefficient		Log Y		$\log \frac{y_1}{y_2}$
				γ_1	γ_2	$\log \gamma_1$	$\log \gamma_2$	
55.10	583.0	0.939	0.835	1.015	31.110	0.0064	1.4929	-1.4865
54.80	651.9	0.920	0.704	1.068	7.048	0.0286	0.8181	-0.3195
55.04	674.6	0.724	0.650	1.251	3.052	0.0972	0.4846	-0.3874
55.00	676.1	0.567	0.629	1.552	2.065	0.1909	0.3150	-0.1241
55.00	674.5	0.498	0.621	1.740	1.819	0.2405	0.2598	-0.0193
55.12	673.2	0.409	0.609	2.065	1.583	0.3150	0.1995	+0.1153
54.97	660.3	0.332	0.595	2.452	1.433	0.3896	0.1562	0.2334
54.98	630.0	0.219	0.560	3.336	1.269	0.5232	0.1035	0.4197
55.14	588.4	0.146	0.520	4.316	1.174	0.6351	0.0697	0.5654
55.10	491.2	0.074	0.431	5.099	1.074	0.7708	0.0311	0.7397
55.16	345.3	0.012	0.173	10.539	1.019	1.0229	0.0080	1.0149

TABLE 3

Vapor-Liquid Equilibrium Data for n-hexane(1)-Benzene(2) System at 760 mm. Hg.

Temp., °C.	Liquid mole Fraction	Vapor mole Fraction	Activity Coefficient		Log γ		$\log \frac{\gamma_2}{\gamma_1}$
			γ_1	γ_2	$\log \gamma_1$	$\log \gamma_2$	
65.82	0.877	0.885	1.067	1.241	0.0229	0.1874	0.1245
69.06	0.770	0.705	1.035	1.267	0.0149	0.0916	0.0667
69.48	0.665	0.703	1.033	1.244	0.0140	0.0940	0.0808
70.00	0.573	0.532	1.049	1.169	0.0253	0.0753	0.0500
70.68	0.479	0.566	1.113	1.124	0.0464	0.0507	0.0043
71.70	0.373	0.475	1.146	1.101	0.0592	0.0418	-0.0174
73.20	0.275	0.395	1.220	1.054	0.0764	0.0229	-0.0635
74.72	0.188	0.300	1.323	1.021	0.1232	0.0090	-0.1142
76.90	0.054	0.177	1.568	1.000	0.1953	0.0000	-0.1953

TABLE 4

Vapor-Liquid Equilibrium Data for n-Hexane(1)-Benzene(3) System at 55°C.

Temp., °C.	Total Pressure mm. Hg.	Liquid Mole Fraction x_1	Vapor Mole Fraction y_1	Activity Coefficient		Log γ		$\log \frac{y_2}{y_1}$
				γ_1	γ_3	$\log \gamma_1$	$\log \gamma_3$	
54.98	486.0	0.877	0.883	1.013	1.415	0.0055	0.1507	0.1452
54.92	485.1	0.770	0.786	1.028	1.385	0.0119	0.1415	0.1296
54.93	468.0	0.573	0.636	1.077	1.223	0.0323	0.0874	0.0551
55.16	445.2	0.375	0.489	1.195	1.106	0.0774	0.0437	-0.0337
54.88	425.0	0.2735	0.405	1.308	1.067	0.1165	0.0282	-0.0883
55.12	402.5	0.176	0.306	1.442	1.031	0.1590	0.0132	-0.1458
55.15	371.9	0.085	0.178	1.603	1.016	0.2049	0.0068	-0.1981
55.00	480.0	0.706	0.735	1.034	1.323	0.0145	0.1216	0.1071
54.92	470.5	0.6005	0.659	1.071	1.232	0.0298	0.0906	0.0608
54.82	453.0	0.495	0.581	1.120	1.170	0.0492	0.0682	0.0190
55.02	409.7	0.206	0.304	1.415	1.035	0.1507	0.0119	-0.1358
55.10	401.4	0.171	0.300	1.452	1.033	0.1620	0.0140	-0.1480
55.04	383.9	0.118	0.227	1.526	1.028	0.1835	0.0119	-0.1716
54.97	371.6	0.086	0.104	1.641	1.015	0.2166	0.0064	-0.2102

TABLE 5

Vapor-Liquid Equilibrium Data for Ethyl Alcohol(2)-Benzene(3) System at 760 mm. Hg.

Temp., °C.	Liquid Mole Fraction x ₂	Vapor Mole Fraction y ₂	Activity Coefficient			Log γ		log $\frac{y_2}{x_2}$
			γ ₂	γ ₃	γ ₂	log γ ₂	log γ ₃	
73.36	0.9188	0.7858	1.044	3.262	0.0187	0.5135	-0.1988	
70.56	0.8270	0.6525	1.000	2.721	0.0000	0.4348	-0.1348	
68.89	0.7340	0.5640	1.129	2.346	0.0526	0.3703	-0.3177	
68.25	0.6290	0.5110	1.234	1.915	0.0913	0.2821	-0.1908	
67.90	0.5230	0.4730	1.396	1.635	0.1418	0.2135	-0.0717	
67.83	0.3640	0.4220	1.782	1.348	0.2509	0.1297	0.1212	
68.17	0.2660	0.3905	2.224	1.217	0.3472	0.0852	0.2620	
69.08	0.1695	0.3475	2.989	1.118	0.4755	0.0483	0.4272	
71.75	0.0675	0.2355	4.551	1.068	0.6591	0.0286	0.6295	

TABLE 6

Vapor-Liquid Equilibrium Data for Ethyl Alcohol(2)-Benzene(3) System at 55°C.

Temp., °C.	Total Pressure mm. Hg.	Liquid Mole Fraction x_2	Vapor Mole Fraction y_2	Activity Coefficient		Logarithm of Activity Coefficient		$\log \frac{y_2}{x_2}$
				γ_2	γ_3	$\log \gamma_2$	$\log \gamma_3$	
55.05	458.8	0.9160	0.7165	3.306	0.0178	0.5193	-0.5015	
54.98	441.6	0.8300	0.6020	2.949	0.0286	0.4696	-0.4410	
54.78	437.4	0.7430	0.5230	2.503	0.0461	0.3984	-0.3523	
55.00	460.0	0.6320	0.4720	2.018	0.0453	0.3049	-0.2596	
55.08	471.0	0.5260	0.4340	1.715	0.1112	0.2342	-0.0930	
55.00	470.0	0.3670	0.3980	1.821	0.2603	0.1358	0.1245	
54.90	463.9	0.2660	0.3690	1.224	0.3636	0.0878	0.2758	
55.08	457.9	0.1590	0.3260	3.343	0.5241	0.0487	0.4754	
54.85	422.8	0.0570	0.2460	6.566	0.8373	0.0165	0.8008	

TABLE 7

Vapor-Liquid Equilibrium Data for n-Hexane(1)-Ethyl Alcohol(2)-Benzene(3) System at 760 mm. Hg.

Run	Temp. °C	Liquid Mole Fraction		Vapor Mole Fraction		Liquid Phase γ		
		n-Hexane x_1	Ethanol x_2	n-Hexane y_1	Ethanol y_2	n-Hexane γ_1	Ethanol γ_2	Benzene γ_3
1	62.01	0.9127	0.0359	0.7195	0.2062	1.0194	11.3559	1.5583
2	64.09	0.7178	0.0252	0.6506	0.1568	1.0574	11.2298	1.2618
3	67.58	0.4802	0.0151	0.5102	0.0842	1.1022	8.6611	1.2004
4	58.89	0.7258	0.2090	0.6058	0.3356	1.1496	3.6494	1.8152
5	59.29	0.7267	0.1454	0.5851	0.3189	1.0941	4.8953	1.4929
6	60.22	0.6378	0.1179	0.5187	0.3013	1.0714	5.4710	1.4196
7	61.02	0.5580	0.0916	0.4924	0.2905	1.1317	6.5514	1.1600
8	62.88	0.4444	0.0712	0.4211	0.2492	1.1433	6.6599	1.1940
9	58.96	0.6394	0.2231	0.5701	0.3210	1.2711	3.2593	1.5980
10	59.53	0.5797	0.1878	0.5200	0.3256	1.2094	3.8281	1.3117
11	61.78	0.3911	0.1435	0.3917	0.2989	1.2529	4.1603	1.2122
12	64.06	0.2965	0.0986	0.3294	0.2621	1.2900	4.8032	1.1379
13	71.40	0.1261	0.0327	0.1806	0.1291	1.3187	5.2255	1.0808
14	58.76	0.5365	0.3358	0.5222	0.3017	1.3465	2.5989	1.5268
15	59.89	0.4575	0.2685	0.4623	0.3112	1.3457	2.7617	1.3984

30.

..... continued

TABLE 7 (continued)

Run	Temp. °C	Liquid Mole Fraction		Vapor Mole Fraction		Liquid Phase γ		
		n-Hexane	Ethanol	n-Hexane	Ethanol	n-Hexane	Ethanol	Benzene
		X ₁	X ₂	Y ₁	Y ₂	Y ₁	Y ₂	Y ₃
16	61.07	0.3784	0.2129	0.4023	0.3202	1.3616	3.0942	1.2697
17	64.86	0.2203	0.1131	0.2731	0.2932	1.4026	4.5250	1.0671
18	58.49	0.4247	0.5427	0.5698	0.4029	1.9726	1.7181	1.7271
19	58.72	0.3968	0.5143	0.5376	0.3909	1.8765	1.7410	1.6362
20	59.23	0.3723	0.4189	0.5107	0.3688	1.8677	1.6852	1.7462
21	59.93	0.3223	0.4460	0.4230	0.3710	1.7456	1.8109	1.7315
22	61.13	0.2021	0.3692	0.3351	0.3804	1.5181	2.1237	1.5176
23	62.48	0.2139	0.2903	0.2939	0.3467	1.6794	2.3264	1.2031
24	63.99	0.1770	0.2195	0.2355	0.3451	1.5483	2.8497	1.1744
25	66.55	0.1128	0.1430	0.1675	0.2987	1.5915	3.3906	1.1103
26	71.89	0.0346	0.0467	0.0789	0.1745	2.0678	4.8461	1.0512
27	59.68	0.2666	0.6378	0.4651	0.4128	2.2400	1.4196	2.5096
28	60.97	0.2211	0.5236	0.3639	0.3929	2.0868	1.5539	1.8072
29	62.26	0.1824	0.4333	0.2902	0.3704	1.9591	1.6718	1.5842
30	65.29	0.1060	0.2293	0.1603	0.3512	1.6874	2.6246	1.1866

TABLE 7 (continued)

Run	Temp. °C	Liquid Mole Fraction		Vapor Mole Fraction		Liquid Phase γ		
		Ethanol		Ethanol		n-Heptane	Ethanol	Benzene
		x ₁	x ₂	y ₁	y ₂			
31	60.73	0.1980	0.6901	0.4265	0.4361	2.7339	1.3223	2.3169
32	61.44	0.1955	0.6083	0.3596	0.4137	2.3268	1.3790	2.1345
33	63.40	0.1263	0.4656	0.2127	0.4155	1.9930	1.6538	1.5653
34	64.48	0.0958	0.3459	0.1564	0.3891	1.8703	1.9961	1.3528
35	63.57	0.0428	0.1462	0.0573	0.3133	1.3459	3.1928	1.1231
36	62.93	0.1147	0.3156	0.3640	0.5197	3.8223	1.2101	2.9139
37	63.76	0.1340	0.7325	0.3037	0.5085	2.6416	1.2710	2.4107
38	63.84	0.0837	0.7232	0.2468	0.5131	3.4487	1.2946	2.1103
39	64.19	0.0718	0.6424	0.1872	0.4679	3.0130	1.3090	2.0244
40	65.17	0.0603	0.5130	0.1245	0.4445	2.3130	1.4922	1.6370
41	70.02	0.0353	0.9150	0.1608	0.7296	4.3762	1.1175	3.0397
42	67.32	0.0294	0.7641	0.1010	0.5763	3.5933	1.1846	2.3550
43	66.82	0.0230	0.5269	0.0461	0.4040	2.1138	1.4738	1.6052

TABLE 8

Vapor-Liquid Equilibrium Data for n-Heptane(1)-Ethyl Alcohol(2)-Benzene(3) System at 55°C.

Run	Temp., °C.	Total Pressure mm. Hg.	Liquid Mole Fraction		Vapor Mole Fraction		Activity Coefficient		
			Heptane x ₁	Ethanol x ₂	Heptane y ₁	Ethanol y ₂	γ ₁	γ ₂	γ ₃
1	55.06	601.1	0.8950	0.0123	0.7367	0.2187	1.022	11.080	1.303
2	55.10	562.7	0.7382	0.0256	0.6566	0.1563	1.032	12.222	1.358
3	55.25	503.2	0.4727	0.0154	0.5227	0.0921	1.141	10.630	1.148
4	54.73	657.5	0.7577	0.1856	0.6307	0.3235	1.143	4.146	1.660
5	54.92	610.0	0.7184	0.1451	0.6090	0.3003	1.140	4.810	1.322
6	55.00	632.9	0.6254	0.1132	0.5320	0.2950	1.114	4.658	1.447
7	55.16	621.9	0.5865	0.1173	0.4803	0.2800	1.048	5.266	1.530
8	54.95	500.7	0.4365	0.0785	0.4155	0.2720	1.146	7.207	1.146
9	55.00	666.5	0.6373	0.2327	0.5935	0.3228	1.265	3.254	1.290
10	54.95	610.0	0.5612	0.2132	0.5136	0.3246	1.214	3.490	1.407
11	55.05	599.3	0.4003	0.1378	0.4184	0.2728	1.294	4.230	1.223
12	55.00	554.1	0.3138	0.0994	0.3229	0.2528	1.180	5.035	1.225
13	55.00	438.9	0.1175	0.0111	0.2051	0.1433	1.585	15.936	1.007
14	55.13	663.6	0.5456	0.3376	0.5577	0.3464	1.397	2.419	1.661

..... continued

14

TABLE 9 (continued)

Run	Temp. °C	Total Pressure mm. Hg.	Liquid Mole Fraction			Vapor Mole Fraction			Activity Coefficient		
			Hexane x ₁	Ethanol x ₂	Heptane x ₃	Hexane y ₁	Ethanol y ₂	Heptane y ₃	γ_1	γ_2	γ_3
15	55.00	637.5	0.4598	0.2712	0.4762	0.3300	0.3300	1.366	2.772	1.405	
16	54.98	609.7	0.3807	0.2074	0.4158	0.3031	0.3031	1.379	3.157	1.274	
17	55.05	538.2	0.2234	0.1022	0.2695	0.2664	0.2664	1.341	4.905	1.022	
18	55.16	669.9	0.4434	0.5348	0.5944	0.3011	0.3011	1.348	1.693	2.237	
19	54.98	661.4	0.3957	0.5279	0.5531	0.3673	0.3673	1.914	1.646	2.109	
20	55.22	646.4	0.3353	0.4467	0.4995	0.3407	0.3407	1.977	1.601	1.759	
21	55.10	629.9	0.2992	0.4611	0.4367	0.3493	0.3493	1.902	1.700	1.709	
22	55.00	609.0	0.2715	0.3715	0.3671	0.3489	0.3489	1.706	2.034	1.465	
23	55.20	579.9	0.2268	0.2806	0.2304	0.3745	0.3745	1.211	2.741	1.413	
24	54.85	543.5	0.1633	0.2007	0.2369	0.3151	0.3151	1.606	3.099	1.197	
25	55.10	506.4	0.1046	0.1192	0.1698	0.3056	0.3056	1.695	4.619	1.043	
26	54.95	411.8	0.0457	0.0378	0.0809	0.1486	0.1486	1.511	7.359	1.006	

..... continued

TABLE 8 (continued)

Run	Temp. °C.	Total Pressure mm. Hg.	Liquid Mole Fraction			Vapor Mole Fraction			Activity Coefficient		
			Hexane X ₁	Ethanol X ₂	Hexane Y ₁	Ethanol Y ₂	Hexane γ ₁	Ethanol γ ₂	Hexane γ ₁	Ethanol γ ₂	γ ₂
27	54.94	635.7	0.2531	0.6329	0.4653	0.4023	0.424	1.450	2.253		
28	55.14	612.0	0.2244	0.5229	0.3783	0.3733	2.125	1.552	1.935		
29	55.16	595.0	0.1930	0.4338	0.3098	0.3712	2.059	1.776	1.430		
30	55.16	521.5	0.1073	0.2342	0.1636	0.3376	1.644	2.690	1.207		
31	55.15	618.7	0.1755	0.6944	0.1349	0.4290	2.833	1.356	2.330		
32	55.05	601.0	0.1735	0.6302	0.3713	0.4755	2.690	1.379	2.083		
33	55.05	558.5	0.1160	0.4594	0.2311	0.3952	2.368	1.669	1.513		
34	55.08	536.0	0.0990	0.3445	0.1553	0.3641	1.945	2.11	1.354		
35	55.10	471.0	0.0393	0.1105	0.0633	0.3062	1.667	3.652	1.095		
36	55.05	560.1	0.0745	0.4425	0.3711	0.437	1.591	1.036	5.137		
37	55.16	518.4	0.0669	0.7925	0.3377	0.4766	1.305	1.170	2.571		

..... continued

TABLE 8 (continued)

Run	Temp. °C.	Total Pressure mm. Hg.	Liquid Mole Fraction		Vapor Mole Fraction		Activity Coefficient		
			Hexane x ₁	Ethanol x ₂	Hexane y ₁	Ethanol y ₂	γ ₁	γ ₂	γ ₃
38	54.73	541.4	0.0333	0.7263	0.2696	0.4437	3.660	1.197	2.518
39	55.00	540.9	0.0736	0.6402	0.2006	0.4413	3.050	1.332	2.069
40	54.98	517.8	0.0585	0.5263	0.1452	0.3992	2.661	1.405	1.740
41	55.10	406.4	0.0300	0.9283	0.1983	0.6768	5.539	1.054	3.679
42	54.96	470.5	0.0275	0.7594	0.1241	0.5254	4.400	1.165	2.366
43	54.80	493.5	0.0230	0.5480	0.0605	0.4473	2.651	1.425	1.710

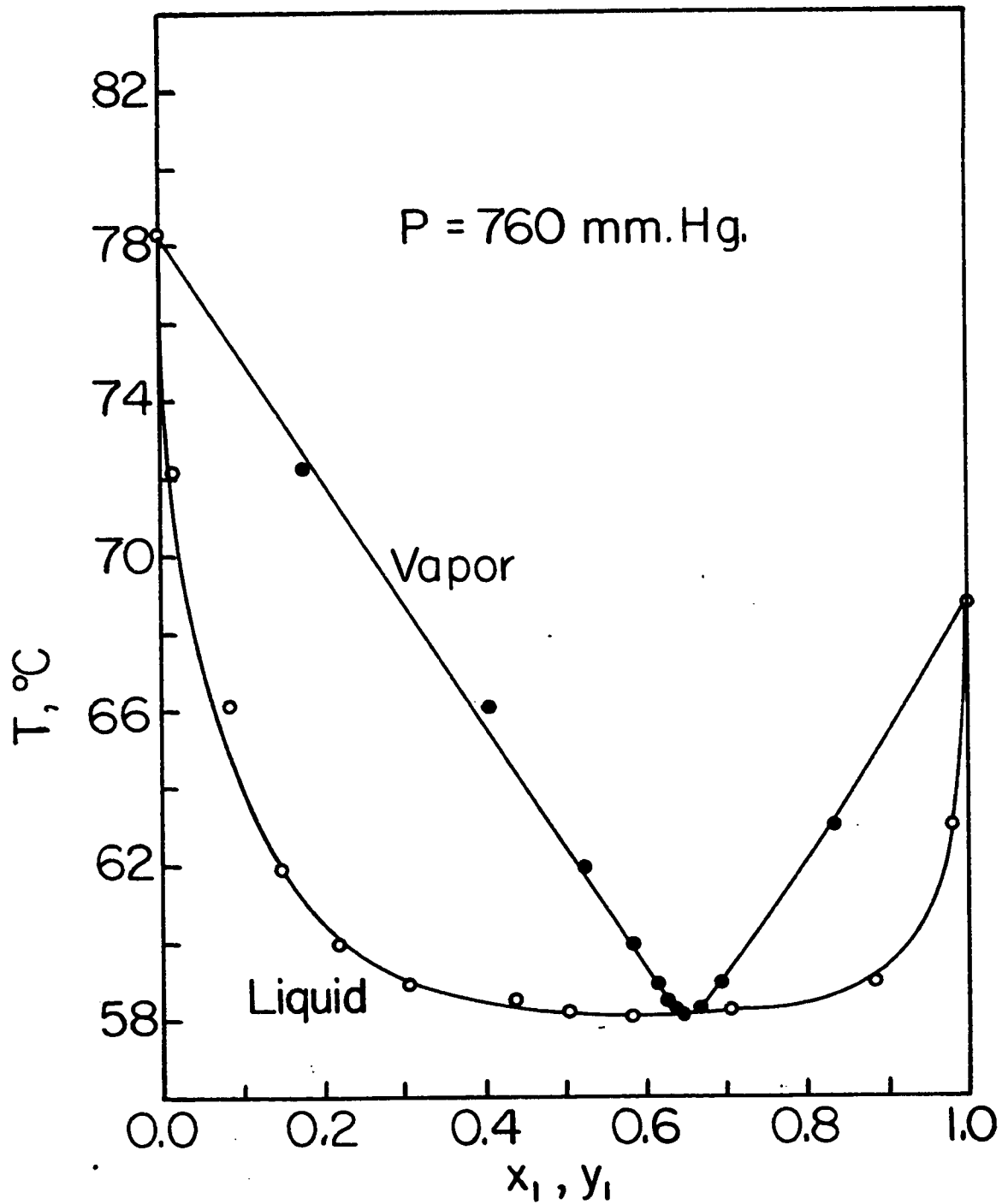


Fig. 1. Temperature vs. composition diagram for n-hexane(1)-ethyl alcohol(2) system at 760 mm. Hg.

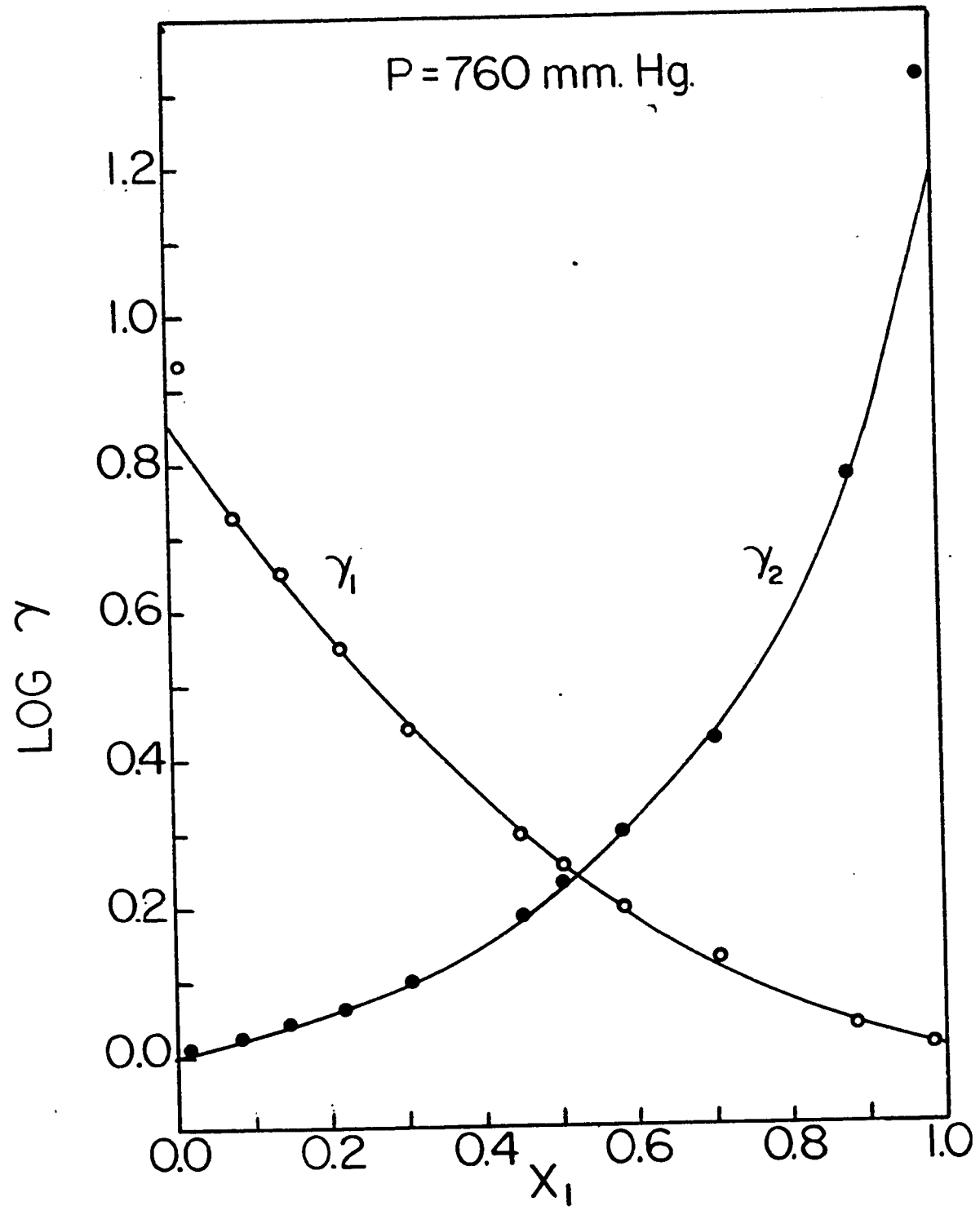


Fig. 2. Logarithmic activity coefficients vs. composition for n-hexane(1)-ethyl alcohol(2) system at 760 mm.Hg.

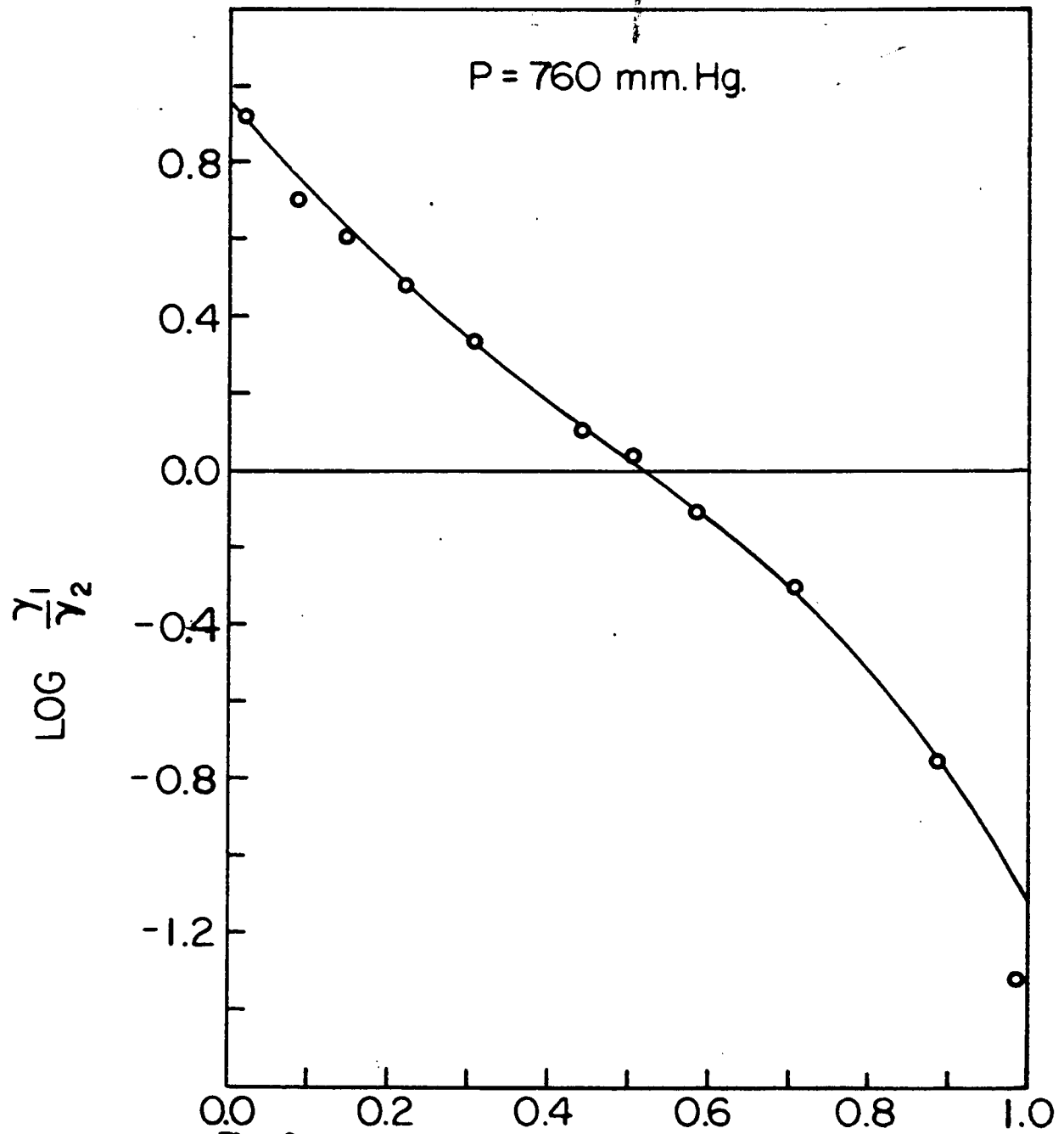


Fig. 3. Logarithm of ratios of γ_1/γ_2 vs. x_1 for n-hexane(1)-ethyl alcohol(2) system at 760 mm. Hg.

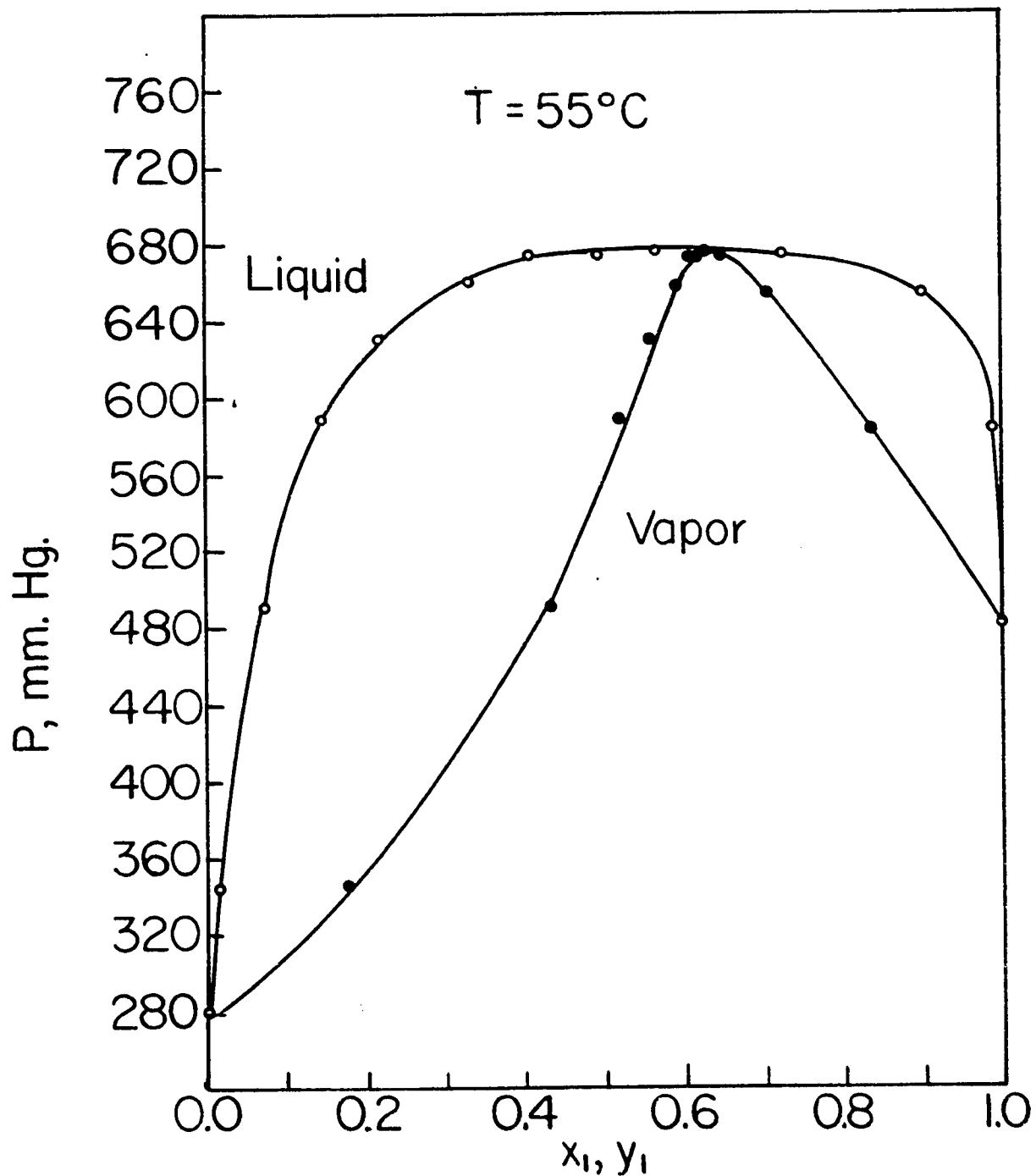


Fig. 4. Total pressure vs. composition diagram for n-hexane(1)-ethyl alcohol(2) system at 55°C .

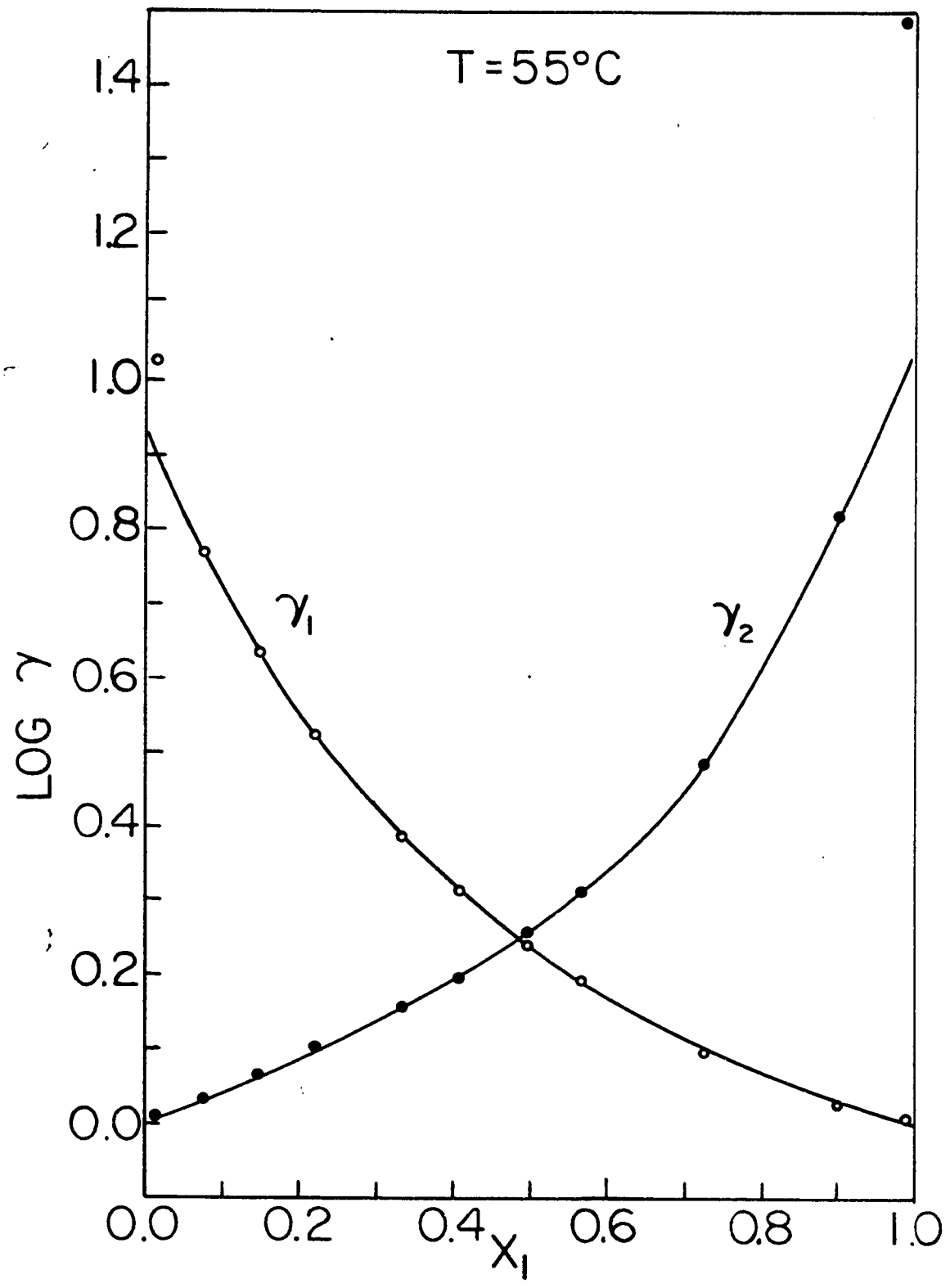


Fig. 5. Logarithmic activity coefficients vs. composition for n-hexane(1)-ethyl alcohol(2) system at 55°C.

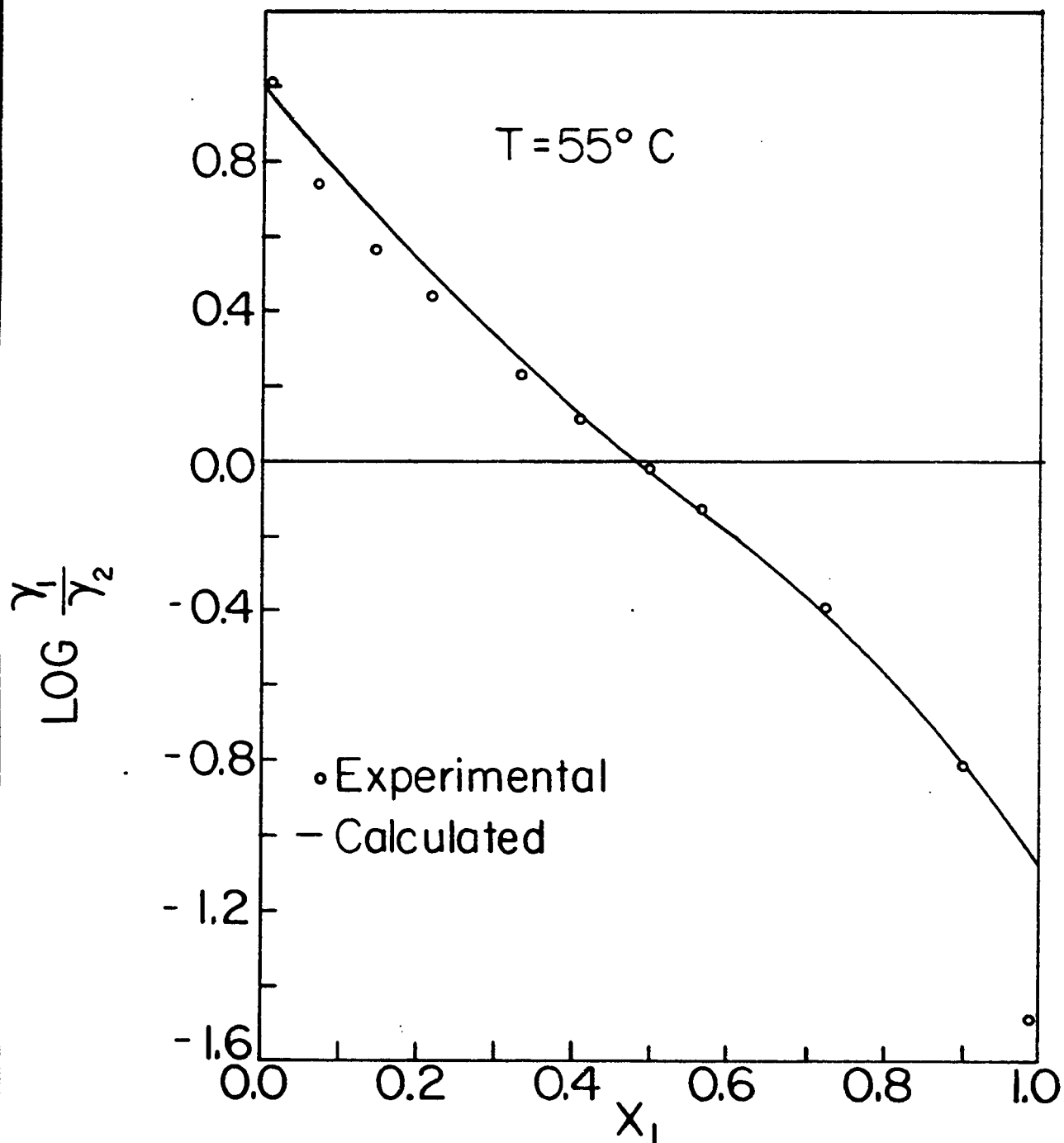


Fig. 6. Logarithm of ratios of γ_1/γ_2 vs. x_1 plot for n-hexane(1)-ethyl alcohol(2) system at 55°C .

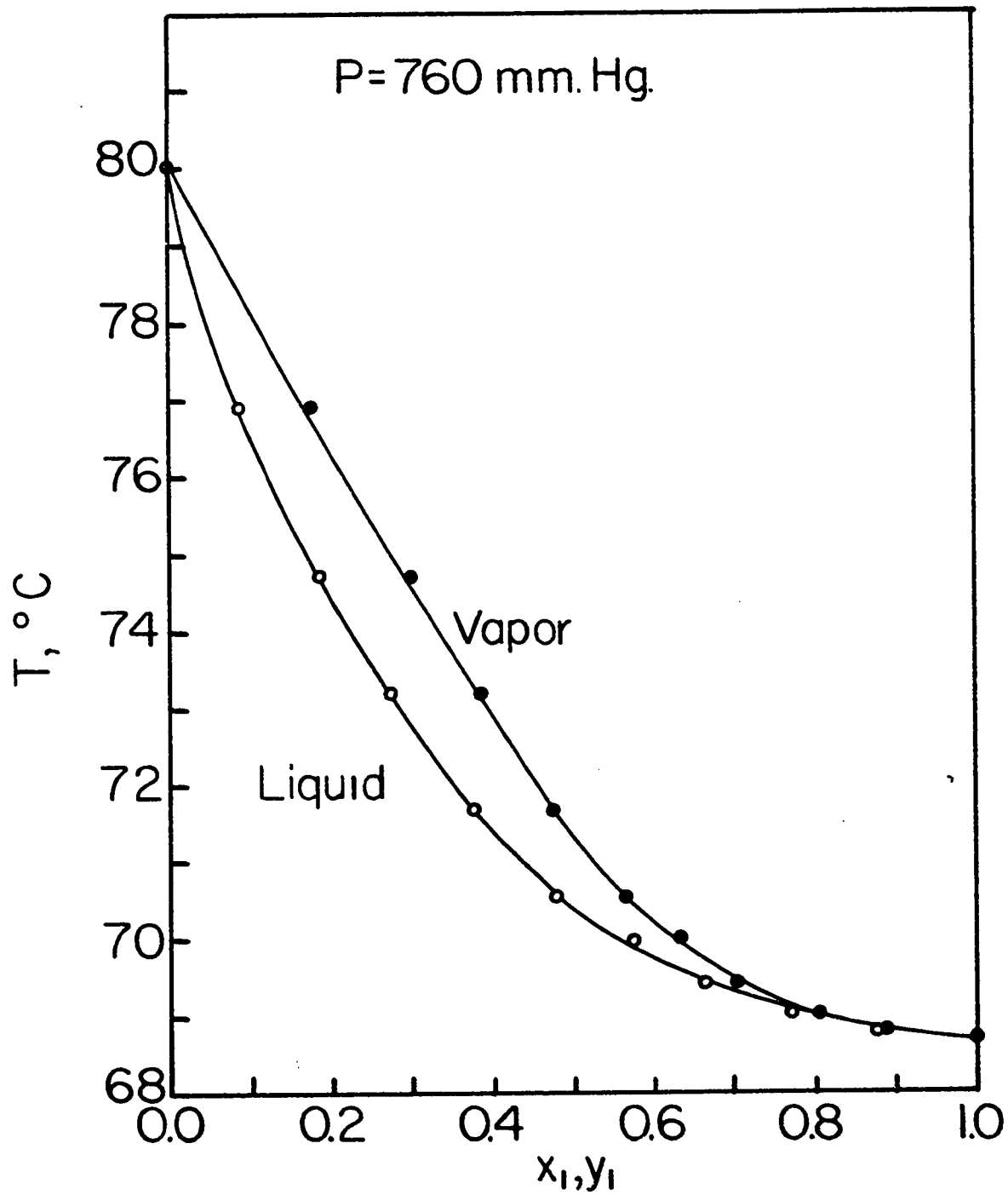


Fig. 7. Temperature vs. composition diagram for n-hexane(1)-benzene(3) system at 760 mm. Hg.

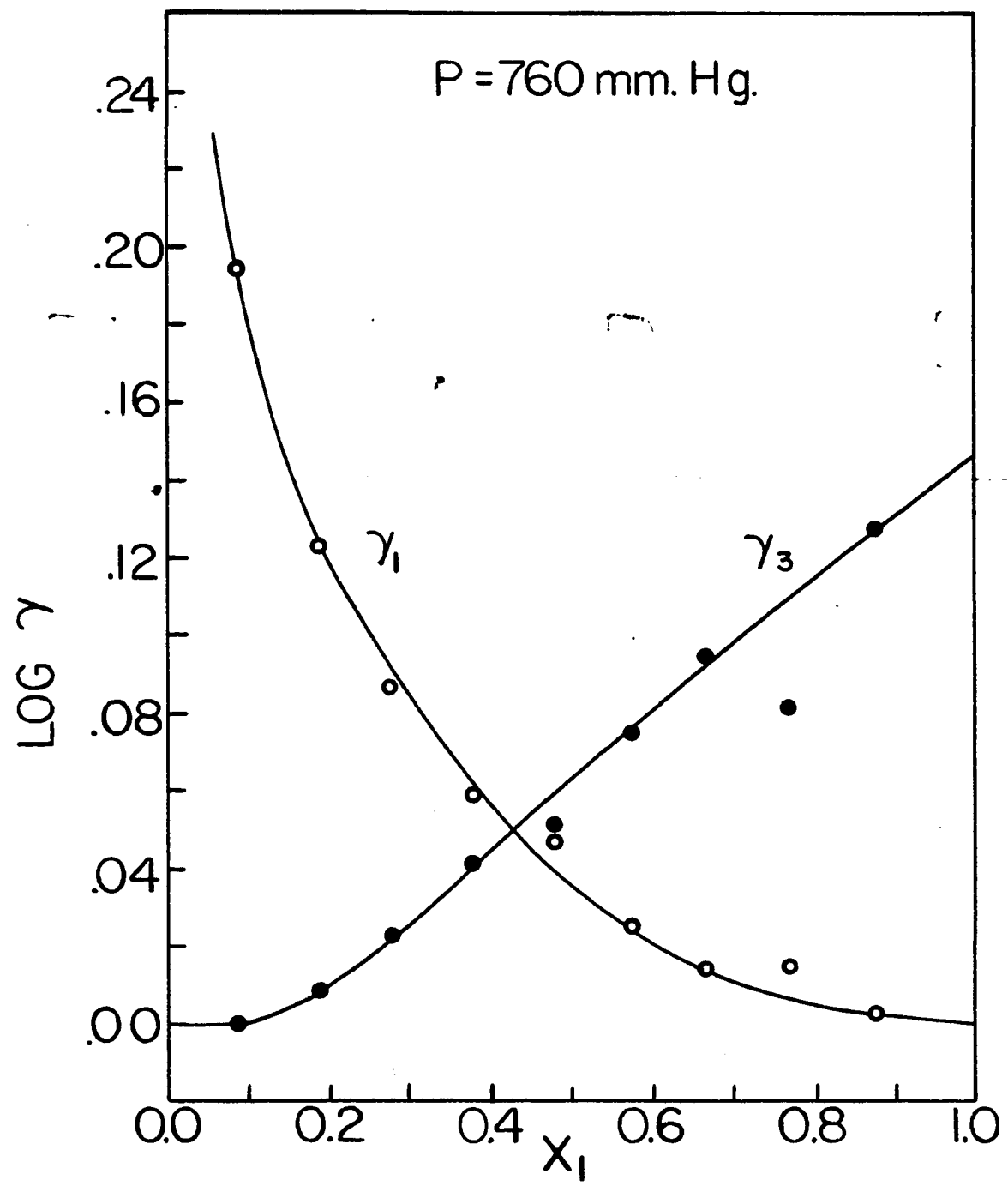


Fig. 8. Logarithmic activity coefficients vs. composition for n-hexane(1)-benzene(3) system at 760 mm. Hg.

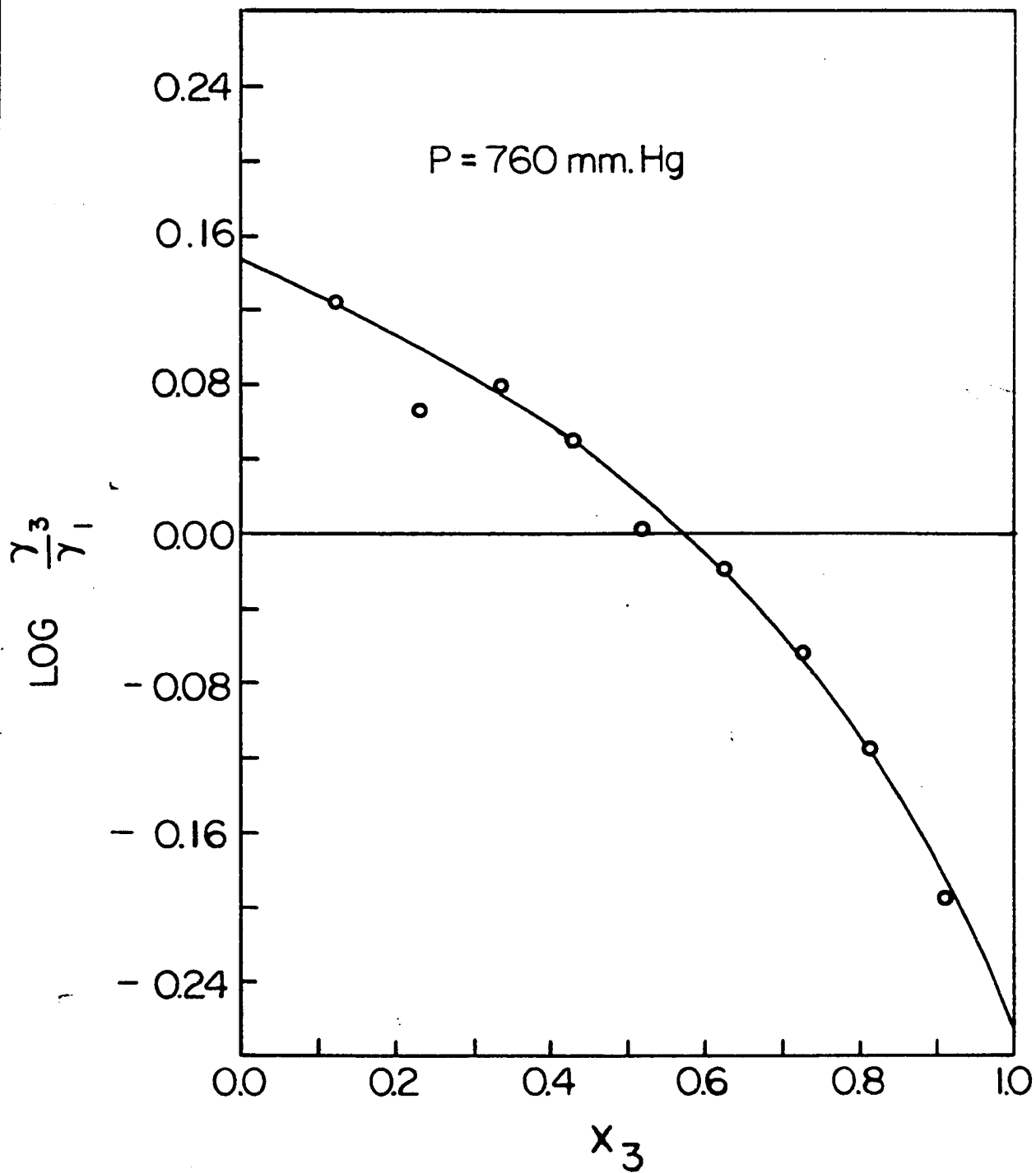


Fig. 9. Logarithm of ratios of γ_3/γ_1 vs. x_3 for n-hexane(1)-benzene(3) system at 760 mm. Hg.

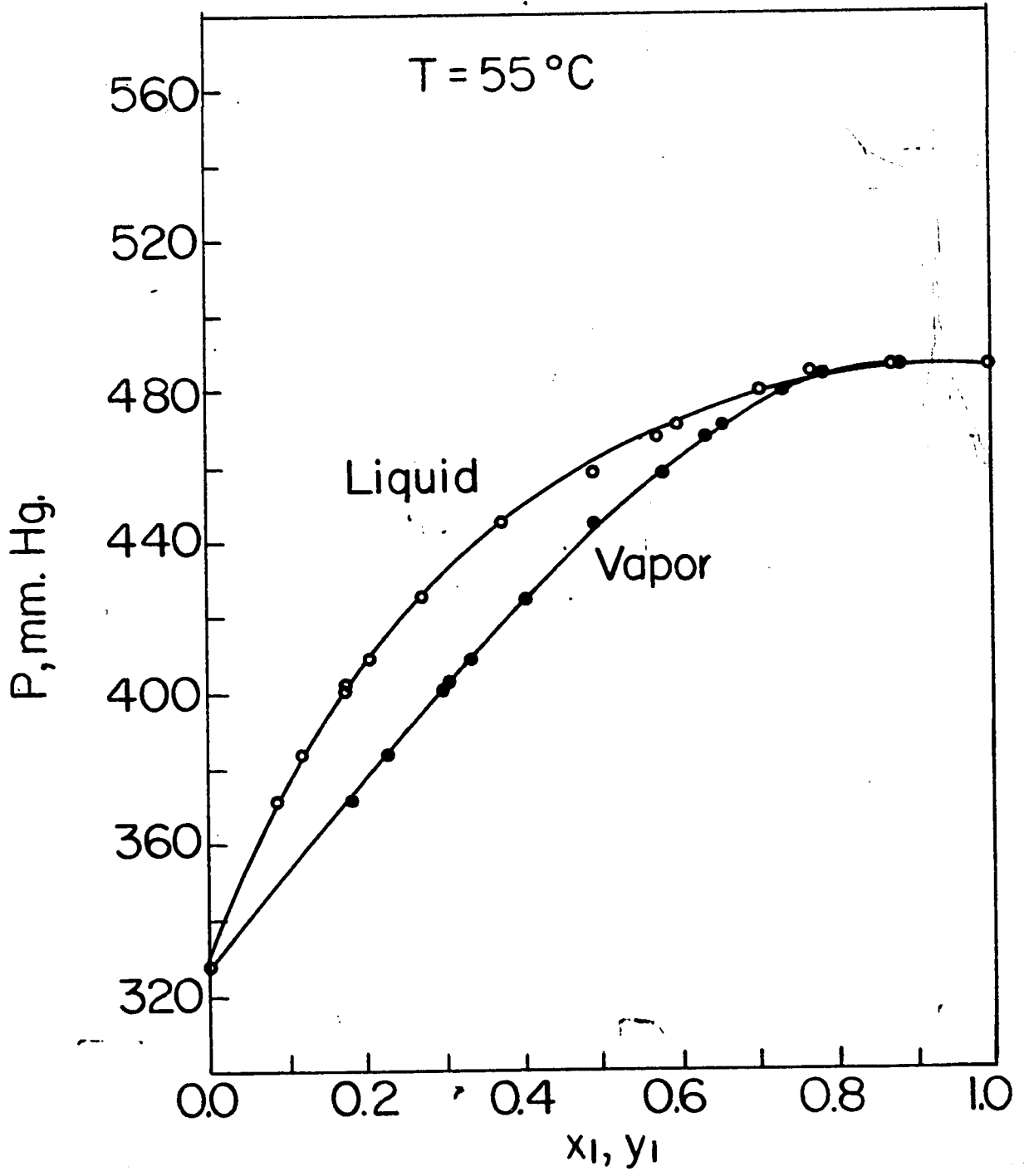


Fig. 10. Total pressure vs. composition diagram for n-hexane(1)-benzene(2) system at 55°C.

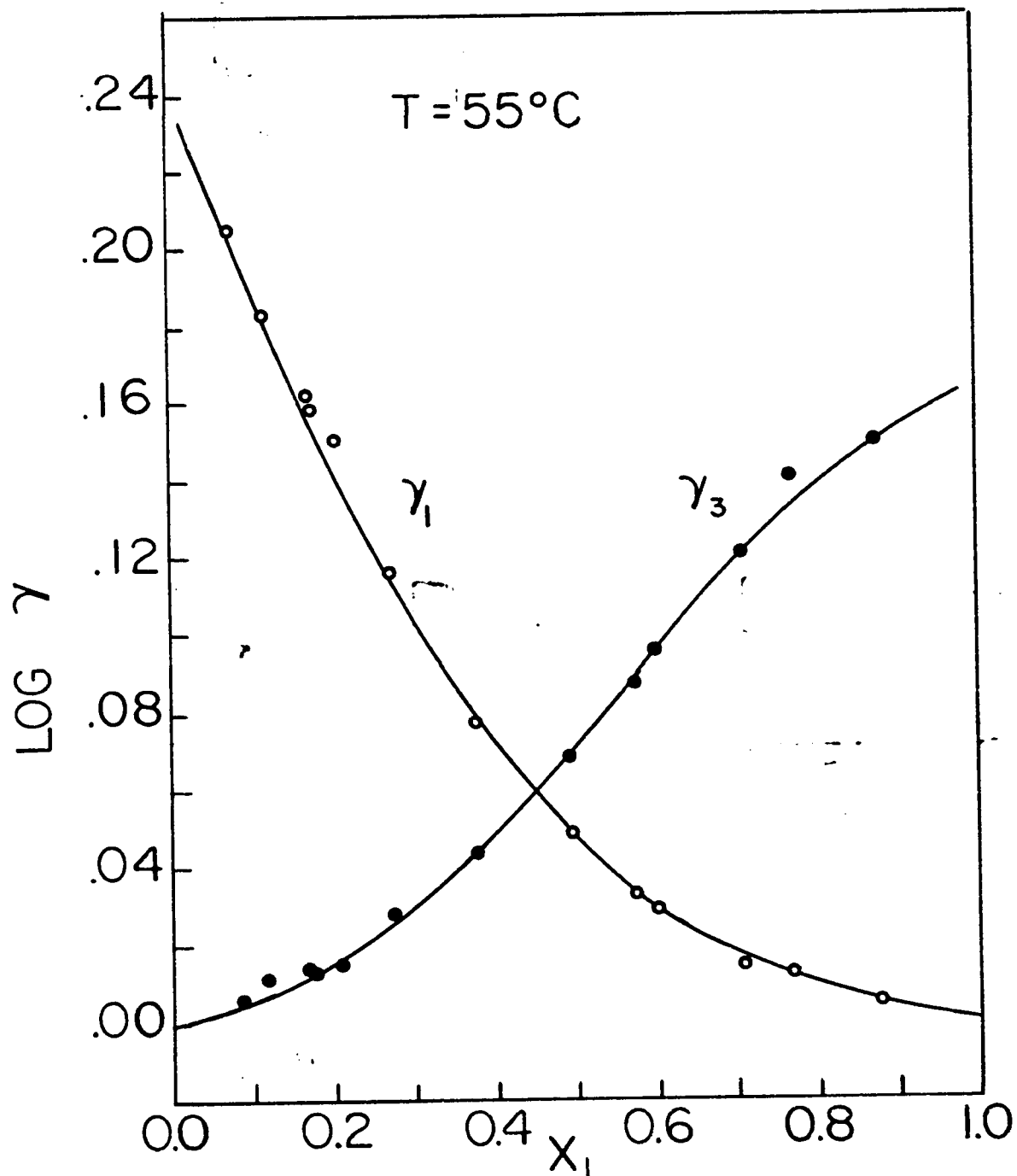


Fig. 11. Logarithmic activity coefficients vs. composition for n-hexane(1)-benzene(3) system at 55°C .

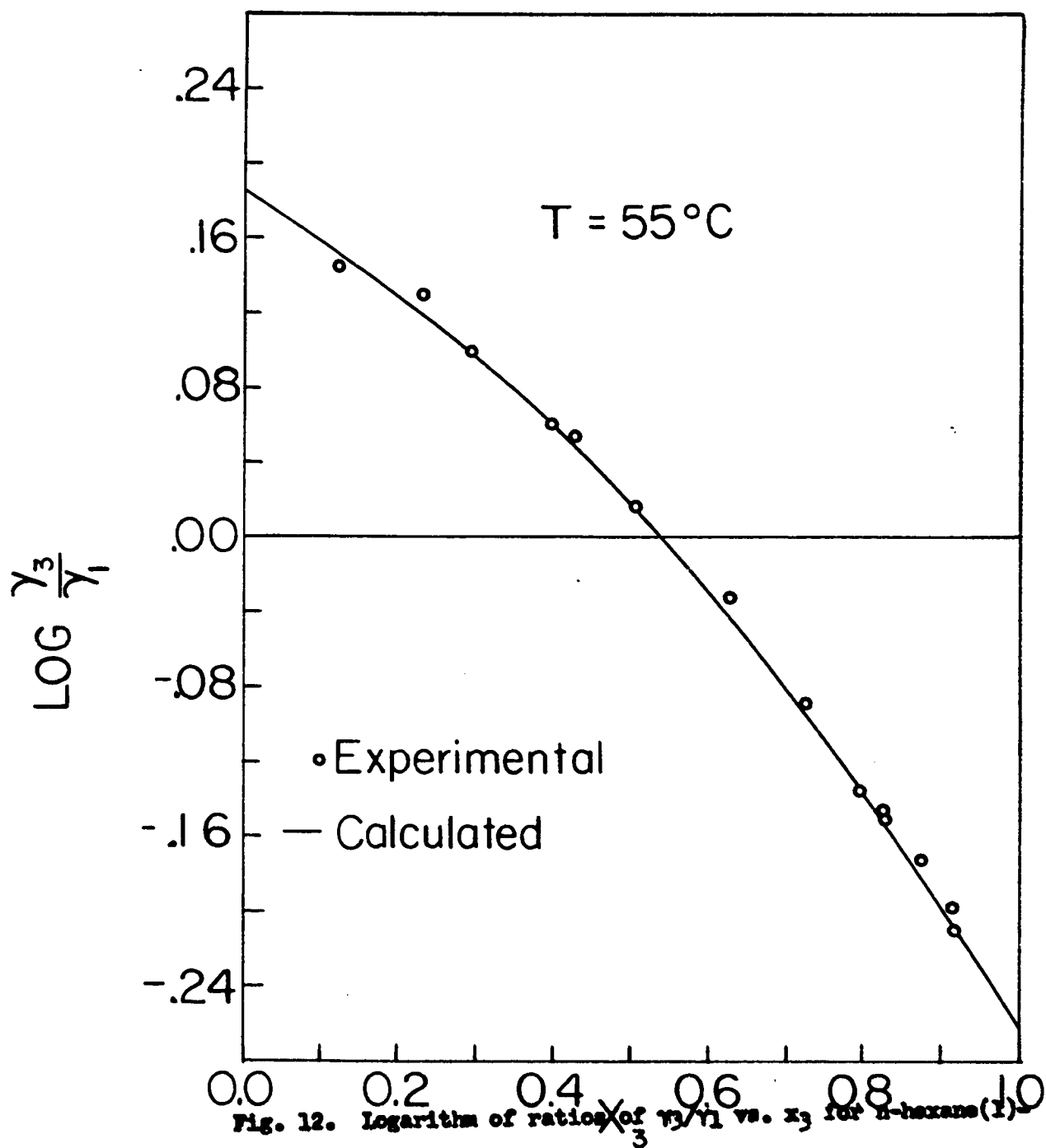


Fig. 12. Logarithm of ratios of γ_3/γ_1 vs. x_3 for n-hexane(1)-benzene(2) system at 55°C .

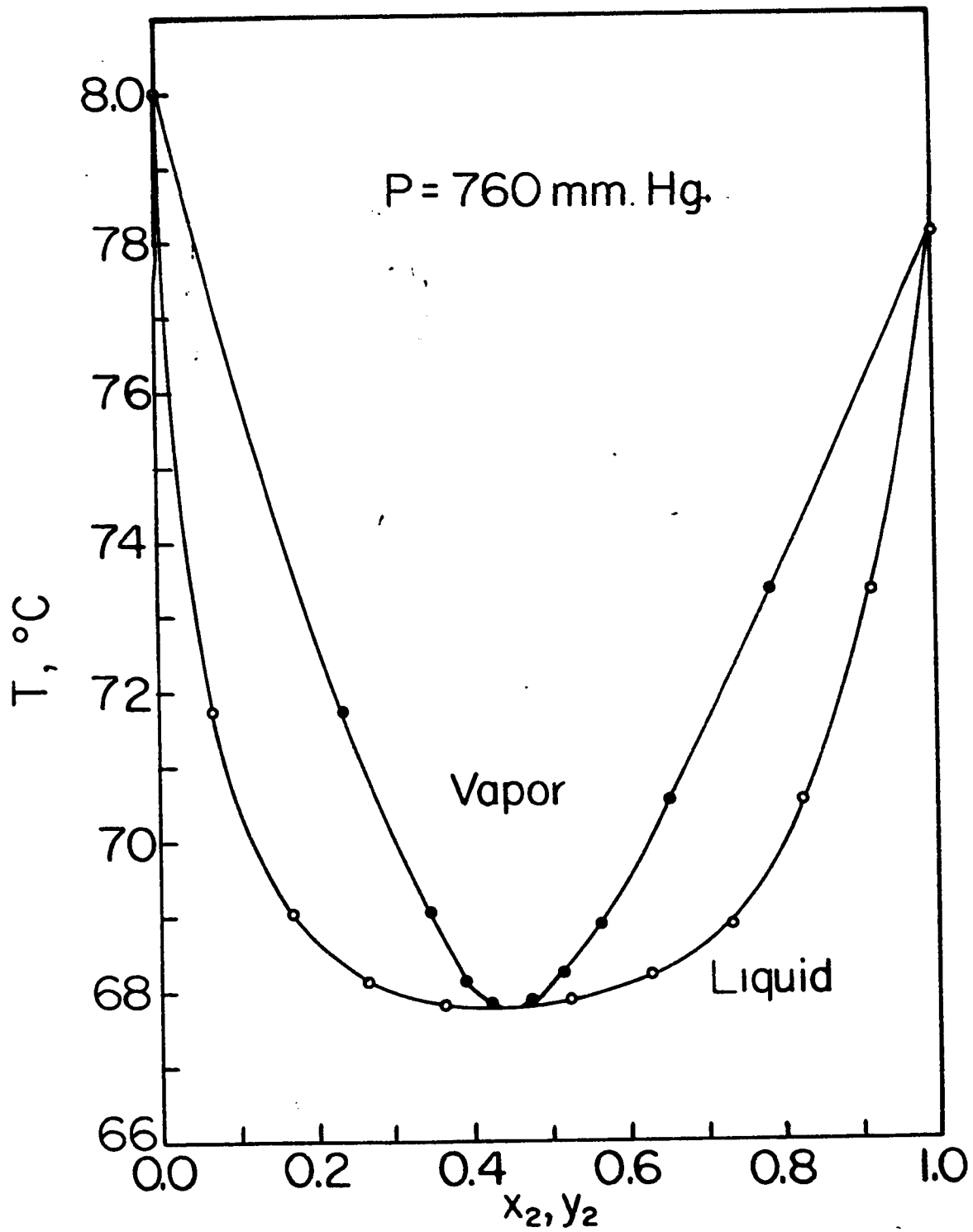


Fig. 13. Temperature vs. composition diagram for ethyl alcohol(2)-benzene(3) system at 760 mm. Hg.

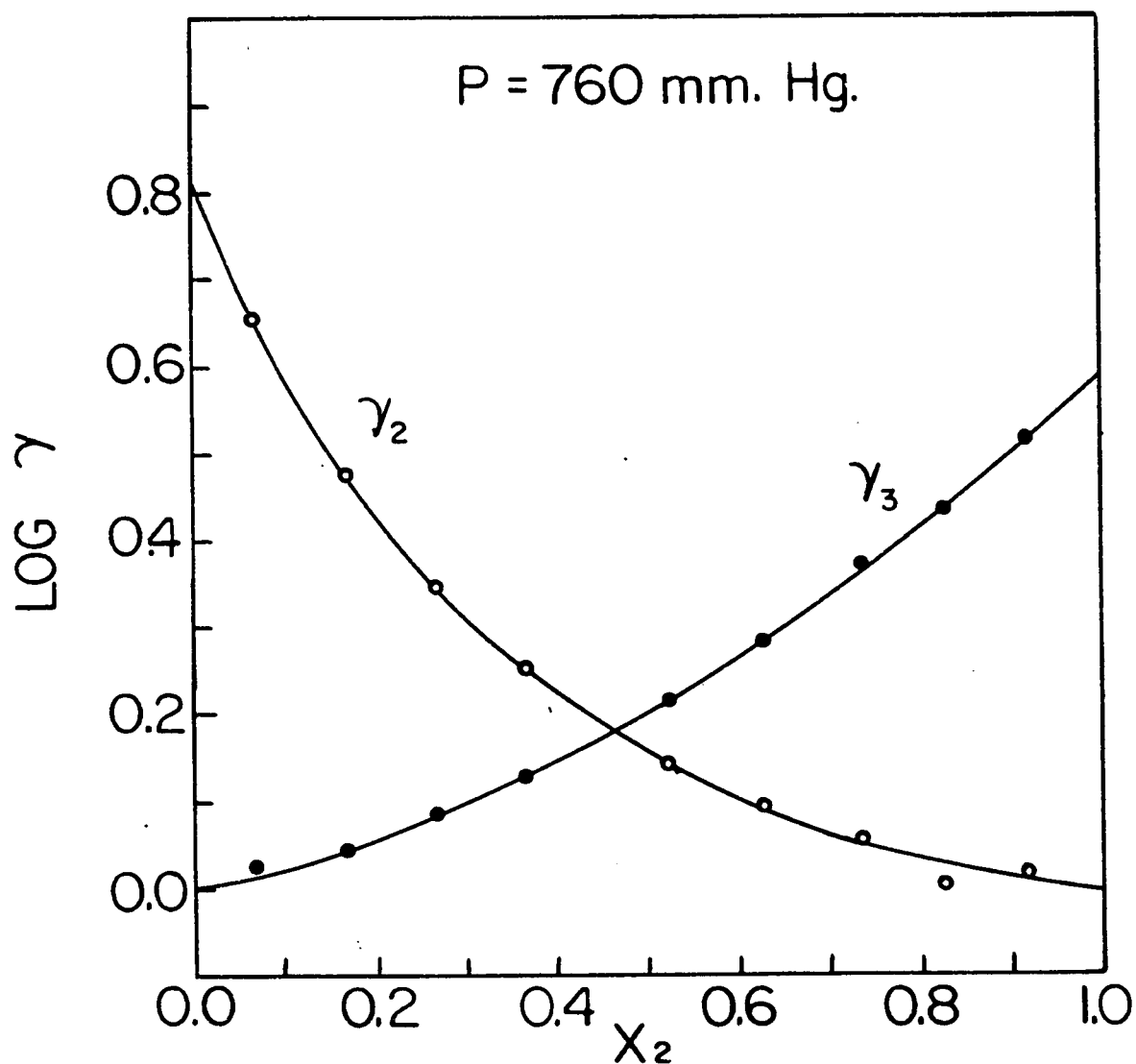


Fig. 14. Logarithmic activity coefficients vs. composition for ethyl alcohol(2)-benzene(3) system at 760 mm. Hg.

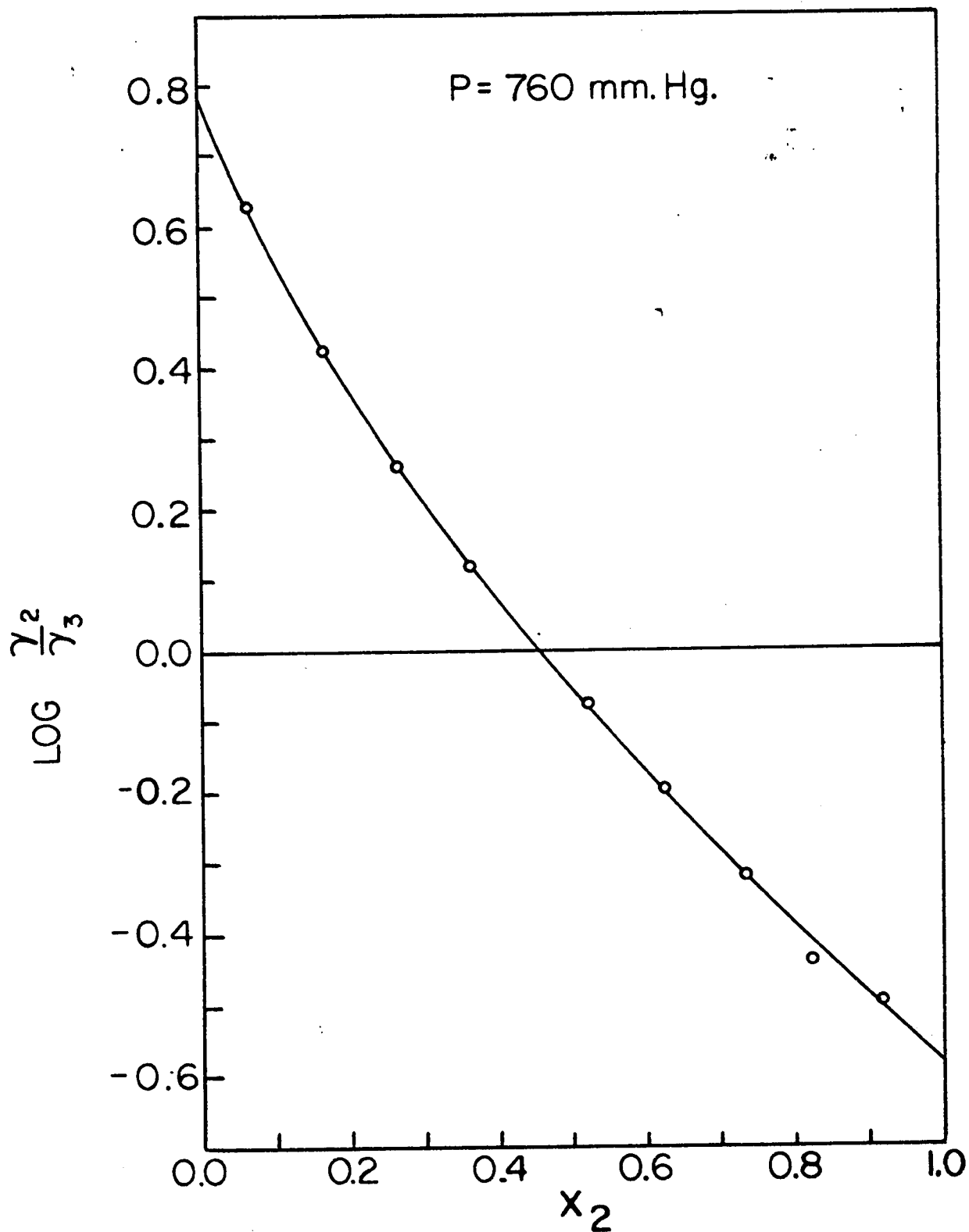


Fig. 15. Logarithm of ratios of γ_2/γ_3 vs. x_2 for ethyl alcohol(2)-benzene(3) system at 760 mm. Hg.

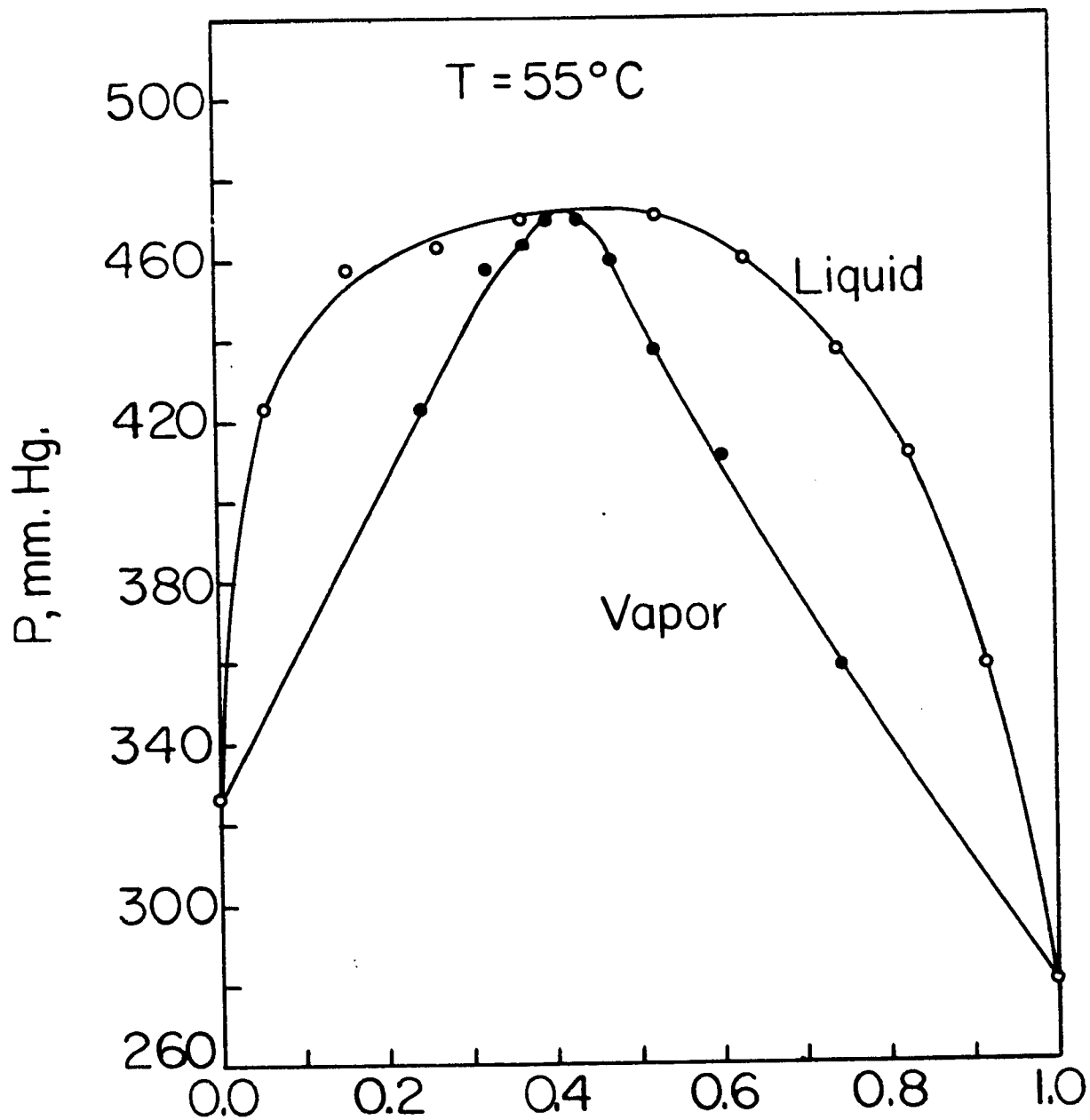


Fig. 16. Total pressure vs. composition diagram for ethyl alcohol(2)-benzene(3) system at 55°C.

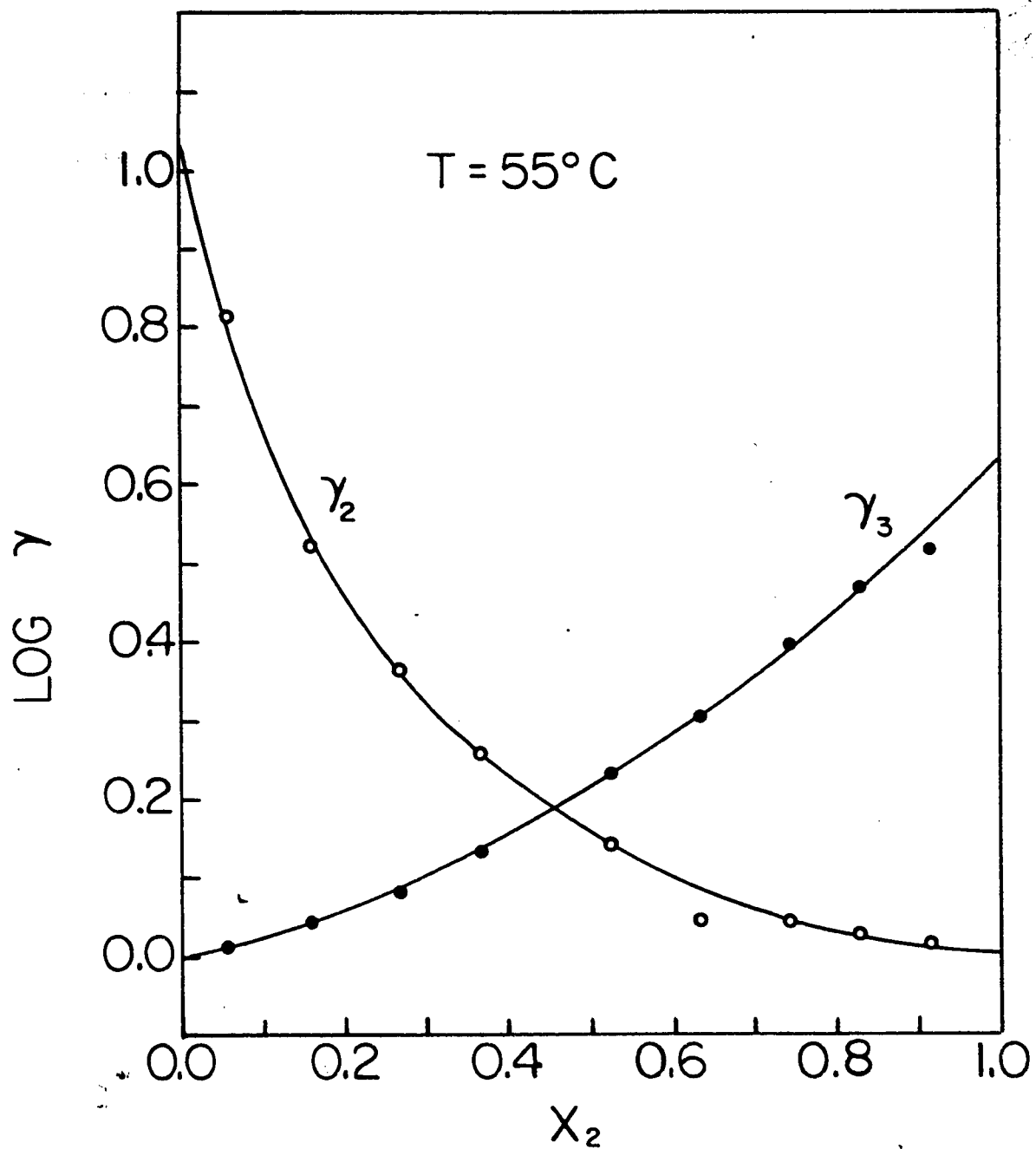


Fig. 17. Logarithmic activity coefficients vs. composition for ethyl alcohol(2)-benzene(3) system at 55°C .

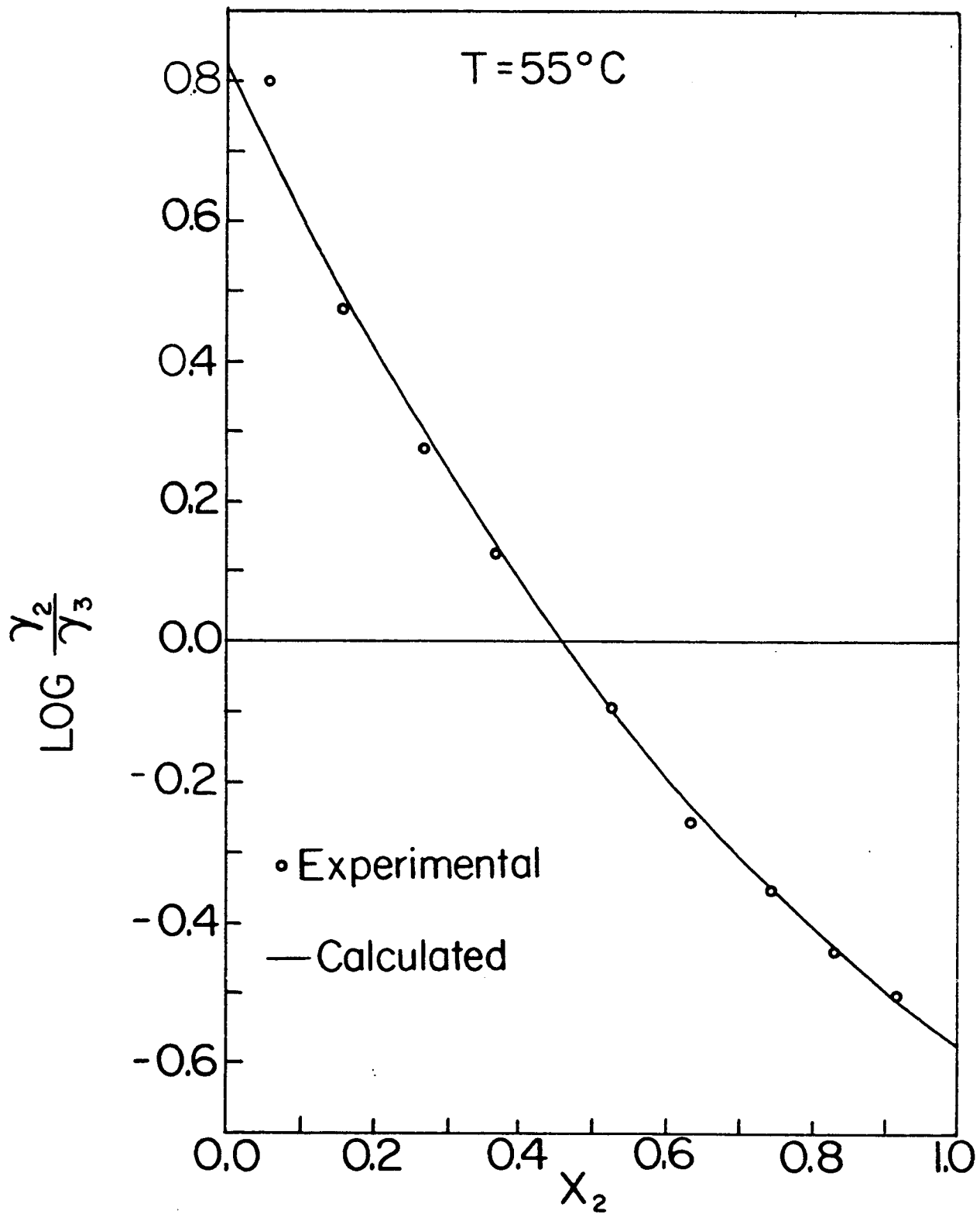
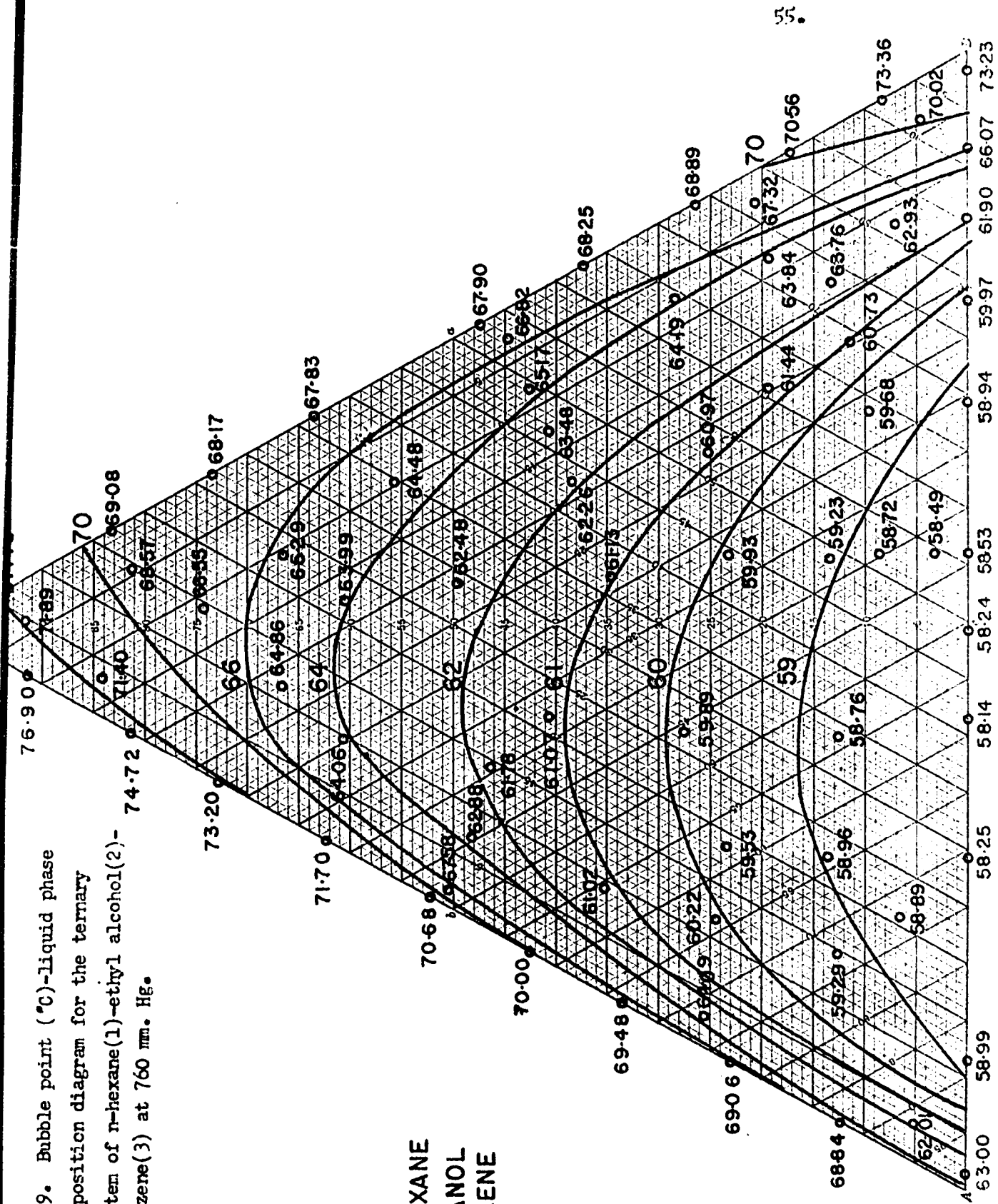


Fig. 18. Logarithm of ratios of γ_2/γ_3 vs. x_2 for ethyl alcohol(2)-benzene(3) system at 55°C .

Fig. 19. Bubble point (°C)-liquid phase composition diagram for the ternary system of n-hexane(1)-ethyl alcohol(2)-benzene(3) at 760 mm. Hg.

A = n-HEXANE
 B = ETHANOL
 C = BENZENE



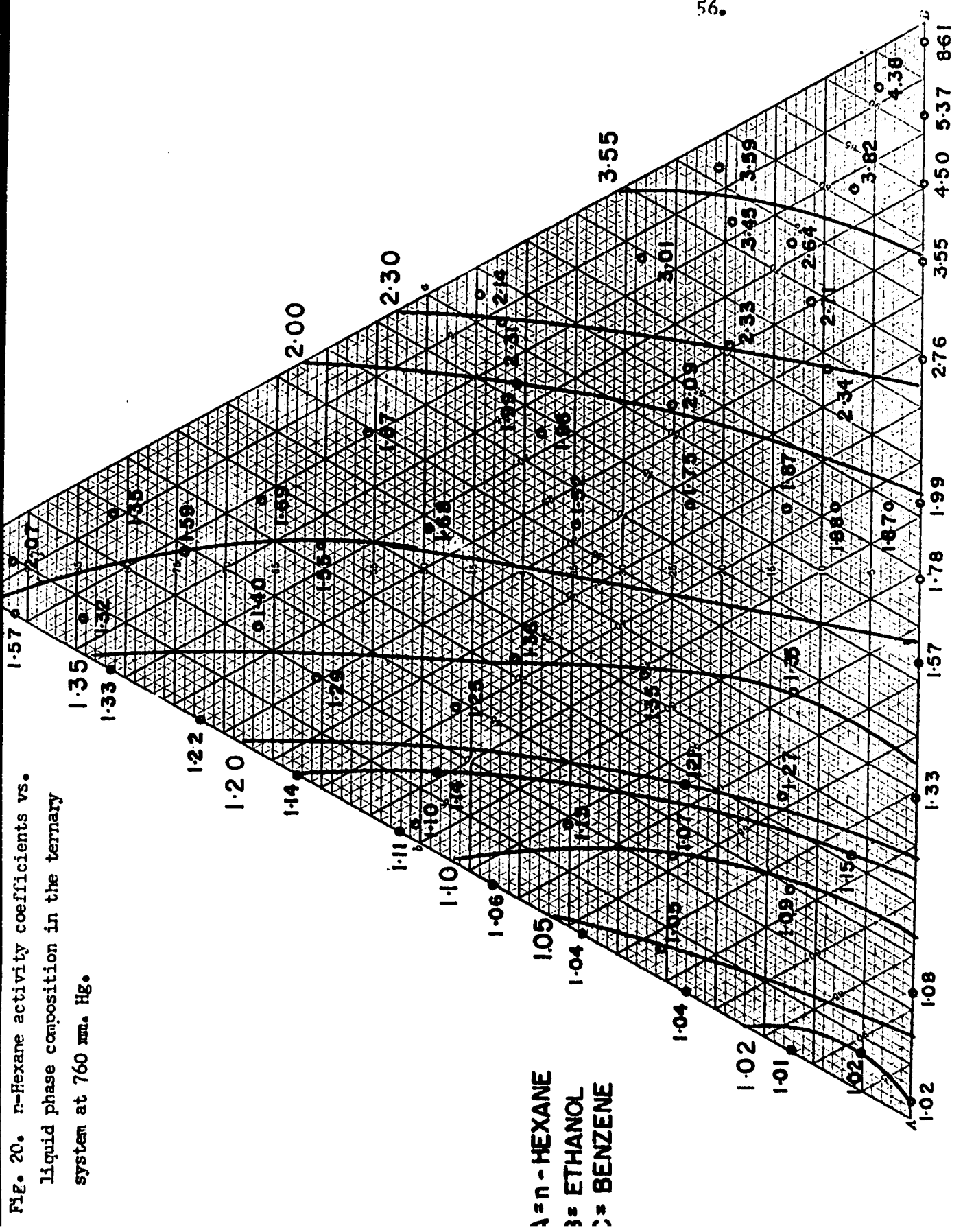


FIG. 20. n-Hexane activity coefficients vs. liquid phase composition in the ternary system at 760 mm. Hg.

Fig. 21. Ethyl alcohol activity coefficients vs. liquid phase composition in the ternary system at 760 mm. Hg.

A = n-HEXANE
 B = ETHANOL
 C = BENZENE

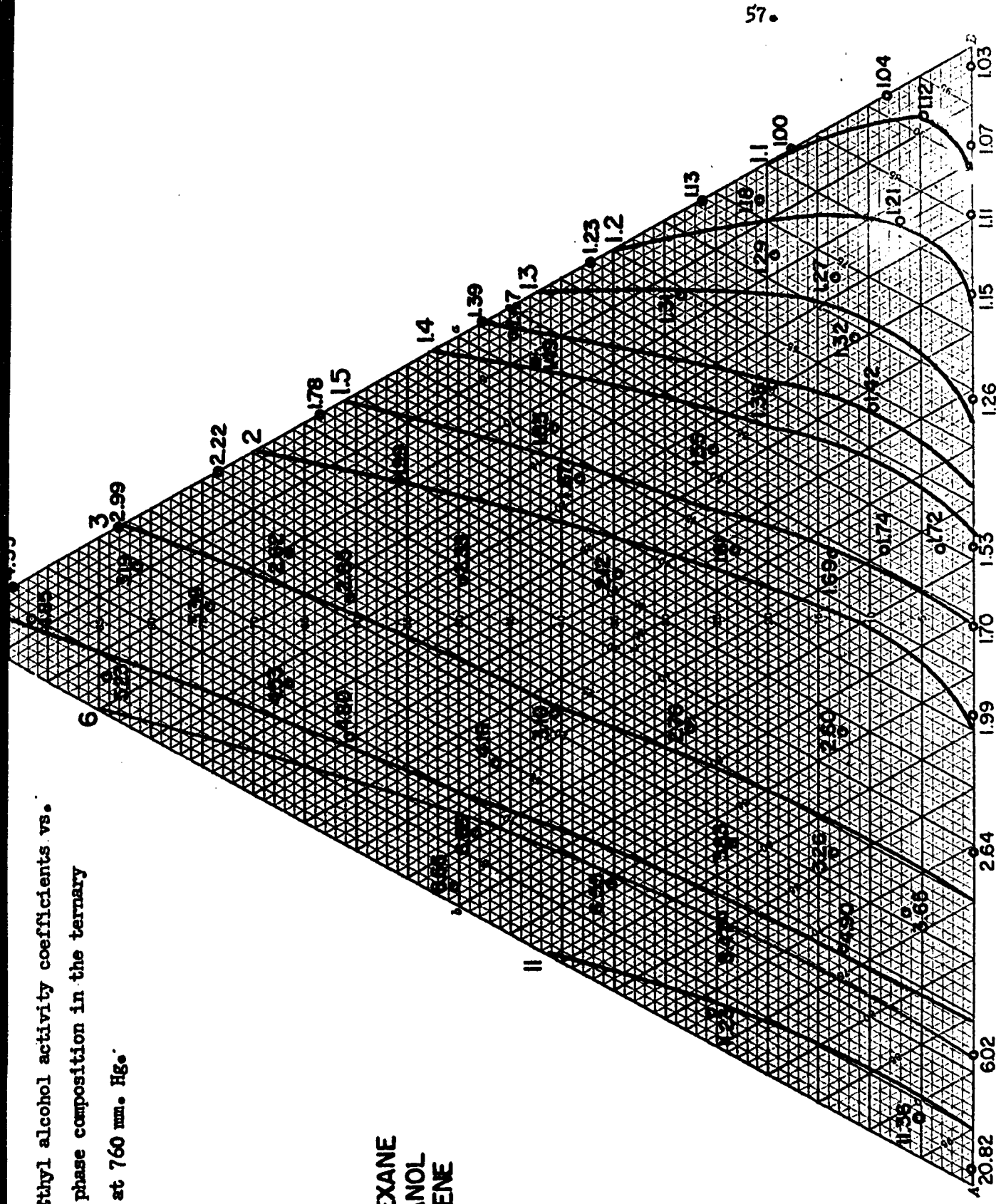


Fig. 22. Benzene activity coefficients vs. liquid phase composition in the ternary system at 760 mm. Hg.

A = n-HEXANE
 B = ETHANOL
 C = BENZENE

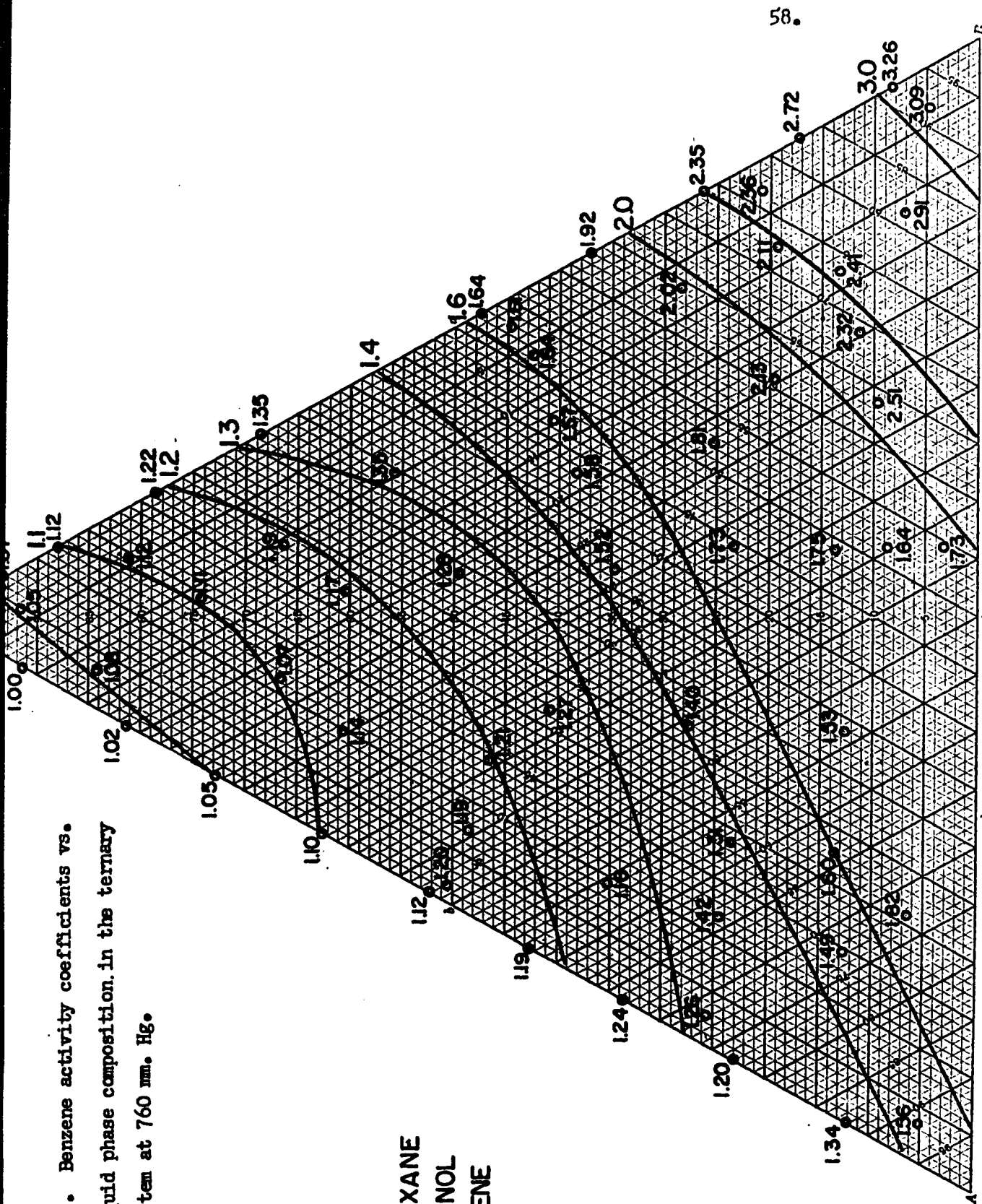


Fig. 23. Total pressure (mm.Hg.)-liquid phase composition diagram for the ternary system of n-hexane(1)-ethyl alcohol(2)-benzene(3) at 55°C.

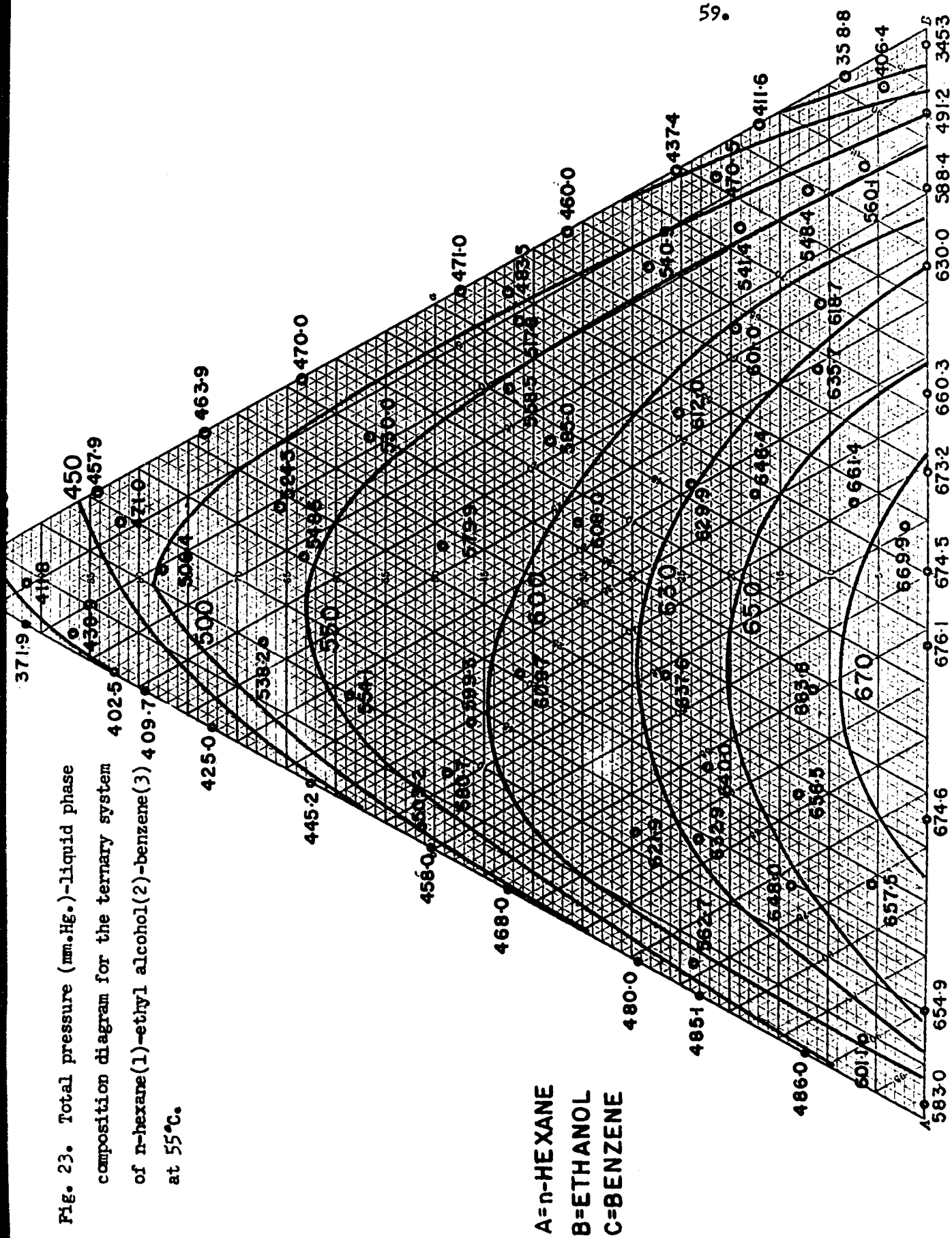
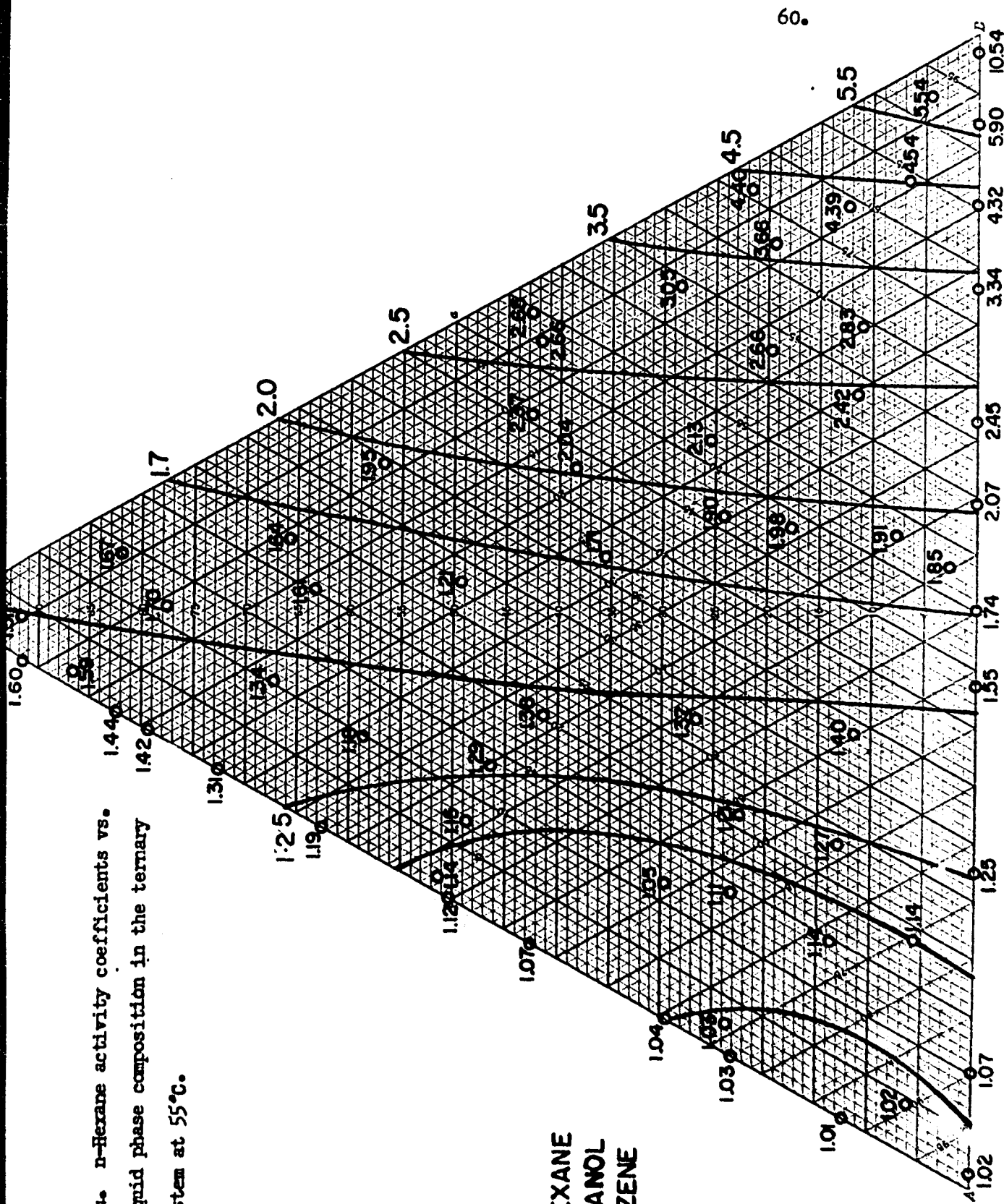
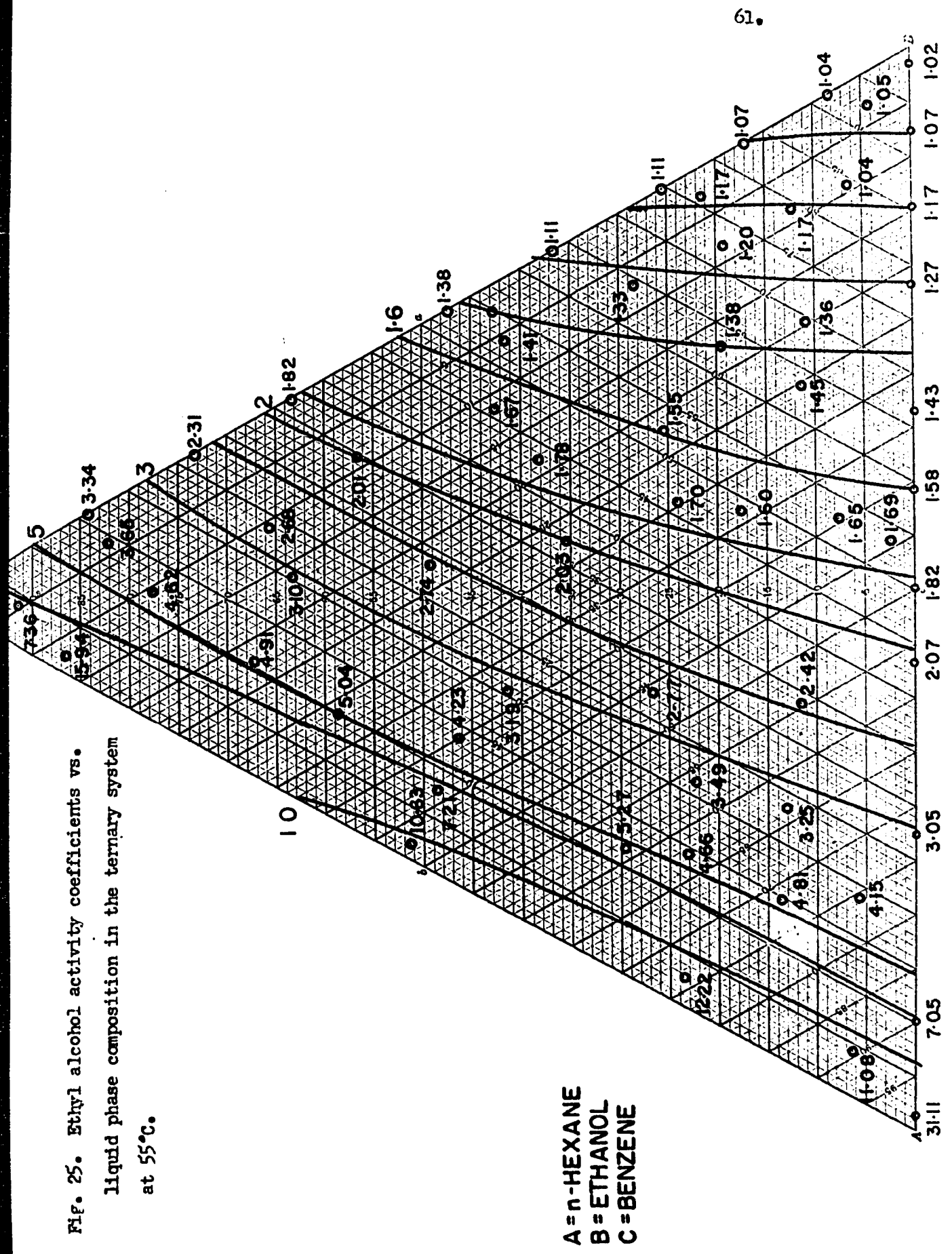


Fig. 24. n-Hexane activity coefficients vs. liquid phase composition in the ternary system at 55°C.



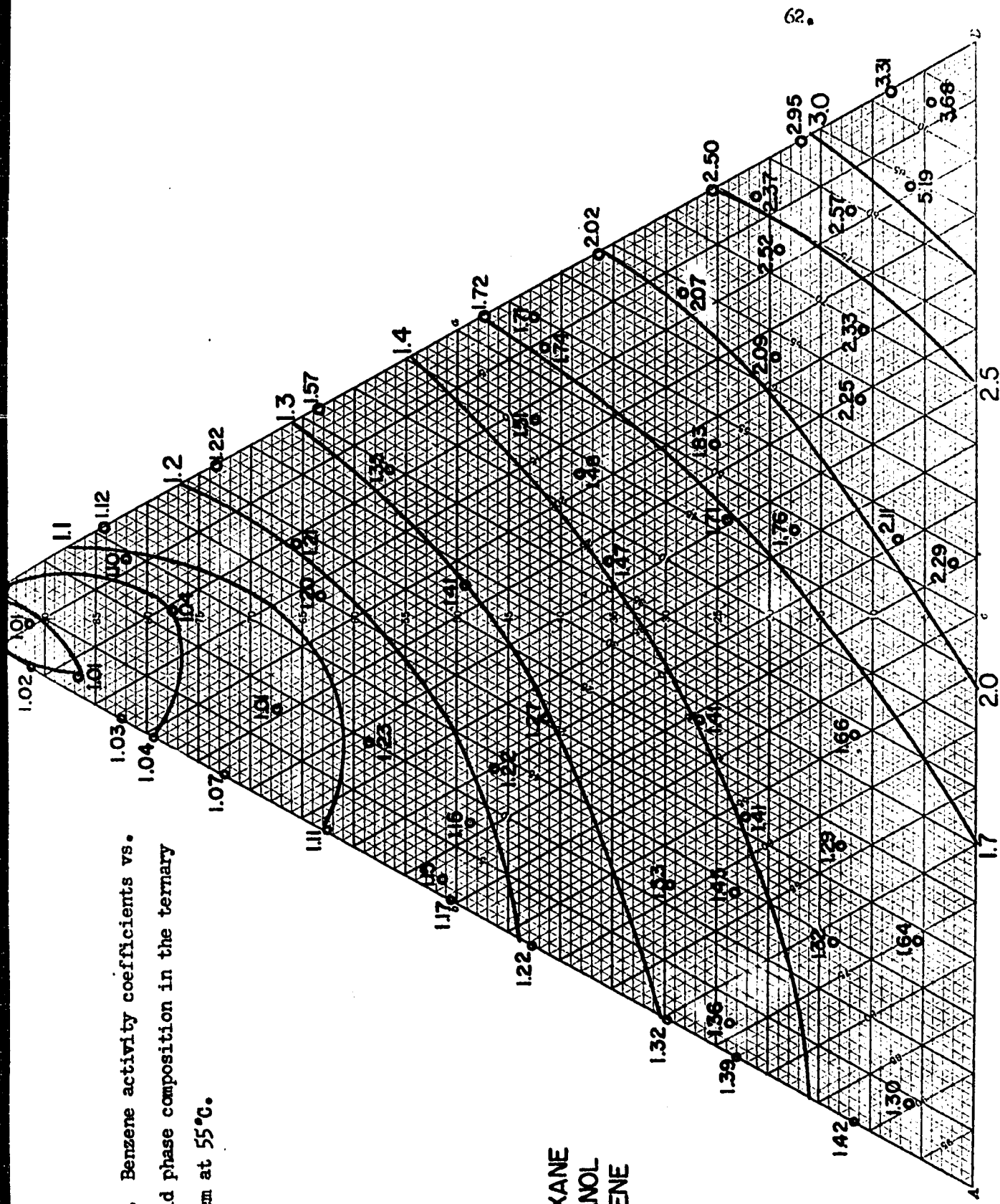
A = n-HEXANE
 B = ETHANOL
 C = BENZENE

Fig. 25. Ethyl alcohol activity coefficients vs. liquid phase composition in the ternary system at 55°C.



A = n-HEXANE
 B = ETHANOL
 C = BENZENE

Fig. 26. Benzene activity coefficients vs. liquid phase composition in the ternary system at 55°C.



A = n-HEXANE
 B = ETHANOL
 C = BENZENE

CORRELATION OF RESULTS

It is intended to correlate the vapor-liquid equilibrium data of the ternary system at 55°C by the method suggested by Redlich and Kister (6).

Redlich-Kister's free energy function for the ternary system is represented by the following equation.

$$Q_{123} = Q_{12} + Q_{23} + Q_{31} + x_1 x_2 x_3 \left[C_{123} + D_1 (x_2 - x_3) + D_2 (x_3 - x_1) + D_3 (x_1 - x_2) + \dots \right] \quad (22)$$

$$\text{where } Q_{123} = x_1 \log \gamma_1 + x_2 \log \gamma_2 + x_3 \log \gamma_3 \quad (23)$$

In Equations 22 and 23, x_1 , x_2 and x_3 are experimentally determined liquid compositions and $\log \gamma_1$, $\log \gamma_2$ and $\log \gamma_3$ are their corresponding liquid phase activity coefficients. Q_{12} , Q_{23} and Q_{31} can be evaluated as follows

$$Q_{12} = x_1 x_2 \left[B_{12} + C_{12} (x_1 - x_2) + D_{12} (x_1 - x_2)^2 + \dots \right] \quad (24)$$

$$Q_{23} = x_2 x_3 \left[B_{23} + C_{23} (x_2 - x_3) + D_{23} (x_2 - x_3)^2 + \dots \right] \quad (25)$$

$$Q_{31} = x_3 x_1 \left[B_{31} + C_{31} (x_3 - x_1) + D_{31} (x_3 - x_1)^2 + \dots \right] \quad (26)$$

B_{12} , C_{12} and D_{12} are obtained from the $\log (\gamma_1/\gamma_2)$ vs. x_1 plot at characteristic liquid compositions in the binary system of 1 and 2.

B_{23} , C_{23} and D_{23} are evaluated from the $\log (\gamma_2/\gamma_3)$ vs. x_2 plot in the binary system of 2 and 3. B_{31} , C_{31} and D_{31} are obtained from the

$\log (\gamma_3/\gamma_1)$ vs. x_3 plot in the binary system of 3 and 1. All binary constants are listed in Table 15.

$$\frac{Q_{123} - Q_{12} - Q_{23} - Q_{31}}{x_1 x_2 x_3} = C_{123} + D_1(x_2 - x_3) + D_2(x_3 - x_1) + D_3(x_1 - x_2) \quad (27)$$

Hence, sets of equations similar to Equation 27 may be obtained from different experimental runs.

In this case, twenty-one reliable experimental runs were chosen for the calculation of the ternary constants. The least square programming on an IBM 650 was employed for the evaluation of the ternary constants. Table 16 presents 21 equations for the IBM 650 programming.

The constants obtained from the IBM 650 programming are as follows:

$$\begin{aligned} C_{123} &= 1.2704051 \\ D_1 &= -1.1604252 \\ D_2 &= -0.78328600 \\ D_3 &= -1.3393105 \end{aligned}$$

The IBM programming also provided the values of the term $\frac{Q_{123}(\text{calcd}) - Q_{12} - Q_{23} - Q_{31}}{x_1 x_2 x_3}$ from which the reliability of the

ternary constants is checked by calculating the term $Q_{123}(\text{calcd.})$. The comparison of experimental and calculated Q_{123} is presented in Table 17.

SAMPLE CALCULATION

(1) Calculation of mole fraction ratios for calibration.

Take Table 1h, run 1 as example.

(a) Mole fraction calculation:

From experiment, a sample has the following composition by weighing.

n-hexane(1) = 1.3868 gms.

ethanol(2) = 3.0054 gms.

benzene(3) = 5.2793 gms.

Therefore,

$$\text{Mole fraction of n-hexane } (x_1) = \frac{w_1/M_1}{w_1/M_1 + w_2/M_2 + w_3/M_3}$$

where M = molecular weight

w = actual weight

$$x_1 = \frac{1.3868/86.172}{1.3868/86.172 + 3.0054/46.068 + 5.2793/78.108}$$

$$= 0.1081$$

$$x_2 = \frac{3.0054/46.068}{1.3868/86.172 + 3.0054/46.068 + 5.2793/78.108}$$

$$= 0.4381$$

$$x_3 = \frac{5.2793/78.108}{1.3868/86.172 + 3.0054/46.068 + 5.2793/78.108}$$

$$= 0.4538$$

(b) Mole fraction ratio calculation

$$\frac{\text{Mole fraction of ethanol}}{\text{Mole fraction of benzene}} = \frac{0.4381}{0.4538} = 0.9654$$

$$\frac{\text{Mole fraction of benzene}}{\text{Mole fraction of n-hexane}} = \frac{0.4538}{0.1081} = 4.1980$$

$$\frac{\text{Mole fraction of ethanol}}{\text{Mole fraction of n-hexane}} = \frac{0.4381}{0.1081} = 4.0527$$

(2) Calculation of mole fractions of unknown.

Take Table 7, run 27 of liquid sample as example.

(a) Evaluation of mole fraction ratio from area ratio.

From experiment one obtained the area ratios as follows.

For Ethanol/Benzene ratio

$$\text{Area ratio} = 4.487$$

From Figure 32,

$$\frac{\text{Mole fraction ratio}}{\text{area ratio}} = 1.4667$$

$$\begin{aligned} \text{Therefore, } x_2/x_3 &= 1.4667 \times 4.487 \\ &= 6.5811 \end{aligned}$$

For Benzene/n-Hexane ratio

$$\text{Area ratio} = 0.2962$$

From Figure 33

$$\frac{\text{Mole fraction ratio}}{\text{area ratio}} = 1.2085$$

$$\begin{aligned} \text{Therefore, } x_3/x_1 &= 1.2085 \times 0.2962 \\ &= 0.3580 \end{aligned}$$

For Ethanol/n-Hexane ratio

$$\text{Area ratio} = 1.3291$$

From Figure 34,

$$\frac{\text{Mole fraction ratio}}{\text{area ratio}} = 1.8000$$

$$\begin{aligned} \text{Therefore } x_2/x_1 &= 1.8000 \times 1.3291 \\ &= 2.3924 \end{aligned}$$

(b) Evaluation of mole fraction

$$\text{Since } x_1 + x_2 + x_3 = 1$$

$$\text{and } x_3/x_1 = 0.3580; \quad x_2/x_1 = 2.3924$$

$$\text{therefore } x_1 + 2.3924 x_1 + 0.358 x_1 = 1$$

$$x_1 = \frac{1}{3.7504} = 0.2666$$

and

$$0.2666 + (0.2666)(2.3924) + x_3 = 1$$

Therefore

$$x_3 = 0.0956$$

Consequently

$$x_2 = 0.6378$$

(3) Evaluation of liquid phase activity coefficients.

Take Table 7, run 27 as example.

$$\text{Since } \gamma_1 = \frac{y_1 P}{x_1 P_1}$$

$$\text{and } P_1 = 566.6 \text{ mm.Hg.}$$

$$\begin{aligned} \text{Therefore } \gamma_1 &= \frac{0.4651 \times 760}{0.2666 \times 566.6} \\ &= 2.3400 \end{aligned}$$

In the same manner,

$$\begin{aligned} \text{at } p_2 &= 346.5 \text{ mm. Hg.} \\ \gamma_2 &= 1.4196 \\ \text{and at } p_3 &= 387.1 \text{ mm. Hg.} \\ \gamma_3 &= 2.5096 \end{aligned}$$

(4) Determination of binary Redlich-Kister constants.

Take the determination of B_{23} , C_{23} , D_{23} at 55°C as example.

From Figure 18, the following characteristic points are obtained.

x_2	0.5	0.7041	0.7887	0.8536
$\log \gamma_2/\gamma_3$	-0.061	-0.316	-0.4	-0.461

The method proposed by Redlich and Kister (6) is employed and the following relations are obtained.

$$\begin{aligned} \text{(a) } 0.5 C_{23} &= -0.061 \\ C_{23} &= -0.122 \end{aligned}$$

$$\begin{aligned} \text{(b) } -0.7071 B_{23} - 0.25 C_{23} &= -0.461 \\ -0.7071 B_{23} - (0.25)(-0.122) &= -0.461 \\ B_{23} &= 0.6951 \end{aligned}$$

$$\begin{aligned} \text{(c) } -0.5773 (B_{23} - 0.3333 D_{23}) &= -0.4 \\ -0.5773 (0.6951 - 0.3333 D_{23}) &= -0.4 \\ D_{23} &= 0.00665 \end{aligned}$$

$$(d) -0.4082 (B_{23} - 0.6667 D_{23}) = -0.316$$

$$-0.4082 (0.6951 - 0.6667 D_{23}) = -0.316$$

$$D_{23} = -0.00145$$

$$\begin{aligned} \text{Average of } D_{23} &= \frac{0.00665 + (-0.00145)}{2} \\ &= -0.00145 \end{aligned}$$

(5) Evaluation of equations in Table 17.

Take run 2 at 55°C as example.

$$\begin{aligned} \text{Since } \frac{Q_{123} - Q_{12} - Q_{23} - Q_{31}}{x_1 x_2 x_3} &= C_{123} + (x_2 - x_1) D_1 + \\ &(x_3 - x_1) D_2 + (x_1 - x_2) D_3 \end{aligned}$$

$$\begin{aligned} \text{where } Q_{123} &= x_1 \log \gamma_1 + x_2 \log \gamma_2 + x_3 \log \gamma_3 \\ &= 0.7382 \times 0.0136 + 0.0256 \times 1.0871 + 0.2363 \times 0.1329 \\ &= 0.0692 \end{aligned}$$

$$\begin{aligned} Q_{12} &= x_1 x_2 \left[B_{12} + C_{12} (x_1 - x_2) + D_{12} (x_1 - x_2)^2 \right] \\ &= (0.7382)(0.0256) \left[0.9532 + (-0.056) \right. \\ &\quad \left. (0.7382 - 0.0256) + (0.1893)(0.7382 - 0.0256)^2 \right] \\ &= 0.0191 \end{aligned}$$

$$\begin{aligned} Q_{23} &= x_2 x_3 \left[B_{23} + C_{23} (x_2 - x_3) + D_{23} (x_2 - x_3)^2 \right] \\ &= (0.0256)(0.2363) \left[0.6951 + (-0.122) \right. \\ &\quad \left. (0.0256 - 0.2363) + (-0.00145)(0.0256 - 0.2363)^2 \right] \\ &= 0.0043 \end{aligned}$$

$$\begin{aligned}
 Q_{31} &= x_3 x_1 \left[B_{31} + C_{31} (x_3 - x_1) - D_{31} (x_3 - x_1)^2 \right] \\
 &= (0.2363)(0.7382) \left[0.22146 + (0.0356) \right. \\
 &\quad \left. (0.2363 - 0.7382) + (0.00037)(0.2363 - 0.7382)^2 \right] \\
 &= 0.0355
 \end{aligned}$$

Finally

$$\begin{aligned}
 &\frac{Q_{123} - Q_{12} - Q_{23} - Q_{31}}{x_1 x_2 x_3} \\
 &= \frac{0.0692 - 0.0191 - 0.0043 - 0.0355}{(0.7382)(0.0256)(0.2363)} \\
 &= 2.2868
 \end{aligned}$$

(6) Consistency Test

Take runs 12, 17, 25, 30 and 24 at 55°C as example.

The following table is obtained from experimental data.

Consistency Test Table

Run	x_1	$\log \eta_1$	$x_1(\log \eta_1) - \log \eta_1$	x_2	$\log \eta_2$	$x_2(\log \eta_2) - \log \eta_2$	x_3	$\log \eta_3$	$x_3(\log \eta_3) - \log \eta_3$
12	0.3138	0.0719	0.02457	0.0994	0.7020	-0.01981	0.5867	0.0873	0.04283
17	0.2234	0.1274	-0.03514	0.1042	0.6906	0.00391	0.6725	0.0051	0.04647
25	0.1046	0.2292	-0.00926	0.1192	0.6645	0.01129	0.7762	0.0182	-0.05938
30	0.1073	0.2159	-0.00252	0.2342	0.4281	0.10560	0.6532	0.0816	-0.03943
24	0.1683	0.2057	+0.02424	0.2007	0.4913	-0.05497	0.6309	0.0781	-0.00360

$$\sum + = 0.21639$$

$$\sum - = 0.22159$$

$$\text{Total} = 0.21639 - 0.22159$$

$$= -0.00524$$

$$\% \text{ Deviation} = \frac{0.21639 - 0.22159}{\frac{0.21639 + 0.22159}{2}} \times 100$$

$$= 2.39\%$$

DISCUSSION

The reliability of the experimental results is discussed as follows:

(1) n-Hexane-Ethanol System

The net area of the $\log \gamma_1/\gamma_2$ vs. x_1 plot for this system is nearly zero at 760 mm.Hg. as shown in Figure 3 and 0.012 at 55°C as shown in Figure 6. However, the binary Redlich-Kister constants evaluated from the plot fit the experimental data reasonably well as illustrated in Figure 6. Thus it is concluded that the experimental data are consistent.

(2) n-Hexane-Benzene System

The difference in area in the $\log \gamma_2/\gamma_1$ vs. x_2 plot for this system is 0.003 at 760 mm.Hg. as shown in Figure 9 and 0.009 at 55°C as shown in Figure 12. The binary Redlich-Kister constants of this system fit the experimental data very well. Thus it is claimed that the data are consistent.

(3) Ethanol-Benzene System

The net area in the $\log \gamma_2/\gamma_3$ vs. x_2 plot is 0.0003 at 760 mm. Hg. as shown in Figure 15 and 0.0016 at 55°C as shown in Figure 18. The binary Redlich-Kister constants of this system also fit the experimental data well as illustrated in Figure 18. Thus it may be concluded that the data are thermodynamically consistent.

(4) The Ternary System

The consistency of the data for the ternary system is checked

by the method of Li and Lu (23). Figure 35 shows the testing of the data at 760 mm.Hg. It appears that the quality of the data is better in the middle region of the triangular plot. The deviation for runs 36, 37 and 38 is 9.36%. However, if point 39 is included, the deviation increases to 26.45% from 9.36%. Hence the point 39 is singled out for consistency test. In conclusion, the data of the ternary system at 760 mm. Hg. might be considered consistent.

The data of the ternary system at 55°C are also tested by the same method. Figure 37 shows the testing. It appears that the data are consistent throughout most of the concentration range of the ternary system, because the deviations are low. However, the data in the region of very high concentration of any component are less consistent. It is due to the fact that the accuracy of analysis is less reliable when one component is in much higher concentration than others. In conclusion, the data at 55°C are considered to be consistent.

It is interesting to mention that no ternary azeotrope is found directly from the experiment. However, an azeotropic ridge (31) joining the two binary azeotropes, namely, n-hexane-ethanol and ethanol-benzene was observed. Figures 36 and 38 illustrate the vapor-liquid equilibrium relationship at 760 mm. Hg. and 55°C, respectively. It is obvious that most of the vapor compositions tend to converge along a path which connects the azeotrope of the two binaries.

The evaluated binary Redlich-Kister constants fit the corresponding binary data well. The calculated ternary constants also fit the ternary system well.

CONCLUSION

The conclusion of this investigation may be outlined as follows.

(1) The modified Gillespie equilibrium still provides quite reliable vapor-liquid equilibrium data.

(2) The technique of analysis for the binary and ternary system proves to be adequate.

(3) The binary Redlich-Kister constants at 55°C are evaluated as follows:

(a) n-Hexane(1)-Ethanol(2) System

$$B_{12} = 0.9532$$

$$C_{12} = -0.056$$

$$D_{12} = 0.1893$$

(b) Ethanol(2)-Benzene(3) System

$$B_{23} = 0.6951$$

$$C_{23} = -0.122$$

$$D_{23} = -0.00145$$

(c) n-Hexane(1)-Benzene(3) System

$$B_{31} = 0.22146$$

$$C_{31} = 0.0356$$

$$D_{31} = 0.00037$$

(4) The ternary Redlich-Kister constants at 55°C calculated from IEM 650 are as follows:

$$G_{123} = 1.2704051$$

$$D_1 = -1.1604252$$

$$D_2 = -0.78328600$$

$$D_3 = -1.3393105$$

(5) Methods of extension of the ternary equilibrium data are also desirable.

APPENDIX I

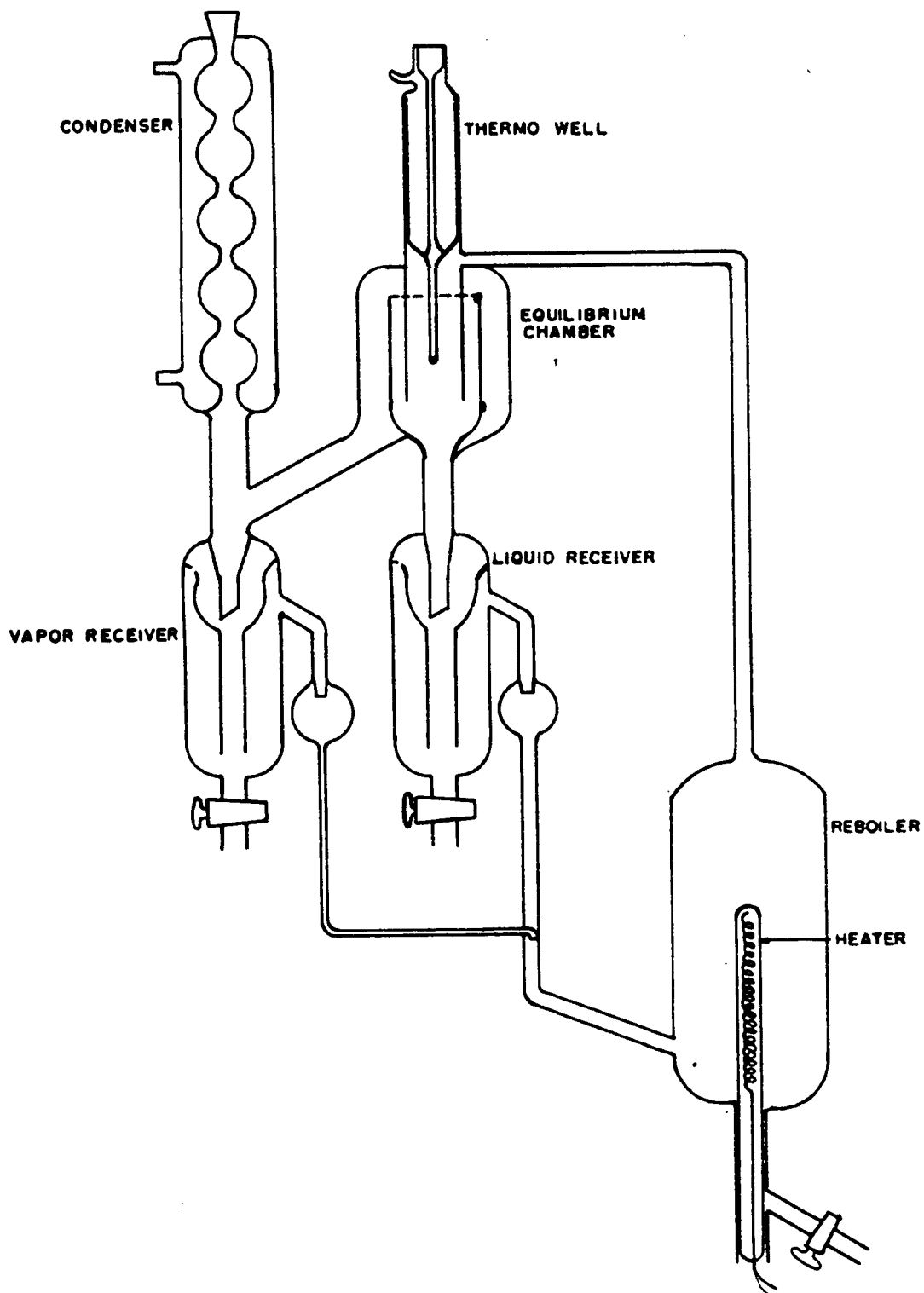


Fig. 27. Modified Gillespie Equilibrium Still

TABLE 9

Operating Conditions for Gas Chromatographic Analysis

Chromatograph:	Perkin-Elmer Model 154-C
Column dimensions:	Two 2-meter x 1/4 inch
Column packings:	Perkin-Elmer Type R Column Polypropylene glycol (UCOM LB-550-X)
Carrier gas:	Helium, flow rate 152 cc/min.
Temperature:	100 °C.
Pressure:	25 psig.
Sample size:	Perkin-Elmer micro-dipper No. 3, 0.005 ml.
Recorder:	L. and N. 0-10 mv. Type G Speedomax Recorder.

TABLE 10

Calibration of Temperature - Absolute Millivolts
For the Copper Constantan Thermocouple

Temperature °C.	E.M.F. Absolute Millivolts
0	0.000
50	2.053
60	2.488
70	2.932
80	3.384
90	3.844
100	4.311

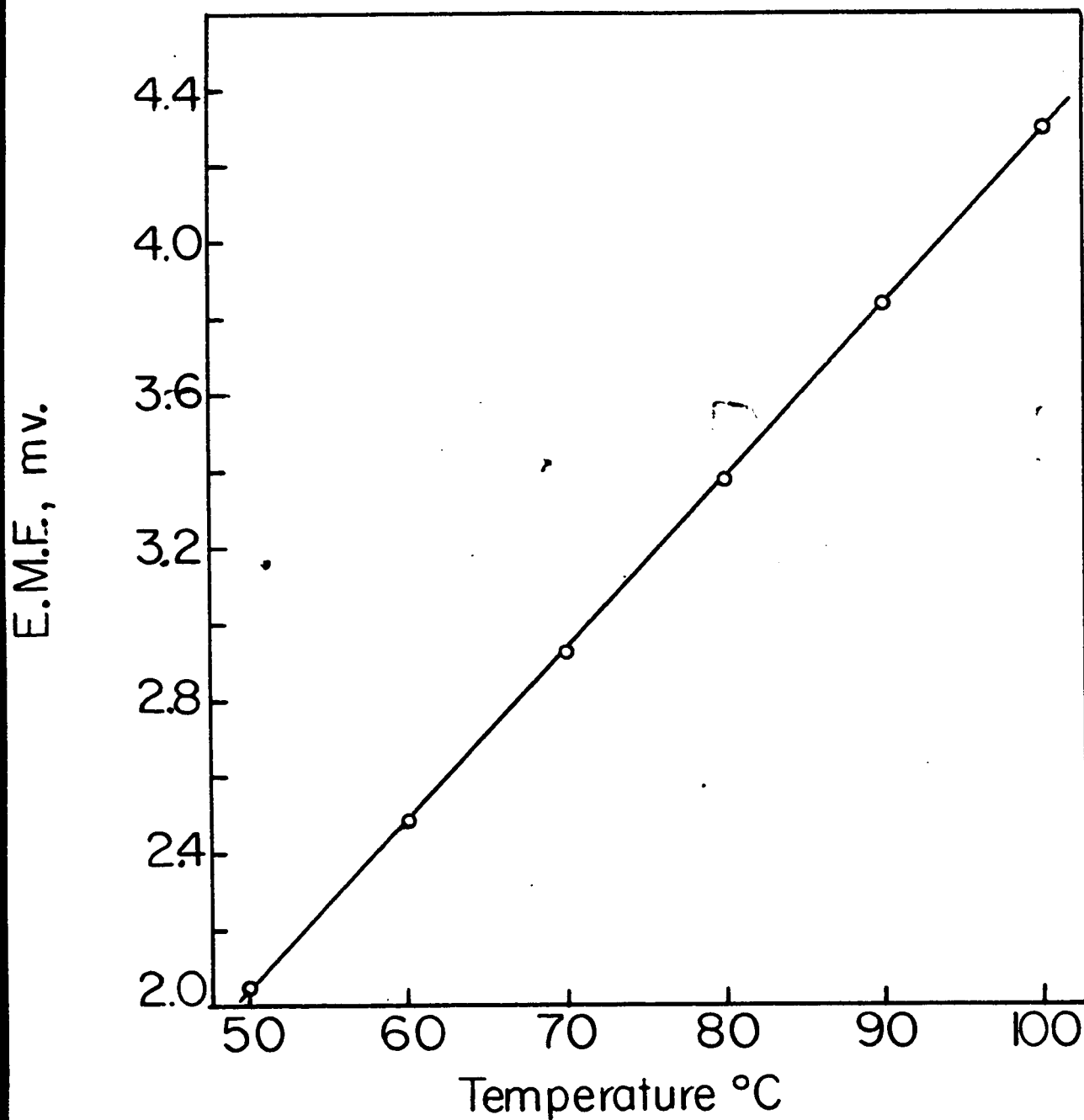


Fig. 28. Calibration curve of copper constantan thermocouple

TABLE 11

Calibration of Composition - Refractive Index
For the System n-Hexane-Benzene

Run	Mole Fraction of n-hexane	Refractive Index at 25°C.
1	0.0000	1.4977
2	0.0248	1.4925
3	0.1121	1.4770
4	0.2191	1.4590
5	0.2318	1.4570
6	0.3932	1.4340
7	0.5059	1.4196
8	0.4889	1.4220
9	0.6882	1.3996
10	0.7072	1.3980
11	0.8968	1.3810
12	0.9151	1.3790
13	1.0000	1.3722

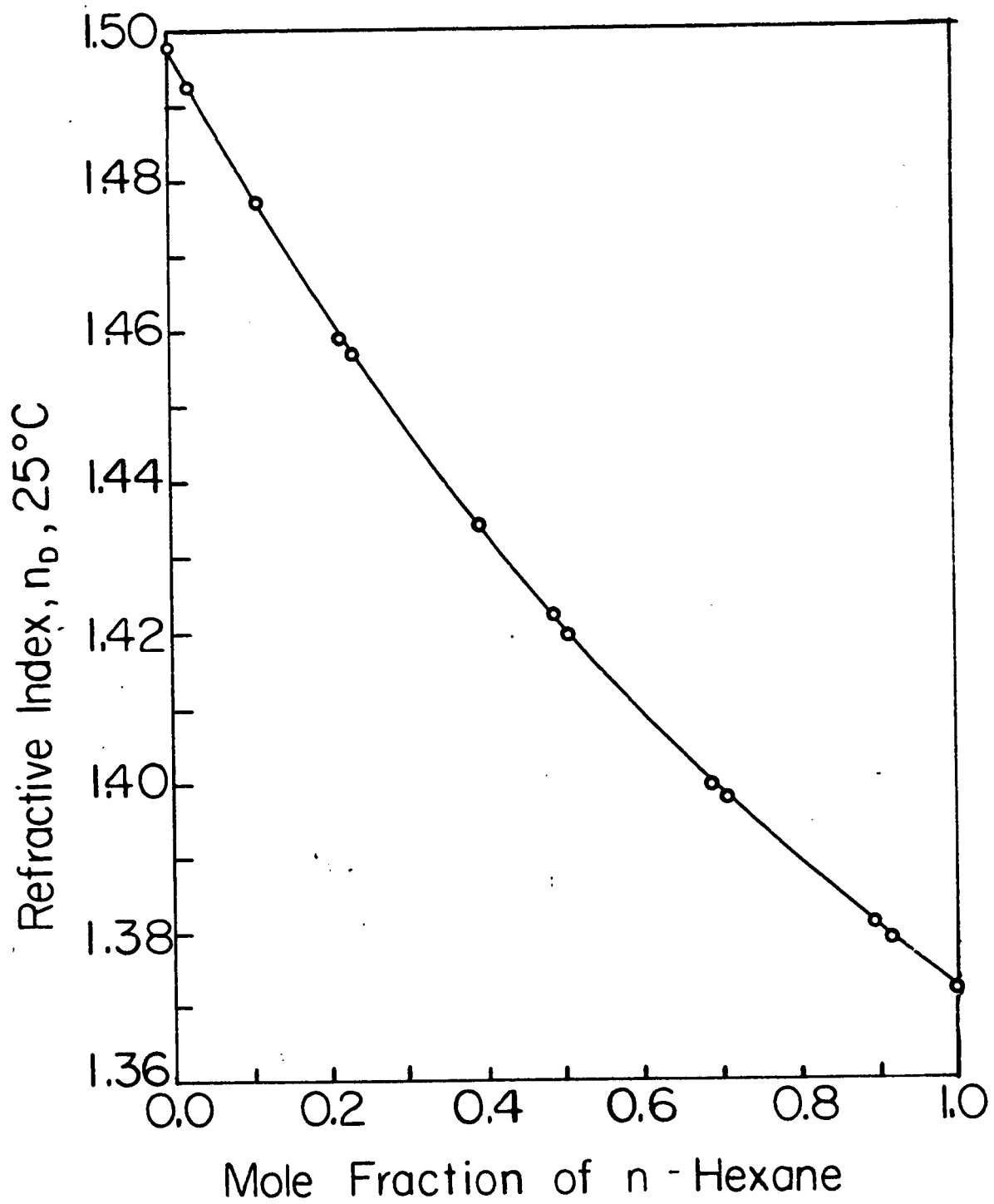


Fig. 29. Calibration curve of composition-refractive index
for the system n-hexane-benzene

TABLE 12

Calibration of Composition - Refractive Index
For the System Ethyl Alcohol-Benzene

Run	Mole Fraction of Ethanol	Refractive Index at 25°C.
1	0.0000	1.4977
2	0.0362	1.4943
3	0.1081	1.4869
4	0.1225	1.4853
5	0.2619	1.4707
6	0.3539	1.4598
7	0.4731	1.4449
8	0.5996	1.4277
9	0.6216	1.4215
10	0.6404	1.4220
11	0.7579	1.4035
12	0.8259	1.3920
13	0.8985	1.3788
14	0.9491	1.3691
15	0.9696	1.3652
16	1.0000	1.3591

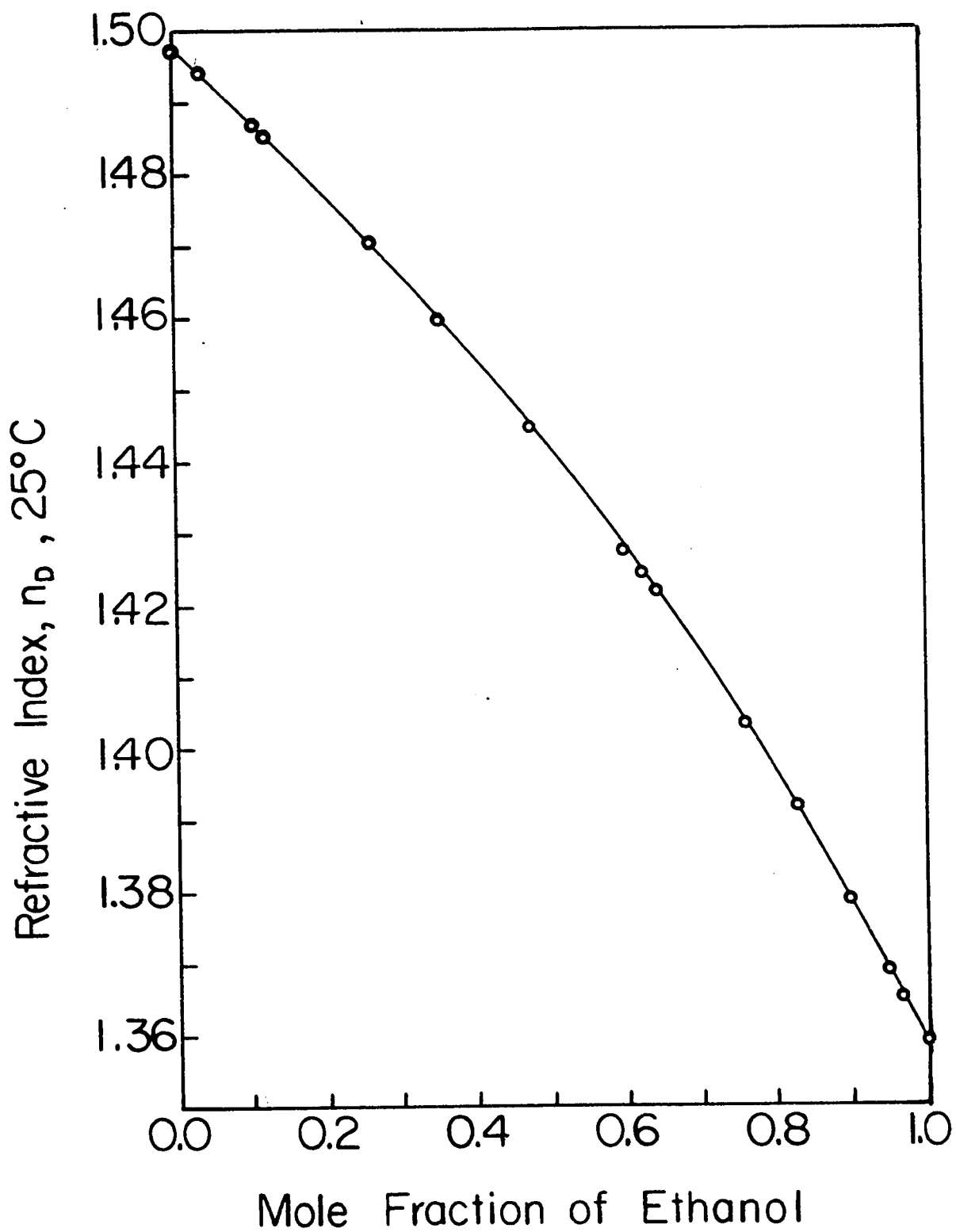


Fig. 30. Calibration curve of composition-refractive index
for the system ethyl alcohol-benzene

TABLE 13

Calibration of Mole Fraction Ratio vs. Area Ratio
For the System of n-Hexane-Ethyl Alcohol

<u>Mole Fraction Ratio</u>	<u>Area Ratio</u>
<u>Ethanol</u> <u>n-Hexane</u>	<u>Ethanol</u> <u>n-Hexane</u>
1.538	0.966
6.321	3.990
6.310	3.743
7.621	4.473
1.044	0.678
1.476	0.888
2.276	1.569
3.333	2.006
0.252	0.176
4.565	2.778
5.734	3.333
1.064	0.662
23.876	14.571
11.690	6.890
8.718	5.386
5.369	3.238
5.911	3.509
2.556	1.667
2.373	1.485
7.888	4.958
5.878	3.504

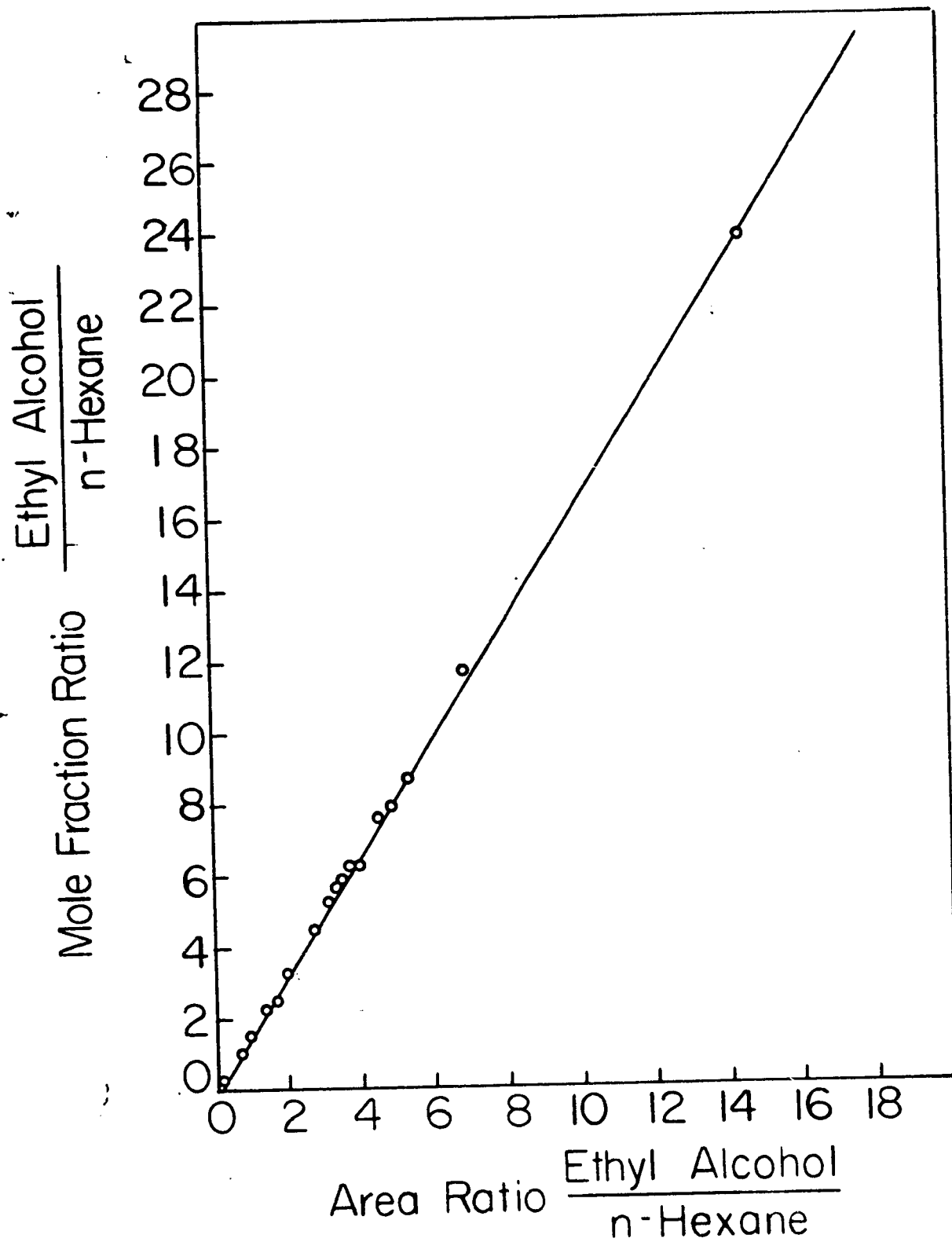


Fig. 11. Calibration curve of (Ethanol/n-Hexane) mole fraction vs. (Ethanol/n-Hexane) area for the binary system of n-hexane-ethanol

TABLE 1h

Calibration of Mole Fraction Ratio vs. Area Ratio
for the System of n-Hexane-Ethyl Alcohol-Benzene

<u>Mole Fraction Ratio</u>			<u>Area Ratio</u>		
<u>Ethanol</u> <u>Benzene</u>	<u>Benzene</u> <u>n-Hexane</u>	<u>Ethanol</u> <u>n-Hexane</u>	<u>Ethanol</u> <u>Benzene</u>	<u>Benzene</u> <u>n-Hexane</u>	<u>Ethanol</u> <u>n-Hexane</u>
0.9654	4.1980	4.0527	0.6884	3.377	2.325
2.9682	4.7480	14.0932	1.9770	3.966	7.841
0.9731	7.6153	7.4102	0.7025	6.311	4.433
2.4940	1.3199	3.2918	1.7399	1.249	2.173
3.4537	1.5218	5.2543	2.4275	1.202	2.917
1.1198	2.0389	2.2831	0.8140	1.686	1.373
2.0288	0.5421	1.0999	1.5091	0.4348	0.656
0.7177	0.9353	0.6713	0.5139	0.8404	0.431
1.9252	0.2666	0.5133	1.3334	0.2329	0.311
0.3426	4.1041	1.4063	0.2528	2.890	0.730
5.2045	1.2152	6.3245	3.7354	0.9742	3.639
15.7880	1.3826	21.8280	10.727	1.060	11.373

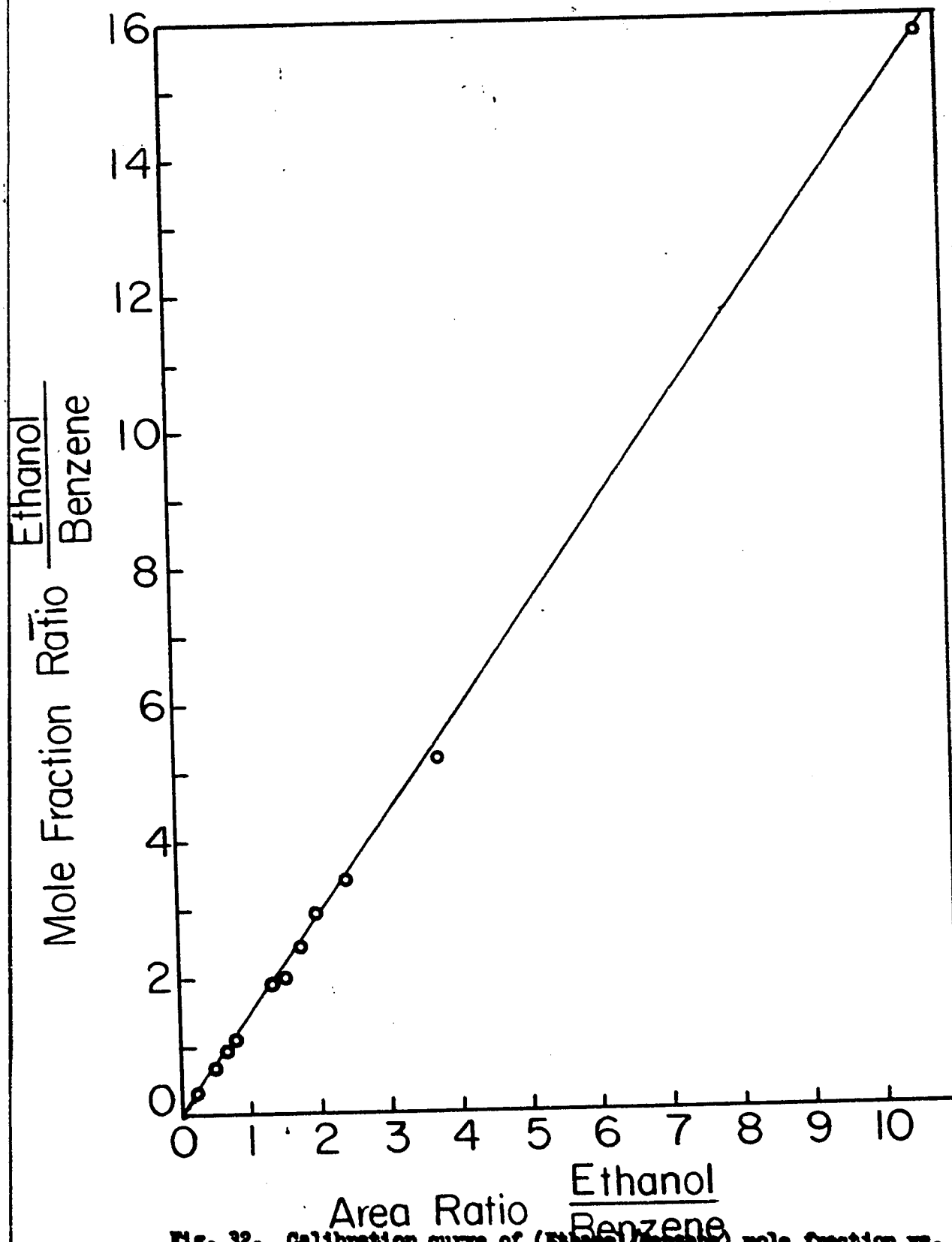


Fig. 32. Calibration curve of (Ethanol/Benzene) mole fraction vs. (Ethanol/Benzene) area for the ternary system

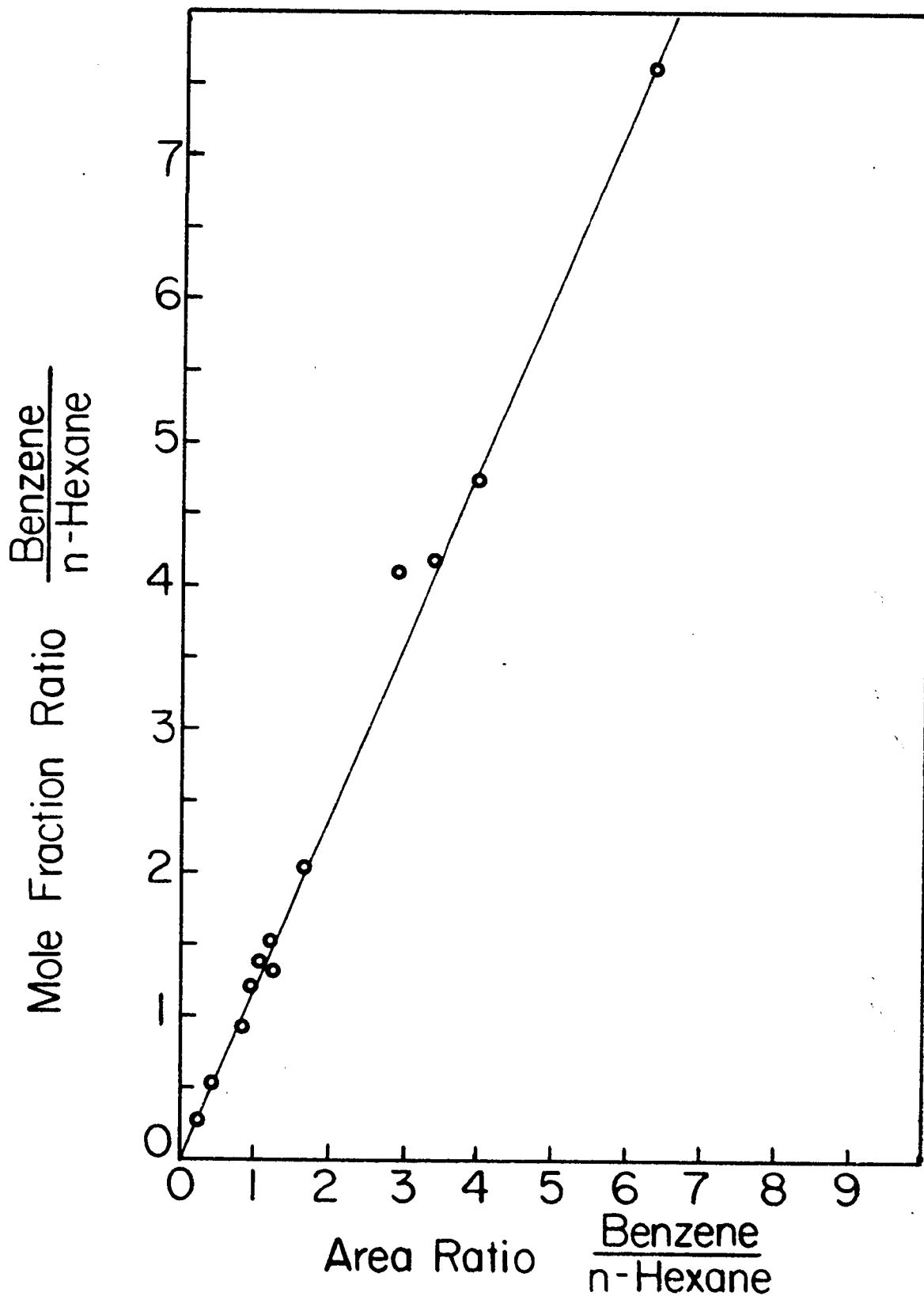


Fig. 33. Calibration curve of (Benzene/n-Hexane) mole fraction vs. (Benzene/n-Hexane) area for the ternary system

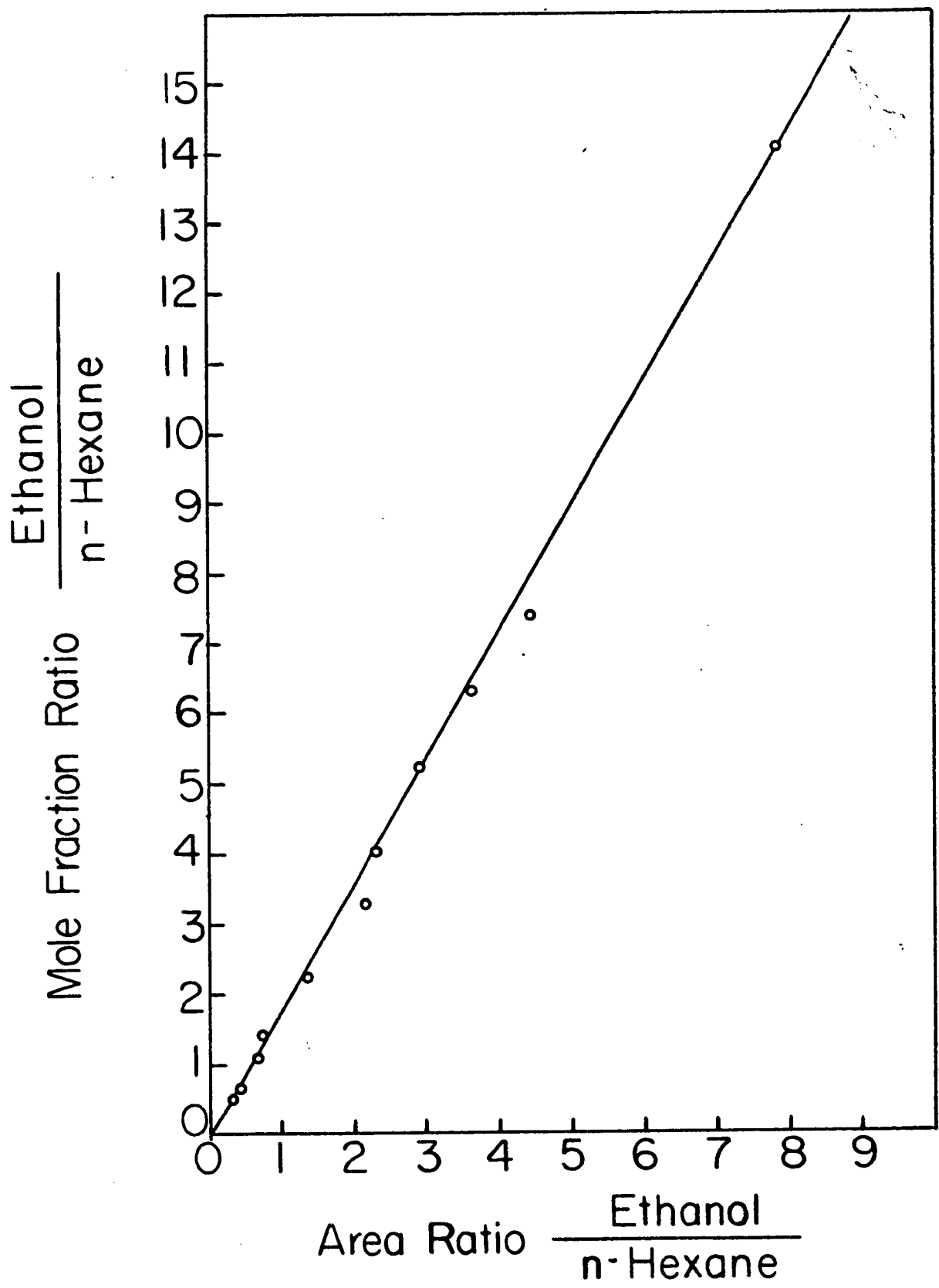


Fig. 34. Calibration curve of (Ethanol/n-Hexane) mole fraction vs. (Ethanol/n-Hexane) area for the ternary system

TABLE 15

Redlich-Kister Constants for the Binary Systems
of n-Hexane-Ethanol, n-Hexane-Benzene and Ethanol-Benzene at 55°C.

System: n-Hexane(1)-Ethanol(2)

$$B_{12} = 0.9532$$

$$C_{12} = -0.056$$

$$D_{12} = 0.1893$$

System: Ethanol(2)-Benzene(3)

$$B_{23} = 0.6951$$

$$C_{23} = -0.122$$

$$D_{23} = -0.00145$$

System: n-Hexane(1)-Benzene(3)

$$B_{31} = 0.22146$$

$$C_{31} = 0.0356$$

$$D_{31} = 0.00037$$

TABLE 16

Equations for Solving the Ternary Constants
in the Redlich-Kister Equation

Run	$C_{123} + (x_2-x_3) D_1 + (x_3-x_1) D_2 + (x_1-x_2) D_3 = \frac{Q_{123}-Q_{12}-Q_{23}-Q_{31}}{x_1 x_2 x_3}$
2	$C_{123} - 0.2107 D_1 - 0.5020 D_2 + 0.7126 D_3 = 2.2888$
3	$C_{123} - 0.4265 D_1 + 0.0392 D_2 + 0.4573 D_3 = 1.7838$
6	$C_{123} - 0.0882 D_1 - 0.3940 D_2 + 0.4822 D_3 = 0.8380$
7	$C_{123} - 0.1789 D_1 - 0.2903 D_2 + 0.4692 D_3 = 1.1275$
8	$C_{123} - 0.4064 D_1 + 0.0484 D_2 + 0.3580 D_3 = 0.9133$
10	$C_{123} - 0.0123 D_1 - 0.3357 D_2 + 0.3480 D_3 = 0.8185$
11	$C_{123} - 0.3242 D_1 + 0.0617 D_2 + 0.2625 D_3 = 1.2078$
12	$C_{123} - 0.4873 D_1 + 0.2729 D_2 + 0.2144 D_3 = 1.4973$
15	$C_{123} + 0.0023 D_1 - 0.1909 D_2 + 0.1886 D_3 = 0.7910$
16	$C_{123} - 0.2044 D_1 + 0.0311 D_2 + 0.1733 D_3 = 0.9046$
21	$C_{123} + 0.2214 D_1 - 0.0595 D_2 - 0.1619 D_3 = 0.6798$
22	$C_{123} + 0.0144 D_1 + 0.0856 D_2 - 0.1000 D_3 = 0.7250$
24	$C_{123} - 0.4302 D_1 + 0.4626 D_2 - 0.0324 D_3 = 1.4272$
25	$C_{123} - 0.6570 D_1 + 0.6716 D_2 - 0.0146 D_3 = 1.4226$
28	$C_{123} + 0.2704 D_1 + 0.0281 D_2 - 0.2985 D_3 = 0.8074$
29	$C_{123} + 0.0508 D_1 + 0.2000 D_2 - 0.2508 D_3 = 0.7204$
30	$C_{123} - 0.4240 D_1 + 0.5509 D_2 - 0.1269 D_3 = 1.2666$
33	$C_{123} + 0.0350 D_1 + 0.3084 D_2 - 0.3434 D_3 = 1.0044$
39	$C_{123} + 0.3540 D_1 + 0.2126 D_2 - 0.5666 D_3 = 2.3852$
40	$C_{123} + 0.1113 D_1 + 0.3565 D_2 - 0.4678 D_3 = 1.2891$
43	$C_{123} + 0.1193 D_1 + 0.4057 D_2 - 0.5250 D_3 = 3.4814$

TABLE 17

Comparison of Experimental and Calculated Q123

Run	$\frac{Q_{123}(\text{expt}) - Q_{12} - Q_{23} - Q_{31}}{x_1 x_2 x_3}$	$\frac{Q_{123}(\text{calcd}) - Q_{12} - Q_{23} - Q_{31}}{x_1 x_2 x_3}$	Q123 (expt)	Q123 (calcd)
2	2.2888	0.9537	0.0692	0.0632
3	1.7836	1.2033	0.0736	0.0715
6	0.8380	1.0355	0.1621	0.1664
7	1.1275	1.0769	0.1512	0.1502
8	0.8133	1.2246	0.1218	0.1286
10	0.8185	1.0815	0.1964	0.2035
11	1.2078	1.2467	0.1735	0.1725
12	1.4973	1.3349	0.1136	0.1106
15	0.7910	1.1646	0.2221	0.2346
16	0.9046	1.2511	0.2008	0.2121
21	0.6798	1.2769	0.2455	0.2653
22	0.7250	1.3205	0.2367	0.2581
24	1.4272	1.4506	0.1825	0.1830

..... continued

TABLE 17 (continued)

Run	$\frac{Q_{123}(\text{expt}) - Q_{12} - Q_{23} - Q_{31}}{x_1 x_2 x_3}$	$\frac{Q_{123}(\text{calcd}) - Q_{12} - Q_{23} - Q_{31}}{x_1 x_2 x_3}$	$Q_{123}(\text{expt})$	$Q_{123}(\text{calcd})$
25	1.4226	1.5263	0.1173	0.1183
26	0.8074	1.3344	0.2397	0.2553
29	0.7204	1.3906	0.2300	0.2504
30	1.2666	1.5008	0.1772	0.1811
33	1.0044	1.4461	0.2219	0.2319
39	2.3052	1.4519	0.2057	0.1931
40	1.2092	1.4885	0.2024	0.2049
43	3.4824	1.5173	0.1939	0.1833

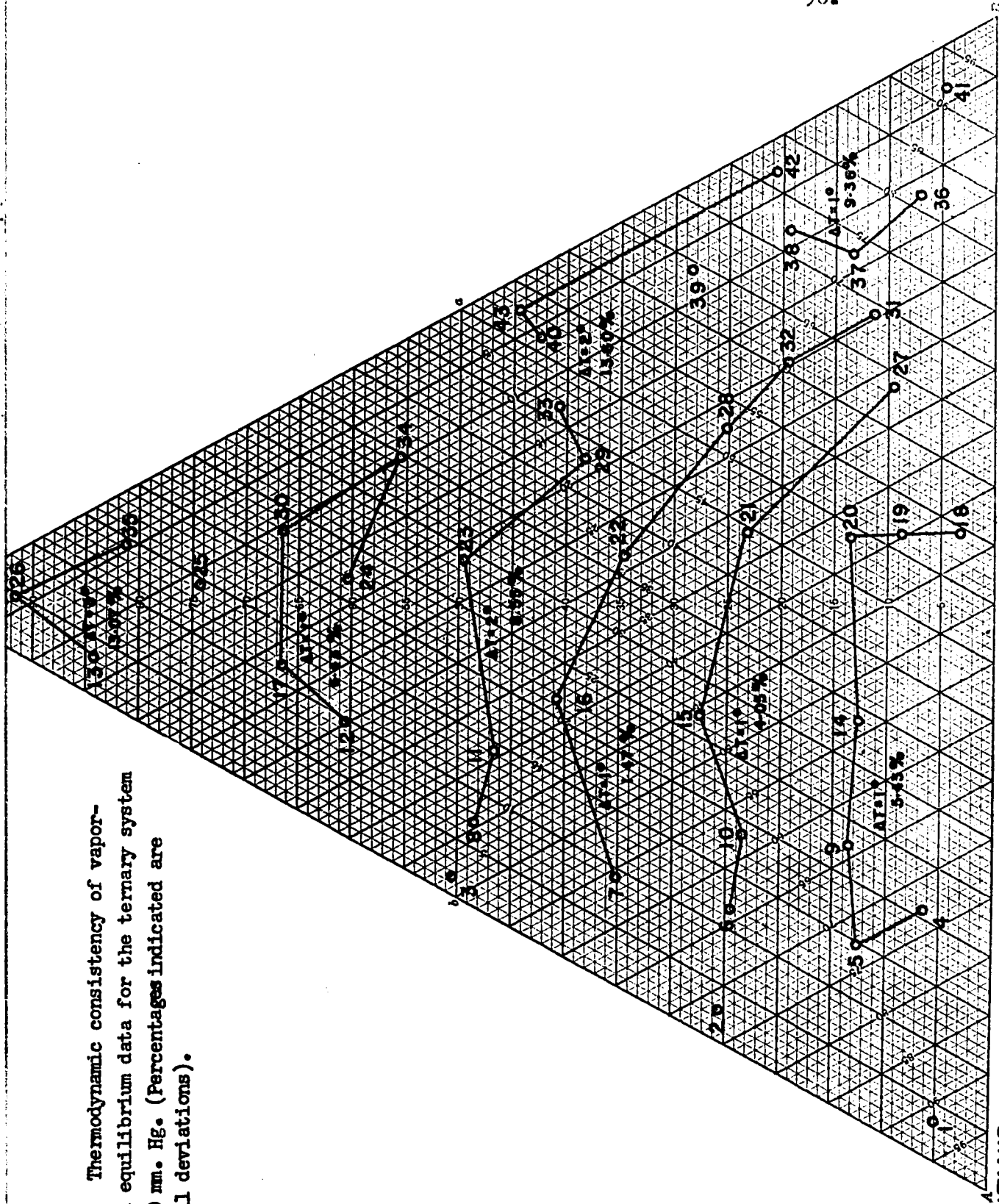


Fig. 35. Thermodynamic consistency of vapor-liquid equilibrium data for the ternary system at 760 mm. Hg. (Percentages indicated are overall deviations).

n-HEXANE

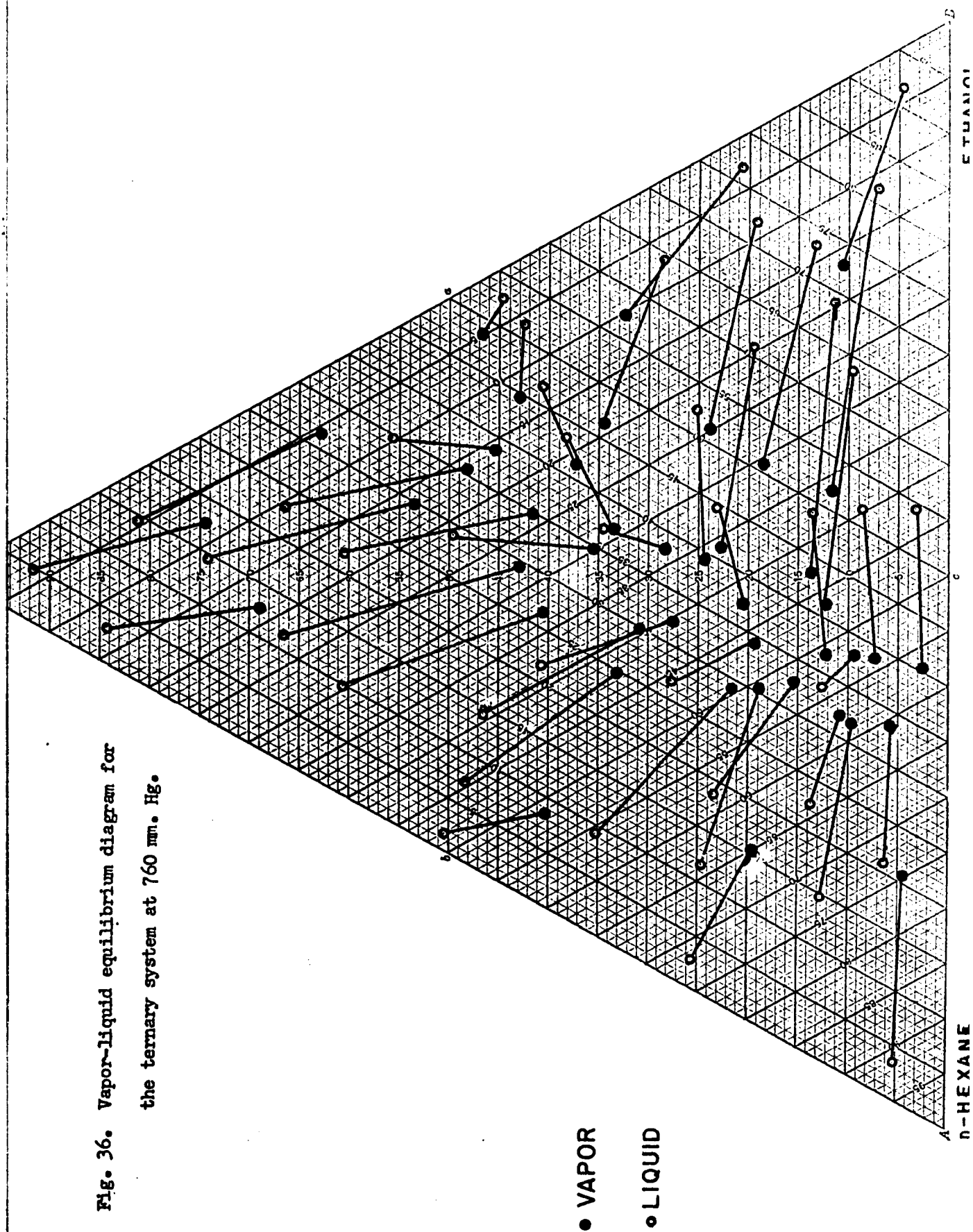


Fig. 36. Vapor-liquid equilibrium diagram for the ternary system at 760 mm. Hg.

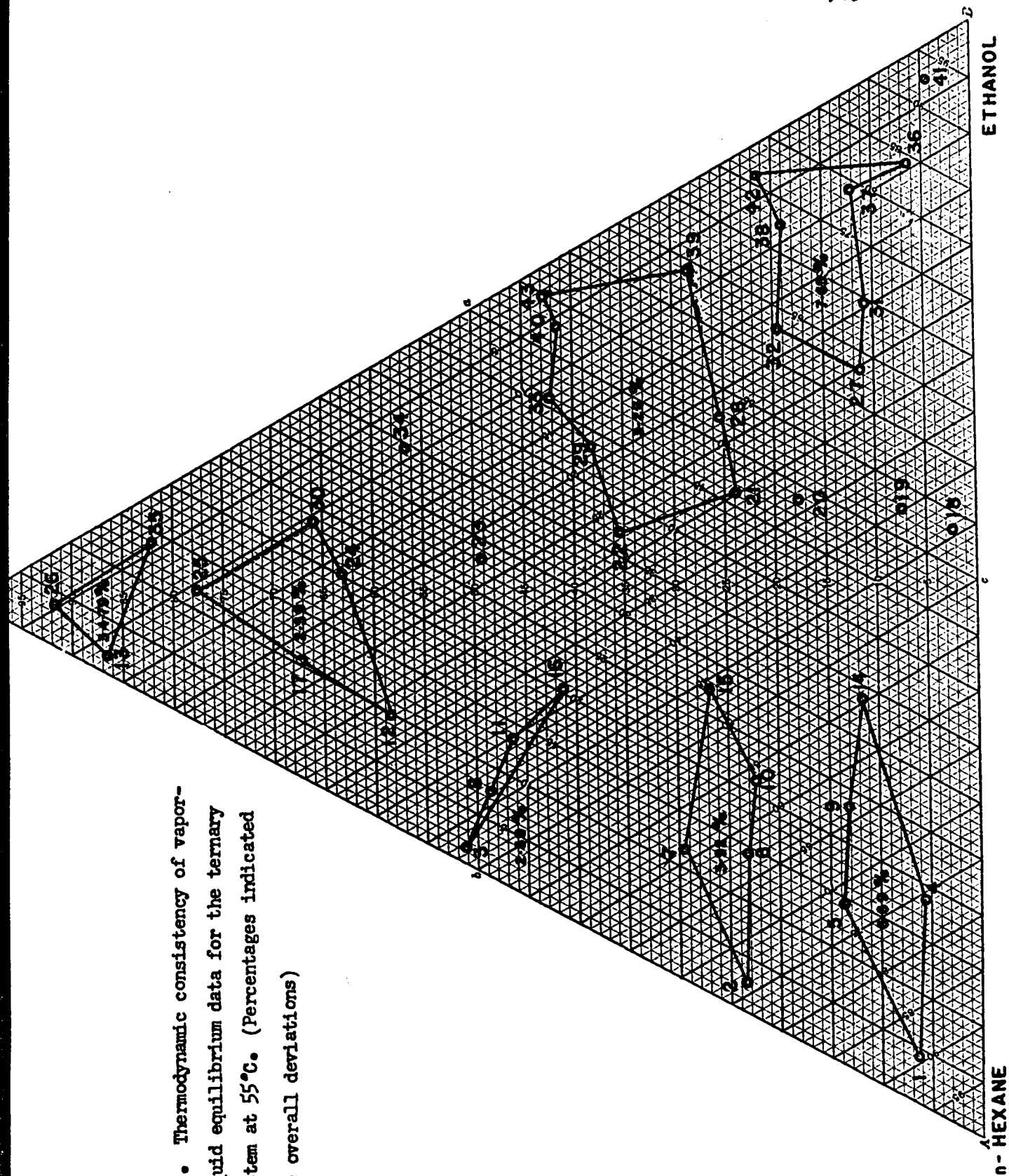


Fig. 37. Thermodynamic consistency of vapor-liquid equilibrium data for the ternary system at 55°C. (Percentages indicated are overall deviations)

n-HEXANE

ETHANOL

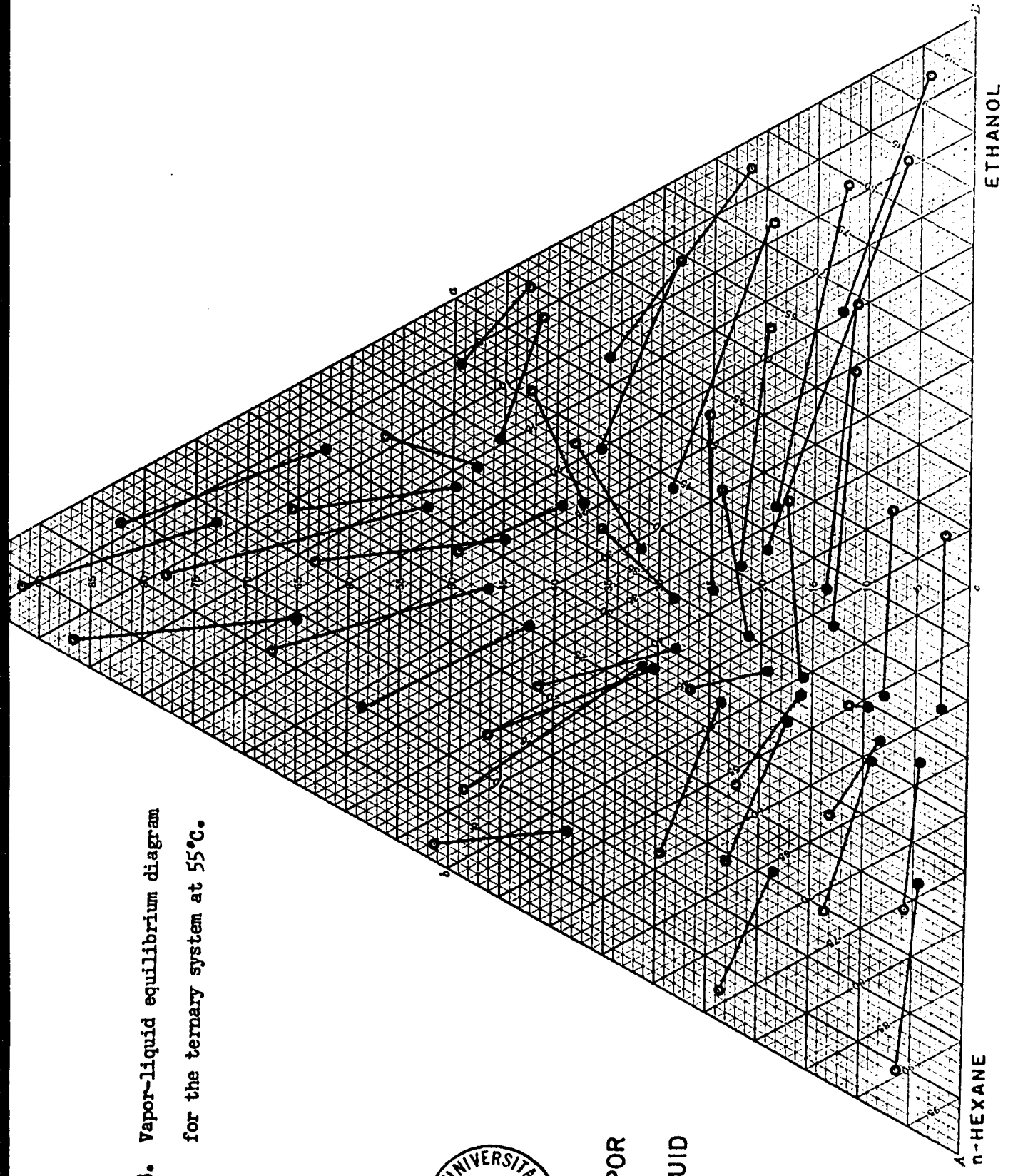


Fig. 38. Vapor-liquid equilibrium diagram for the ternary system at 55°C.



● VAPOR

○ LIQUID

PART II

Prediction of Binary Vapor-Liquid Equilibrium Data

INTRODUCTION

Although numerous experimentally determined vapor-liquid equilibrium data are available in the literature (32, 33), methods which permit extension of these values are still desired. There are many methods proposed for extending and predicting purposes (10, 34, 35, 36, 37, 38, 39). In order to extend data to various temperature and pressure conditions, most of the available methods generally require data obtained at two or more conditions (isothermal and/or isobaric) as primary information. The methods developed from the Gibbs-Duhem equation that involve the conversion of equilibrium data to activity coefficients and its subsequent reconversion to equilibrium compositions suffer from laborious calculations. The algebraic methods using equations which relate directly vapor-liquid equilibrium compositions are simple to use, but suffer from the drawback of not providing boiling points or total pressures for the isobaric and isothermal conditions respectively. It seems desirable to develop an extrapolation method which would provide complete equilibrium values (temperature-equilibrium compositions for isobaric conditions and total pressure-equilibrium compositions for isothermal conditions) at various conditions, using minimum experimental values as primary information and yet is simple to use. This investigation proposes an empirical method which permits the prediction of complete binary vapor-liquid equilibrium values under various conditions, isothermal and isobaric, if the equilibrium data for the system concerned are available over the complete concentration range at any one isothermal or isobaric condition.

PROPOSED METHOD

For a binary solution which deviates from the Raoult's law, the relationships between the equilibrium compositions may be expressed by

$$P y_1 = x_1 \gamma_1 P_1 \quad (28)$$

$$P y_2 = x_2 \gamma_2 P_2 \quad (29)$$

and

$$P = x_1 \gamma_1 P_1 + x_2 \gamma_2 P_2 \quad (30)$$

at low pressures. At high pressures and if the vapor phase obeys the Lewis-Randall ideal-solution rule over the complete concentration range, all the pressure terms of Equations 28 to 30 may be replaced by fugacities evaluated from the properties of the pure components.

If the liquid solution is an ideal one, the quantities γ_1 and γ_2 are equal to unity, and

$$x_1^* = \frac{P - P_2}{P_1 - P_2} \quad (31)$$

and

$$y_1^* = \left(\frac{P - P_2}{P_1 - P_2} \right) \left(\frac{P_1}{P} \right) \quad (32)$$

Therefore, for systems which have ideal liquid solution and ideal vapor phase over the range of conditions interested, the evaluation of $t-x-y$ and $P-x-y$ for isobaric and isothermal conditions, respectively, may be obtained by using Equations 31 and 32 in a simple manner.

In this investigation, pseudo mole fractions, x_1' and y_1' are defined by using the right-hand sides of Equations 31 and 32 respectively, for non-ideal liquid solutions. For a given P - t - x - y measurement, the pseudo mole fractions may be evaluated using the experimentally measured values by means of Equations 31 and 32. It is assumed that these calculated values are constant, corresponding to the experimental x and y values. In other words, the relationships between x and x' , and y and y' are assumed to be constant, independent of variations in temperature and pressure. These relationships calculated from the basic information are used for predicting equilibrium data at other conditions. The proposed method is limited to non-azeotropic solutions.

If the basic information available is a set of isobaric data (t - x - y at P_1) and if one is interested in predicting equilibrium data at another total pressure, P_2 , the prediction may be carried out as follows:

(1) Using the basic information, calculate x_1' and y_1' at regular intervals (for example, 0.1 mole fraction) of x_1 and y_1 by means of Equations 31 and 32.

(2) Calculate x_1' and y_1' at P_2 between the boiling points of the pure components at P_2 . This may proceed in the following manner:

- (a) Select a temperature
- (b) Evaluate the vapor pressures of the pure components at this temperature.

(c) Calculate x_1' and y_1' using Equations 31 and 32, in which all the pressure terms (P_2 , p_1 and p_2) are now known quantities.

(d) Plot $t-x_1'$ and $t-y_1'$.

(3) Evaluate $t-x_1$ and $t-y_1$ from the x_1' and y_1' values obtained in step 1 and from the plot $t-x_1'-y_1'$ obtained in step 2. The resulted $t-x_1-y_1$ plot gives the equilibrium data desired at the condition P_2 . There is no trial-and-error procedure involved.

If the basic information available is a set of isobaric data but equilibrium data at an isothermal condition is desired, the following procedure may be followed:

(1) Calculate x_1' and y_1' at regular intervals as before.

(2) Calculate total pressure values at the isothermal condition in question using the following expressions:

$$P = x_1' (P_1 - P_2) + P_2 \quad (33)$$

and

$$P = \frac{P_1 P_2}{P_1 - (P_1 - P_2) y_1'} \quad (34)$$

The x_1' and y_1' values obtained from step 1 may be substituted directly into these expressions. Since the values x_1' and y_1' of step 1 are obtained at regular intervals of mole fractions, the total pressures obtained from Equation 33 would correspond to x values at regular intervals at the isothermal condition concerned and similarly, the total pressures obtained from Equation 34 would correspond to y values at regular intervals at the same isothermal condition. A plot of $P-x_1-y_1$

would provide the complete equilibrium values at the desired temperature.

Should the basic information available be a set of equilibrium data obtained at an isothermal condition, the same procedure as presented above may be employed for predicting equilibrium values at other conditions.

In the event when it is desirable to predict equilibrium values at more than one condition, further predictions may be carried out using the Other's reference plot (38, 40) as an alternate procedure. Other assumed that the ratio of the latent heat of vaporization of a pure component to that of a reference substance at the same temperature is constant. A linear relationship is obtained relating the vapor pressure of the pure component and the vapor pressure of the reference substance on a log-log plot. Or

$$\log p = a + b \log P_{\text{ref}} \quad (35)$$

This relationship may also be applied to solutions of fixed compositions. Thus, from the basic information and the values predicted at one condition, two reference plots may be constructed, the $t-x$ and $P-x$ values may be obtained directly from a reference plot concerning the liquid compositions and the $t-y$ and $P-y$ values may be obtained directly from a reference plot concerning the vapor compositions. A replotting of $t-x-y$ or $P-x-y$ would provide the equilibrium values at the isobaric or isothermal conditions desired.

TESTING THE PROPOSED METHOD

The proposed method has been tested for eight non-azeotropic systems measured at nineteen different experimental conditions. The predicted results are summarized in Table 18. It may be seen from the table that for the systems methylcyclohexane-toluene and 2,2,4-trimethylpentane-toluene, only $t-x$ values are predicted. This is due to the fact that the selected basic information for the system methylcyclohexane-toluene provides only reliable $t-x$ data (16) and for the system 2,2,4-trimethylpentane-toluene the selected basic information does not include the $t-y$ values. The deviations are evaluated at 0.1 mole fraction intervals in x and y with the exception of the system 2,2,4-trimethylpentane-toluene, where the selected basic information provides the boiling point data only at 0.2 liquid mole fraction intervals.

The maximum and the average deviations in boiling point predictions are 1.9°C and 0.4°C, respectively. The maximum and the average deviations in total pressure predictions are 1.4 mm.Hg. and 0.5 mm.Hg., respectively. Although the agreement between the calculated and the experimental total pressure values seems to be better than the agreement between the calculated and the experimental boiling point values, the difference in agreement may very well be contributed to the difference in quality of the experimental data. In general, all the predicted values may be considered to be in good agreement with the experimental values.

The proposed method has also been tested for the following azeotropic systems: methanol-benzene, ethanol-toluene, acetone-chloroform, benzene-cyclohexane, and ethanol-water. The calculated boiling point and total pressure values deviate considerably from the experimental data. It is therefore suggested that the proposed method be limited to non-azeotropic systems.

SAMPLE CALCULATIONS

The prediction of vapor-liquid equilibrium data for the system heptane-ethylbenzene at 100 mm.Hg. illustrates the procedure of the calculation. The pseudo-mole fractions x_1' and y_1' are calculated from the experimental equilibrium data at 760 mm.Hg. For example, at $x_1 = 0.30$, the boiling point $t = 117.48^\circ\text{C}$ at 760 mm.Hg. At this temperature,

$$P_1 = 1293 \text{ mm. Hg.}$$

and

$$P_2 = 145.5 \text{ mm. Hg.}$$

Therefore

$$x_1' = 0.3711$$

similarly, at

$$y_1 = 0.30$$

$$t = 127.35^\circ\text{C}$$

$$P_1 = 1666 \text{ mm. Hg.}$$

$$P_2 = 594.7 \text{ mm. Hg.}$$

and

$$y_1' = 0.3382$$

The calculated x_1' and y_1' values at 0.1 mole fraction intervals are listed in Table 19.

At $P = 100 \text{ mm. Hg.}$, the boiling points of the pure components are 41.77°C and 74.11°C for heptane and ethylbenzene, respectively.

Between these two temperatures, x_1' and y_1' are evaluated. For example, at $t = 66.0^\circ\text{C}$,

$$P_1 = 261.6 \text{ mm. Hg.}$$

$$P_2 = 72.06 \text{ mm. Hg.}$$

$$x_1' = 0.1174$$

and

$$y_1' = 0.3856$$

The calculated x_1' and y_1' values are plotted with the temperature as shown in Figure 39. From this figure, the boiling points at 100 mm. Hg. corresponding to the x_1' and y_1' values as listed in Table 19, are evaluated. For example, at $x_1' = 0.3711$, $t = 57.0^\circ\text{C}$, this is the boiling point of $x_1 = 0.30$ at 100 mm. Hg. Similarly, at $y_1' = 0.3382$, $t = 67.2^\circ\text{C}$, this is the boiling point corresponding to $y_1 = 0.30$. The t - x and t - y values obtained in this manner are plotted and compared with the experimental values (2) in Figure 40. In this figure, the predicted t - x - y values for the same system at 300 mm. Hg. are also presented and compared with the experimental values.

CONCLUSION

An empirical method is proposed which permits the prediction of binary vapor-liquid equilibrium data under various conditions (t - x - y values at isobaric conditions and P - x - y values at isothermal conditions) if equilibrium data for the system concerned are available over the complete concentration range at any one condition, isothermal or isobaric. The proposed method is simple to use and does not involve any trial-and-error procedure. It is, however, limited to non-azeotropic binary solutions. The proposed method has been tested with eight systems at nineteen experimental conditions. Good agreements are obtained in all cases.

APPENDIX II

TABLE 18

Comparison of Experimental and Calculated Values

System	Basic Information	Conditions Predicted	Liquid Phase	Deviations	
				Ave.	Max.
1. Carbon Tetrachloride-Benzene	P-x-y at 70°C (41)	P-x-y at 40°C (41)	1.3 mm.Hg.	0.8	1.4
			1.1		
2. Carbon Tetrachloride-Cyclohexane	P-x-y at 70°C (42)	P-x-y at 40°C (42)	-0.3 mm.Hg.	0.1	-0.2
			0.1		
3. Heptane-Ethylbenzene	t-x-y at 760 mm.Hg. (2)	t-x-y at 100 mm.Hg. (2)	0.6°C.	0.3	-0.3
			0.2		
4. Heptane-Toluene	t-x-y at 760 mm.Hg. (2)	t-x-y at 150 mm.Hg. (2)	-0.5°C.	0.2	-0.7
			0.3		
5. Methylcyclohexane-Toluene	t-x-y at 760 mm.Hg. (43)	t-x-y at 400 mm.Hg. (44)	1.9°C.	0.6	-0.3
			0.1		
		t-x-y at 300 mm.Hg. (2)	1.1°C.	0.4	0.2
		t-x-y at 200 mm.Hg. (44)	-0.7°C.	0.4	
		t-x-y at 200 mm.Hg. (44)	0.9°C.	0.5	

.... continued

TABLE 18 (continued)

System	Basic Information	Conditions Predicted	Liquid Phase Max.	Deviations	
				Phase Ave.	Vapor Phase Max. Ave.
6. Naphthalene- <i>n</i> -Tetradecane	t-x-y at 760 mm.Hg. (45)	t-x-y at 200 mm.Hg. (45)	0.5°C	0.3	1.2 0.7
		t-x-y at 400 mm.Hg. (45)	-1.0°C.	0.6	-1.0 0.7
		t-x-y at 100 mm.Hg. (45)	-1.0°C.	0.6	1.8 0.8
		t-x-y at 50 mm.Hg. (45)	-0.8°C.	0.5	1.5 0.7
		t-x-y at 20 mm.Hg. (45)	0.8°C.	0.3	1.3 0.7
7. <i>n</i> -Octane-Ethylbenzene	t-x-y at 760 mm.Hg. (46)	t-x-y at 10 mm.Hg. (45)	1.5°C.	0.6	1.8 1.1
		t-x-y at 200 mm.Hg. (46)	0.6°C.	0.2	0.4 0.2
		t-x-y at 500 mm.Hg. (46)	0.2°C.	0.1	0.3 0.1
8. 2,2,4-Trimethylpentane-	t-x-y at 760 mm.Hg. (47)	t-x-y at 50 mm.Hg. (46)	-0.5°C.	0.3	-0.5 0.3
		t-x-y at 1.06 atm. (47)	0.3°C.	0.2	
		t-x-y at 2.02 atm. (47)	0.6°C.	0.6	

TABLE 19

Pseudo Mole Fraction Values Calculated for System
Heptane-ethylbenzene from the Experimental
Equilibrium Data at 760 mm. Hg.

x_1	x_1'	y_1	y_1'
0.1	0.1388	0.1	0.1173
0.2	0.2602	0.2	0.2262
0.3	0.3711	0.3	0.3382
0.4	0.4728	0.4	0.4485
0.5	0.5651	0.5	0.5579
0.6	0.6532	0.6	0.6621
0.7	0.7387	0.7	0.7594
0.8	0.8255	0.8	0.8484
0.9	0.9134	0.9	0.9293

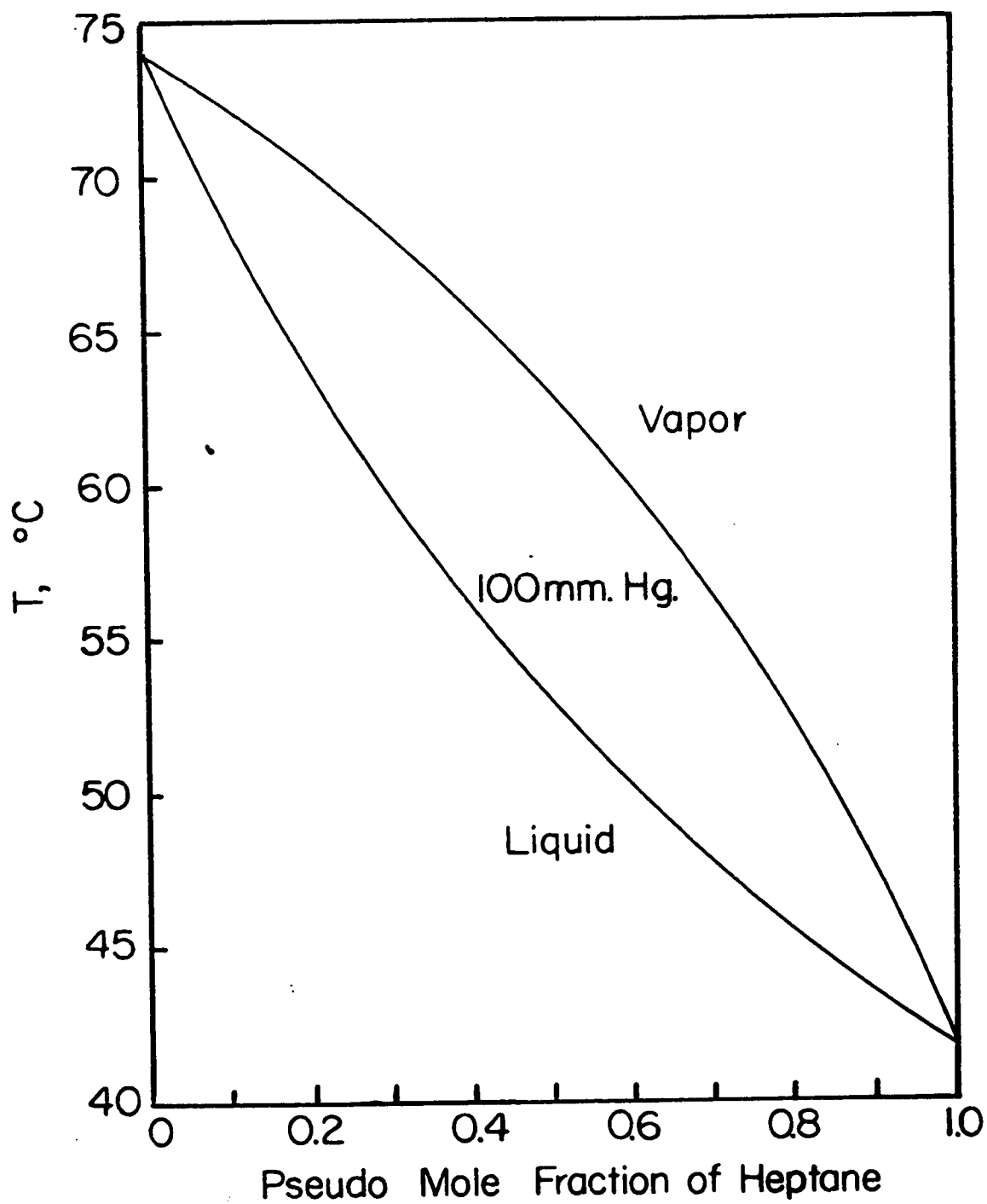


Fig. 39. Calculated t - x '- y ' values for the system heptane-ethyl benzene at 100 mm. Hg.

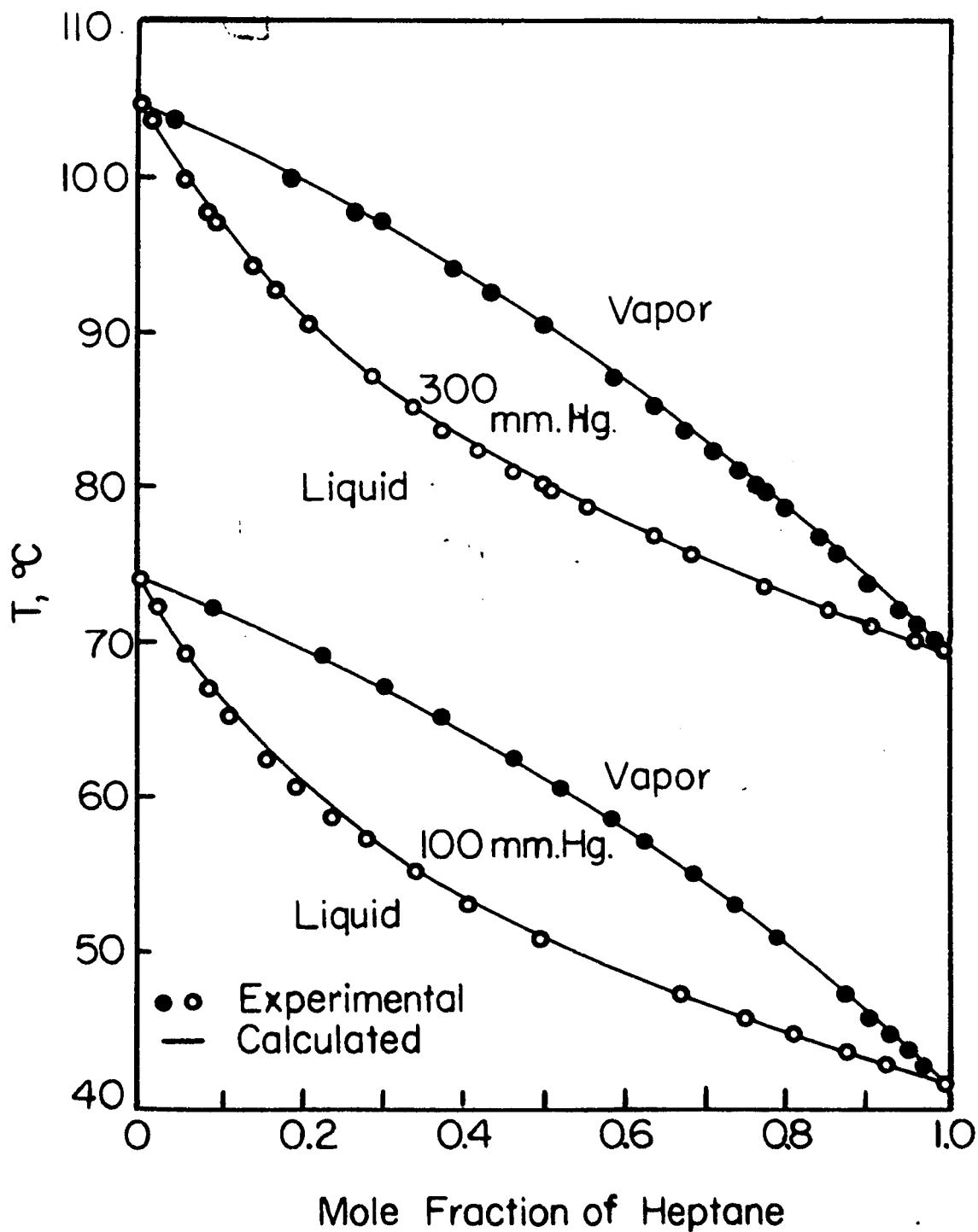


Fig. 40. Predicted vapor-liquid equilibrium curve and data (2) for the system heptane-ethylbenzene

Prediction of Binary Vapor-Liquid Equilibrium Data

JAMES C. K. HO and BENJAMIN C.-Y. LU

Department of Chemical Engineering, University of Ottawa,
Ottawa, Ontario, Canada

This handy method gives temperatures or pressures, as well as equilibrium data

ALTHOUGH numerous experimentally determined vapor-liquid equilibrium data are available in the literature, methods which permit extension of these values are still desired. In order to extend data to various temperature and pressure conditions, most of the available methods generally require data obtained at two or more conditions—*isothermal and/or isobaric*—as primary information. The methods developed from the Gibbs-Duhem equation that involve the conversion of equilibrium data to activity coefficients and its subsequent reconversion to equilibrium compositions suffer from laborious calculations. The algebraic methods using equations which relate directly vapor-liquid equilibrium compositions are simple to use, but suffer from the drawback of not providing boiling points or total pressures for the *isobaric and isothermal* conditions, respectively. It seems desirable to develop an extrapolation method which would provide complete equilibrium values (temperature-equilibrium compositions for *isobaric* conditions and total pressure-equilibrium compositions for *isothermal* conditions) at various conditions, using minimum

experimental values as primary information and yet is simple to use. This investigation proposes an empirical method which permits the prediction of complete binary vapor-liquid equilibrium values under various conditions, *isothermal and isobaric*, if the equilibrium data for the system concerned are available over the complete concentration range at any one *isothermal or isobaric* condition.

Proposed Method

For a binary solution which deviates from the Raoult's law, the relationships between the equilibrium compositions may be expressed by

$$\pi y_1 = x_1 \gamma_1 p_1 \quad (1)$$

$$\pi y_2 = x_2 \gamma_2 p_2 \quad (2)$$

$$\pi = x_1 \gamma_1 p_1 + x_2 \gamma_2 p_2 \quad (3)$$

at low pressures. At high pressures and if the vapor phase obeys the Lewis-Randall ideal-solution rule over the complete concentration range, all the pressure terms of Equations 1 to 3 may be replaced by fugacities evaluated from the properties of the pure components.

If the liquid solution is an ideal one, the quantities γ_1 and γ_2 are equal to unity, and

$$x_1^o = \frac{\pi - p_2}{p_1 - p_2} \quad (4)$$

$$y_1^o = \left(\frac{\pi - p_2}{p_1 - p_2} \right) \left(\frac{p_1}{\pi} \right) \quad (5)$$

Therefore, for systems which have ideal liquid solution and ideal vapor phase over the range of conditions interested, the evaluation of *t-x-y* and π -*x-y* for *isobaric and isothermal* conditions, respectively, may be obtained by using Equations 4 and 5 in a simple manner.

In this investigation, pseudo mole fractions, x_1' and y_1' are defined by using the right-hand sides of Equations 4 and 5, respectively, for nonideal liquid solutions. For a given π -*t-x-y* measurement, the pseudo mole fractions may be evaluated using the experimentally measured values by means of Equations 4 and 5. It is assumed that these calculated values are constant, corresponding to the experimental *x* and *y* values. In other words, the relationships between *x* and x' , and *y* and y' are assumed to be constant, independent of variations in temperature and pressure. These relationships calculated from the basic information are used for predicting equilibrium data at other conditions. The proposed method is limited to nonazeotropic solutions.

Applying the Method

● If the basic information available is a set of *isobaric* data (*t-x-y* at π_1), and if one is interested in predicting equilibrium data at another total pressure, π_2 , the prediction may be carried out as follows:

A. Using the basic information, calculate x_1' and y_1' at regular intervals (for example, 0.1 mole fraction) of x_1 and y_1 by means of Equations 4 and 5.

B. Calculate x_1' and y_1' at π_2 between the boiling points of the pure components at π_2 . This may proceed in the following manner:

Select a temperature.
Evaluate the vapor pressures of the pure components at this temperature.

Calculate x_1' and y_1' using Equations 4 and 5, in which all the pressure terms— π_2 , p_1 , and p_2 —are now known quantities. Plot *t-x'* and *t-y'*.

What you need

► Equilibrium data for the system over the complete composition range at any one *isothermal or isobaric* condition

What you can do

► Calculate temperature and composition at various total pressure conditions

► Calculate pressure and composition at various temperature conditions

Where procedure applies

► Nonazeotropic systems only

C. Evaluate $t - x_1$ and $t - y_1$ from the x_1' and y_1' values obtained in step A and from the plot $t - x_1' - y_1'$ obtained in step B. The resulted $t - x_1 - y_1$ plot gives the equilibrium data desired at the condition π_2 . There is no trial-and-error procedure involved.

• If the basic information available is a set of isobaric data but equilibrium data at an isothermal condition is desired, the following procedure may be followed:

A. Calculate x_1' and y_1' at regular intervals as before.

B. Calculate total pressure values at the isothermal condition in question using the following expressions:

$$\pi = x_1'(\rho_1 - \rho_2) + \rho_2 \quad (6)$$

$$y_1' = \frac{\rho_1 \rho_2}{\rho_1 - (\rho_1 - \rho_2) x_1'} \quad (7)$$

The x_1' and y_1' values obtained from step A may be substituted directly into these expressions. Since the values x_1' and y_1' of step A are obtained at regular intervals of mole fractions, the total pressures obtained from Equation 6 would correspond to x values at regular intervals at the isothermal condition concerned and, similarly, the total pressure obtained from Equation 7 would correspond to y values at regular intervals at the same isothermal condition. A plot of $\pi - x_1 - y_1$ would provide the complete equilibrium values at the desired temperature.

• Should the basic information available be a set of equilibrium data obtained at an isothermal condition, the same procedure as presented above may be employed for predicting equilibrium values at other conditions.

In the event it is desirable to predict equilibrium values at more than one condition, further predictions may be carried out using Othmer's reference

plot (4, 5) as an alternate procedure. Othmer assumed that the ratio of the latent heat of vaporization of a pure component to that of a reference substance at the same temperature is constant. A linear relationship is obtained relating the vapor pressure of the pure component and the vapor pressure of the reference substance on a log-log plot. Or

$$\log p = a + b \log p_{ref.} \quad (8)$$

This relationship may also be applied to solutions of fixed compositions. Thus, from the basic information and the values predicted at one condition, two reference plots may be constructed, the $t-x$ and $\pi-x$ values may be obtained directly from a reference plot concerning the liquid compositions and the $t-y$ and $\pi-y$ values may be obtained directly from a reference plot concerning the vapor compositions. A replotting of $t-x-y$ or $\pi-x-y$ would provide the equilibrium values at the isobaric or isothermal conditions desired.

Testing The Proposed Method

The proposed method has been tested for eight nonazeotropic systems measured at nineteen different experimental conditions. The predicted results are summarized in Table I, which shows that for the systems methylcyclohexane-toluene and 2,2,4-trimethylpentane-toluene, only $t-x$ values are predicted. This is due to the fact that the selected basic information for the system methylcyclohexane-toluene provides only reliable $t-x$ data (9) and for the system 2,2,4-trimethylpentane-toluene the selected basic information does not include the $t-y$ values. The derivations are evaluated at 0.1 mole fraction intervals in x and y with the exception of the

system 2,2,4-trimethylpentane-toluene, where the selected basic information provides the boiling point data only at 0.2 liquid mole fraction interval.

The maximum and the average deviations in boiling point predictions are 1.9° C. and 0.4° C., respectively. The maximum and the average deviations in total pressure predictions are 1.4 and 0.5 mm. of Hg, respectively. Although the agreement between the calculated and the experimental total pressure values seems to be better than the agreement between the calculated and the experimental boiling point values, the difference in agreement may very well be contributed to the difference in quality of the experimental data. In general, all the predicted values may be considered to be in good agreement with the experimental values.

The proposed method has also been tested for the following azeotropic systems: methanol-benzene, ethanol-toluene, acetone-chloroform, benzene-cyclohexane, and ethanol-water. The calculated boiling point and total pressure values deviate considerable from the experimental data. It is therefore suggested that the proposed method be limited to nonazeotropic systems.

Sample Calculations

The prediction of vapor-liquid equilibrium data for the system heptane-ethylbenzene at 100 mm. of Hg illustrates the procedure of the calculation. The pseudo-mole fractions x_1' and y_1' are calculated from the experimental equilibrium data at 760 mm. of Hg. For example, at $x_1 = 0.30$, the boiling point $t = 117.48^\circ$ C. at 760 mm. of Hg. At this temperature.

$$p_1 = 1293 \text{ mm. Hg}$$

Table I. Comparison of Experimental and Calculated Values

System	Basic Information	Conditions Predicted	Deviations			
			Liquid Phase		Vapor Phase	
			Max.	Av.	Max.	Av.
Carbon tetrachloride-benzene	$\pi-x-y$ at 70° C. (8)	$\pi-x-y$ at 40° C. (8)	1.3 mm. Hg	0.8	1.4	1.1
Carbon tetrachloride-cyclohexane	$\pi-x-y$ at 70° C. (7)	$\pi-x-y$ at 40° C. (7)	-0.3 mm. Hg	0.1	-0.2	0.1
Heptane-ethylbenzene	$t-x-y$ at 760 mm. (5)	$t-x-y$ at 100 mm. (5)	0.6° C.	0.3	-0.3	0.2
		$t-x-y$ at 300 mm. (5)	-0.5° C.	0.2	-0.7	0.3
Hexane-toluene	$t-x-y$ at 760 mm. (5)	$t-x-y$ at 150 mm. (5)	1.9° C.	0.6	-0.3	0.1
		$t-x-y$ at 300 mm. (5)	1.1° C.	0.4	0.2	0.2
Methylcyclohexane-toluene	$t-x-y$ at 760 mm. (6)	$t-x-y$ at 400 mm. (10)	-0.7° C.	0.4		
		$t-x-y$ at 200 mm. (10)	0.9° C.	0.5		
Naphthalene-n-tetradecane	$t-x-y$ at 760 mm. (8)	$t-x-y$ at 400 mm. (8)	-1.0° C.	0.6	-1.0	0.7
		$t-x-y$ at 200 mm. (8)	0.5° C.	0.3	1.2	0.7
		$t-x-y$ at 100 mm. (8)	-1.0° C.	0.6	1.8	0.8
		$t-x-y$ at 50 mm. (8)	-0.8° C.	0.5	1.5	0.7
		$t-x-y$ at 20 mm. (8)	0.8° C.	0.3	1.3	0.7
n-Octane-ethylbenzene	$t-x-y$ at 760 mm. (11)	$t-x-y$ at 10 mm. (8)	1.5° C.	0.6	1.8	1.1
		$t-x-y$ at 500 mm. (11)	0.2° C.	0.1	0.3	0.1
		$t-x-y$ at 200 mm. (11)	0.6° C.	0.2	0.4	0.2
2,2,4-Trimethylpentane-toluene	$t-x-y$ at 760 mm. (1)	$t-x-y$ at 50 mm. (11)	-0.5° C.	0.3	-0.5	0.3
		$t-x-y$ at 4.06 atm. (1)	0.3° C.	0.2		
		$t-x-y$ at 2.02 atm. (1)	0.6° C.	0.6		

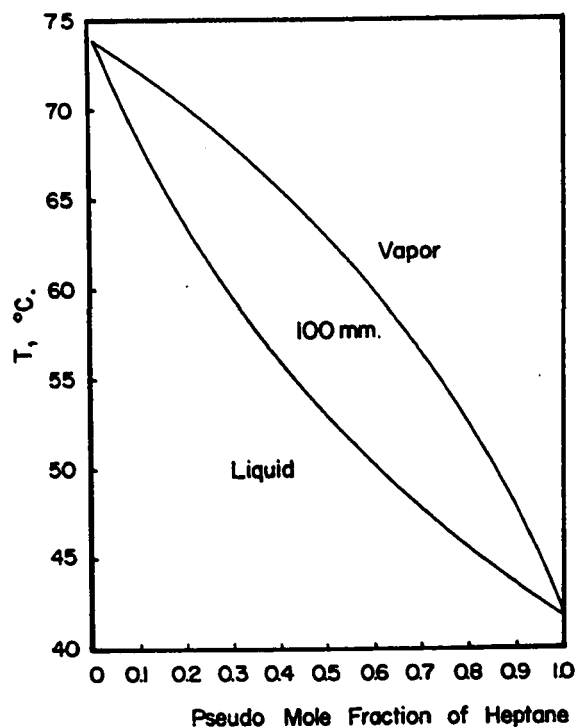


Figure 1. Calculated t - x' - y' values for the system heptane-ethylbenzene at 100 mm. of Hg

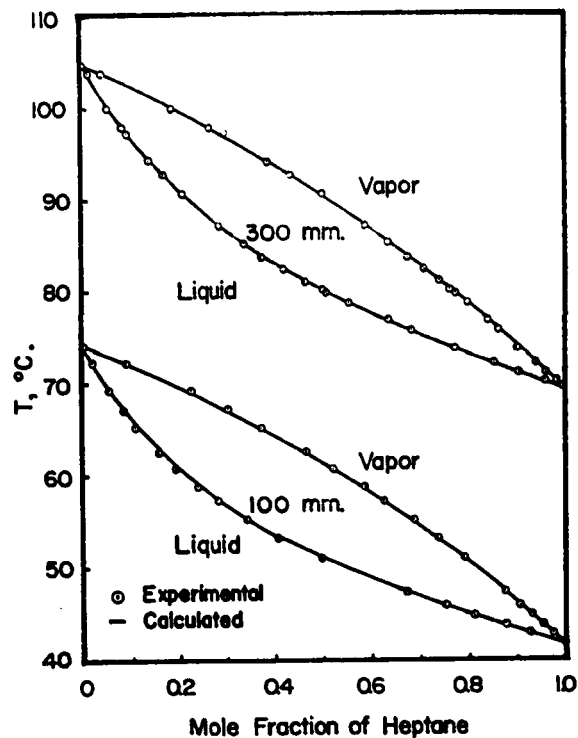


Figure 2. Predicted vapor-liquid equilibrium curve and data (3) for the system heptane-ethylbenzene

and

$$p_2 = 445.5 \text{ mm. of Hg}$$

Therefore

$$x_1' = 0.3711$$

Similarly, at

$$\begin{aligned} y_1 &= 0.30 \\ t &= 127.35^\circ \text{ C.} \\ p_1 &= 1666 \text{ mm. of Hg} \\ p_2 &= 594.7 \text{ mm. of Hg} \end{aligned}$$

and

$$y_1' = 0.3382$$

The calculated x_1' and y_1' values at 0.1 mole fraction intervals are listed in Table II.

At $\pi = 100$ mm. of Hg, the boiling points of the pure components are 41.77° C. and 74.11° C. for heptane and ethylbenzene, respectively. Between these two temperatures, x_1' and y_1' are

~~evaluated. For example, at $t = 66.0^\circ \text{ C.}$, two temperatures, x_1' and y_1' are evaluated. For example, at $t = 66.0^\circ \text{ C.}$,~~

$$p_1 = 261.6 \text{ mm. of Hg}$$

$$p_2 = 72.06 \text{ mm. of Hg}$$

$$x_1' = 0.1474$$

and

$$y_1' = 0.3856$$

The calculated x_1' and y_1' values are plotted with the temperature as shown in Figure 1. From this figure the boiling points at 100 mm. of Hg corresponding to the x_1' and y_1' values as listed in Table II are evaluated. For example, at $x_1' = 0.3711$, $t = 57.0^\circ \text{ C.}$, this is the boiling point of $x_1 = 0.30$ at 100 mm. of Hg. Similarly at $y_1' = 0.3382$, $t = 67.2^\circ \text{ C.}$, this is the boiling point corresponding to $y_1 = 0.30$. The t - x and t - y values obtained in this manner are plotted and compared with the experimental values (3) in Figure 2. In this figure, the predicted t - x - y values for the same system at 300 mm. of Hg are also presented and compared with the experimental values.

Acknowledgment

The authors are indebted to the National Research Council of Canada for financial support.

Nomenclature

t = boiling temperature
 p = vapor pressure
 π = total pressure
 x = liquid mole fraction
 y = vapor mole fraction
 γ = liquid activity coefficients

Superscript

$^\circ$ = ideal conditions
 $'$ = pseudo condition

Subscript

1 = component 1
 2 = component 2

Literature Cited

- (1) Gelus, E., Marple, S., Jr., Miller, M. E., *IND. ENG. CHEM.* **41**, 1757 (1949).
- (2) Haynes, S., Jr., Van Winkle, Matthew, *Ibid.*, **46**, 334 (1954).
- (3) Myers, H. S., *Ibid.*, **47**, 2215 (1955).
- (4) Othmer, D. F., *Ibid.*, **32**, 841 (1940).
- (5) Othmer, D. F., Gilmont, R., *Ibid.*, **36**, 858 (1944).
- (6) Quiggle, D., Fenske, M. R., *J. Am. Chem. Soc.* **55**, 1829 (1937).
- (7) Scatchard, G., Wood, S. E., Mochel, J. M., *Ibid.*, **61**, 3206 (1939).
- (8) Scatchard, G., Wood, S. E., Mochel, J. M., *Ibid.*, **62**, 712 (1940).
- (9) Thijsen, H. A. C., *Chem. Eng. Sci.* **4**, 75 (1955).
- (10) Weber, J. H., *IND. ENG. CHEM.* **47**, 454 (1955).
- (11) Yang, C. P., Van Winkle, Matthew, *Ibid.*, **47**, 293 (1955).

Table II. Pseudo Mole Fraction Values Are Calculated for System Heptane-Ethylbenzene from the Experimental Equilibrium Data at 760 Mm. Hg

x_1	x_1'	y_1	y_1'
0.1	0.1388	0.1	0.1173
0.2	0.2602	0.2	0.2262
0.3	0.3711	0.3	0.3382
0.4	0.4728	0.4	0.4485
0.5	0.5651	0.5	0.5579
0.6	0.6532	0.6	0.6621
0.7	0.7387	0.7	0.7594
0.8	0.8255	0.8	0.8484
0.9	0.9134	0.9	0.9293

RECEIVED for review December 1, 1960
 ACCEPTED February 9, 1961

ACKNOWLEDGEMENT

The author wishes to express his indebtedness to Dr. Benjamin C.-Y. Lu for his valuable suggestions and guidance in the course of this work.

Financial assistance from the National Research Council of Canada is greatly acknowledged.

The author is also very grateful to the Royal Military College of Canada, Kingston, Ontario, for permitting him to complete part of the thesis at the College.

He wishes to thank the graduate students of the Department, particularly Mr. A. Malek and Mrs. K.S.Y. Wu for valuable discussions held during the investigation, and Miss O. Boshko of the Computing Centre of Ottawa University.

NOTATION

A, B	=	constants of Margules equation
A, B	=	constants of van Laar equation
a, b	=	any two points on the same curve in a triangular plot (Part I of Thesis)
a, b	=	constants of Othmer's reference plot (Part II of Thesis)
B_{11}	=	second coefficient in the virial equation of state
B_{11}, B_{12}, B_{22}	=	coefficients associated with interaction parameter as defined by Equation 1
B_{12}, C_{12}, D_{12}	=	constants of Redlich-Kister equations in binary systems
B_{23}, C_{23}, D_{23}	=	
B_{31}, C_{31}, D_{31}	=	constants of Redlich-Kister equations in ternary systems
G_{123}, D_1, D_2, D_3	=	
exp.	=	exponent
ΔH^M	=	isobaric and isothermal heat of mixing
log	=	common logarithms
P	=	total pressure
P_c	=	critical pressure
P	=	vapor pressure
Q	=	$(G^E/2.303 RT)$ = excess free energy function
R	=	gas constant
S	=	$2 B_{12} - B_{11} - B_{22}$ = interaction parameter
T	=	absolute temperature

- T_r = reduced temperature
 t = temperature
 v^* = molal volume of the liquid in the vapor state
 x = mole fraction of component in liquid phase
 y = mole fraction of component in vapor phase
 z_1 = exp. $\frac{(p_1 - P)(V_1^* - B_{11})}{RT}$
 z_2 = exp. $\frac{y_2^2 SP}{RT}$
 γ = liquid phase activity coefficient

Subscripts

- 1 = component 1
 2 = component 2
 3 = component 3
 12 = components 1 and 2
 23 = components 2 and 3
 31 = components 3 and 1
 123 = components 1, 2 and 3
 1 = component 1

Superscripts

- ° = ideal condition (Part II of Thesis)
 ' = pseudo condition (Part II of Thesis)

REFERENCES

1. Tongberg, C. O., and Johnston, F., Ind. Eng. Chem., 25, 733 (1933).
2. Myers, H. S., Ind. Eng. Chem., 47, 2215 (1955).
3. Wehe, A. H., and Coates, J., A.I.Ch.E. Journal, 1, 241 (1955).
4. Barbaudy, J., J. Chim. Phys., 24, 1 (1927).
5. Sinor, J. E., and Weber, J. H., J. Chem. Eng. Data, 5, 243 (1960).
6. Redlich, O., and Kister, A. T., Ind. Eng. Chem., 40, 345 (1948).
7. Benedict, M., Johnson, C. A., Solomon, E., and Rubin, L. G., Trans. Am. Inst. Chem. Engrs., 41, 371 (1945).
8. Scheibel, E. G., Ind. Eng. Chem., 41, 1076 (1949).
9. Margules, M., Sitzber. Akad. Wiss. Wien. Math. naturw. Klasse, (II) 104, 1243 (1895).
10. Carlson, H. C., and Colburn, A. P., Ind. Eng. Chem., 34, 581 (1942).
11. van Laar, J. J., Z. Physik. Chem., 72, 723 (1910).
12. van Laar, J. J., Z. Physik. Chem., 185, 35 (1929).
13. Redlich, O., Kister, A. T., and Turnquist, C. E., Chem. Eng. Progr. Symposium Series 48, No. 2, 49 (1952).
14. Ho, J. C. K., Boshko, O., and Lu, B. C.-Y., Can. J. Chem. Eng., 39, 205 (1961).
15. Lu, B. C.-Y., Spinner, I. H., and Ho, J. C. K., Can. J. Chem. Eng. 40, 16 (1962).
16. Thijsen, H. A. G., Chem. Eng. Sci., 4, 75 (1955).
17. Herington, E. F. G., J. Inst. Petrol., 37, 457 (1951).

18. Krishnamurty, V. V. G., and Rao, C. V., J. Sci. Ind. Research (India) 14 B, 188 (1955).
19. Krishnamurty, V. V. G., and Rao, C. V., J. Sci. Ind. Research (India) 15 B, 55 (1956).
20. Herington, E. F. G., Research (London) 3, 41 (1950).
21. Herington, E. F. G., J. Appl. Chem. (London) 2, 11, 19 (1952).
22. Colburn, A. P., and Schoenborn, E. M., Trans. A.I.Ch.E., 41, 221 (1945).
23. Li, J. C. M., and Lu, B. C.-Y., Can. J. Chem. Eng. 37, 117 (1959).
24. Am. Petrol. Inst. Research Project 44, Carnegie Inst. Technol., Pittsburgh, Pa., 1953.
25. Dreisbach, R. R., "Physical Properties of Chemical Substances", Dow Chemical Co., Midland, Mich., 1952.
26. Robinson, C. S., and Gilliland, E. R., "Elements of Fractional Distillation", 4th Ed., P. 3, McGraw-Hill, New York, 1950.
27. Gillespie, D. T. C., Ind. Eng. Chem. Anal. Ed. 18, 575 (1956).
28. Gilmont, R., Anal. Chem., 23, 157 (1951).
29. Severns, W. H., Jr., Sesonke, A., Perry, R. H., and Pigford, R. L., A.I.Ch.E. Journal, 1, 401 (1955).
30. Wagner, I. F., and Weber, J. H., Ind. Eng. Chem. Eng. Data Ser. 3, 220 (1958).
31. Ricci, J. E., The Phase Rule and Heterogeneous Equilibrium, P. 207, Van Nostrand Co., New York, 1951.

32. Chu, J. C., "Distillation Equilibrium Data", Reinhold, New York, 1950.
33. Chu, J. C., Wong, S. L., Levy, S. L., and Paul, R., "Vapor-Liquid Equilibrium Data", J. W. Edwards Publisher, Inc., Ann Arbor, Michigan (1956).
34. Johnson, A. I., Huang, C. J., Barry, T. W., and Michelliepis, C., Chem. in Canada, P. 25, Jan., 1955.
35. Lu, B. C.-Y., A.I.Ch.E. Journal, 2, 525 (1956).
36. Lu, B. C.-Y., Can. J. Chem. Eng., 37, 193 (1959).
37. Lu, B. C.-Y., and Graydon, W. F., Ind. Eng. Chem., 49, 1058 (1957).
38. Othmer, D. F., and Gilment, R., Ind. Eng. Chem., 36, 858 (1944).
39. Spinner, E. H., Lu, B. C.-Y., and Graydon, W. F., Ind. Eng. Chem., 48, 147 (1956).
40. Othmer, D. F., Ind. Eng. Chem., 32, 841 (1940).
41. Scatchard, G., Wood, S. E., and Mochel, J. H., J. Am. Chem. Soc., 62, 712 (1940).
42. Scatchard, G., Wood, S. E., and Mochel, J. H., J. Am. Chem. Soc., 61, 3206 (1939).
43. Quiggle, D., and Fenske, M. R., J. Am. Chem. Soc., 55, 1829 (1937).
44. Weber, J. H., Ind. Eng. Chem., 47, 454 (1955).
45. Haynes, S. Jr., and van Winkle, M., Ind. Eng. Chem., 46, 334 (1954).
46. Yang, C. P., and van Winkle, M., Ind. Eng. Chem., 47, 293 (1955).
47. Gelus, F., Marple, S. Jr., and Miller, M. E., Ind. Eng. Chem., 41 1757 (1949).

